

A General Framework For Constructing Locally Self-Normalized Multiple-Change-Point Tests

Cheuk Hin Cheng ^{*1} and Kin Wai Chan ^{†2}

¹Department of Statistics, The Chinese University of Hong Kong.

May 3, 2022

Abstract

We propose a general framework to construct self-normalized multiple-change-point tests with time series data. The only building block is a user-specified one-change-point detecting statistic, which covers a wide class of popular methods, including cumulative sum process, outlier-robust rank statistics and order statistics. Neither robust and consistent estimation of nuisance parameters, selection of bandwidth parameters, nor pre-specification of the number of change points is required. The finite-sample performance shows that our proposal is size-accurate, robust against misspecification of the alternative hypothesis, and more powerful than existing methods. Case studies of NASDAQ option volume and Shanghai-Hong Kong Stock Connect turnover are provided.

Keywords: Change-point analysis; non-parametric; self-normalization; time series; multiple change points

*Email: andychengcheukhin@link.cuhk.edu.hk

†Email: kinwaichan@sta.cuhk.edu.hk

1 Introduction

Testing structural stability is of paramount importance in statistical inference. There is considerable amount of literature and practical interest of testing existence of change points (CPs). Csörgö and Horváth (1988, 1997) provided comprehensively both classical parametric and non-parametric approaches for the at most one change (AMOC) problem. For detection of multiple CPs, one method is to assume a fixed or bounded number of CPs (m). The test statistics are constructed by dividing the data into segments and maximizing a sum of AMOC-type statistics computed within each segment; see Antoch and Jarušková (2013) and Shao and Zhang (2010). Since the true number of CPs (M) is usually unknown in practice, several information criteria (Yao, 1988; Lee, 1995) have been proposed for estimating M . We remark that such approaches are vulnerable to misspecification of M and the computational cost is often scaled exponentially with m . Another approach relies on sequential estimation via binary segmentation (Vostrikova, 1981; Bai and Perron, 1998). This class of methods sequentially performs AMOC-type tests and produces CP estimates if the no-CP null hypothesis is rejected. The same procedure is repeated on each of the two subsamples split at the estimated CP until no segment can be split further. Since the structural difference between data before and after a particular CP may be weakened in the presence of other CPs, the AMOC-type tests may inevitably lose power under the multiple-CP situation.

To improve power, localization can be used. Bauer and Hackl (1980) introduced the moving sum (MOSUM) approach. Chu *et al.* (1995) and Eichinger and Kirch (2018) later applied MOSUM to CPs detection. This method selects a local window size and performs inference on each local subsample. To avoid selection of the window size, Fryzlewicz (2014) proposed wild binary segmentation, which randomly draws subsamples without fixing the window size. Both algorithms attempt to find a subsample which contains only one CP to boost power without specifying m . However, the above methods require consistent and robust estimation of nuisance parameters. For example, the long-run variance (LRV) σ^2 of the partial sum usually appears in a test statistic in the form of $T_n(\sigma^2) = L_n/\sigma^2$, where L_n satisfies $L_n \xrightarrow{d} \sigma^2 \mathbb{L}$ under the null for some pivotal distribution \mathbb{L} , and “ \xrightarrow{d} ” denotes

convergence in distribution. Unfortunately, estimating σ^2 can be non-trivial and may require tuning a bandwidth parameter (Andrews, 1991). Worse still, Kiefer and Vogelsang (2005) found that different selected bandwidths can noticeably influence the tests.

To avoid the challenging estimation of σ^2 , Lobato (2001) first proposed to use a self-normalizer (SN) V_n that satisfies $V_n \xrightarrow{d} \sigma^2 \mathbb{V}$ for some pivotal \mathbb{V} so that V_n cancels out the nuisance σ^2 in L_n to form a self-normalized test statistic $T'_n = L_n/V_n \xrightarrow{d} \mathbb{L}/\mathbb{V}$ under the null. Shao and Zhang (2010) later modified the SN for handling the AMOC problem. In the multiple-CP problem, Zhang and Lavitas (2018) proposed a self-normalized test which intuitively scans for the first and last CPs. However, it may sacrifice power when larger changes take place in the middle. Moreover, applying their proposed test to CP location estimation is non-trivial.

In this paper, we propose a general framework combining self-normalization and localization to construct a powerful multiple-CP test, which is applicable to a broad class of time series models including both short-range and long-range dependent data. Our method also allows utilization of outlier-robust change detecting statistics to improve size accuracy and power. The proposed method is driven by principles which generalize one-CP test statistic to a multiple-CP test statistic. Our proposed test is shown to be locally powerful asymptotically. Recursive formula is derived for fast computation.

The remaining part of the paper is structured as follows. We first review the self-normalization idea proposed by Shao and Zhang (2010) under the AMOC problem in Section 2. Our proposal is demonstrated by using the CUSUM process as motivation in Section 3. Limiting distribution, consistency and local power analysis are also provided. In Section 4, detailed principles and the most general form of our proposed test are presented with examples of applying rank and order statistics. The extensions to test for structural changes of other parameters, long range dependent and multivariate time series are also provided. In Section 5, the differences between different self-normalized approaches will be comprehensively discussed. Some implantation issues are also discussed. Simulation experiments are presented in Section 6, which shows promising size accuracy and substantial improvement of power over existing methods. The paper ends with real-data analysis of

the NASDAQ option volume in Section 7.1 and the Shanghai-Hong Kong Stock Connect turnover in Section 7.2. Proofs of main results, additional simulation results, critical values, recursive formulas and algorithms can be found in the Appendix.

2 Introduction of self-normalization

Consider the signal-plus-noise model: $X_i = \mu_i + Z_i$, where $\mu_i = \mathbb{E}(X_i)$ for $i = 1, \dots, n$ and $\{Z_i : i \in \mathbb{Z}\}$ is a stationary noise sequence. The AMOC testing problem is formulated as follows:

$$H_0 : \mu_1 = \dots = \mu_n, \tag{2.1}$$

$$H_1 : \exists 0 < k_1 < n, \quad \mu_1 = \dots = \mu_{k_1} \neq \mu_{k_1+1} = \dots = \mu_n. \tag{2.2}$$

Let $\xi_{k_1, k_2} = \sum_{i=k_1}^{k_2} X_i$ if $1 \leq k_1 \leq k_2 \leq n$; $\xi_{k_1, k_2} = 0$ otherwise. Define the CUSUM process

$$C_n(\lfloor nt \rfloor) = n^{-1/2} \sum_{i=1}^{\lfloor nt \rfloor} (X_i - n^{-1} \xi_{1, n}), \quad t \in [0, 1], \tag{2.3}$$

where $\lfloor nt \rfloor$ is the largest integer part of nt . The limiting distribution of functional of (2.3) relies on the following assumption.

Assumption 2.1. As $n \rightarrow \infty$, $\{n^{-1/2} \sum_{i=1}^{\lfloor nt \rfloor} Z_i : t \in [0, 1]\} \Rightarrow \{\sigma \mathbb{B}(t) : t \in [0, 1]\}$, where $\sigma^2 = \lim_{n \rightarrow \infty} \text{Var}(\xi_{1, n})/n \in (0, \infty)$ is the long-run variance (LRV), $\mathbb{B}(\cdot)$ is the standard Brownian motion and “ \Rightarrow ” denotes convergence in distribution in the Skorokhod space (Billingsley, 1999).

Assumption 2.1 is known as a functional central limit theorem (FCLT) or Donsker’s invariance principle. Under standard regularity conditions (RCs), Assumption 2.1 is satisfied. For example, Herrndorf (1984) proved the FCLT for the dependent data under some mixing conditions; Wu (2007) later showed the strong convergence for stationary processes using physical and predictive dependence measures. Under the null hypothesis H_0 , by continuous mapping theorem, we have $\{C_n(\lfloor nt \rfloor) : t \in [0, 1]\} \Rightarrow \{\sigma \{\mathbb{B}(t) - t\mathbb{B}(1)\} : t \in [0, 1]\}$.

Classically, the celebrated Kolmogorov–Smirnov (KS) test statistic, defined as $\text{KS}_n(\sigma) = \sup_{k=1, \dots, n} |C_n(k)/\sigma|$, can be used for the AMOC problem. Since σ is typically unknown, we need to estimate it by a consistent $\hat{\sigma}$ no matter under H_0 or H_1 ; see [Chan \(2022\)](#) and [Chan \(2022+\)](#) for some possible estimators. Hence, $\text{KS}_n(\hat{\sigma}) \xrightarrow{d} \mathbb{KS} := \sup_{t \in (0,1)} |\mathbb{B}(t) - t\mathbb{B}(1)|$, which is known as the Kolmogorov distribution. [Shao and Zhang \(2010\)](#) proposed to bypass the estimation of σ by normalizing $C_n(k)$ by a non-degenerate standardizing random process called a self normalizer:

$$V_n(k) = n^{-2} \left\{ \sum_{i=1}^k \left(\xi_{1,i} - \frac{i}{k} \xi_{1,k} \right)^2 + \sum_{i=k+1}^n \left(\xi_{i,n} - \frac{n-i+1}{n-k} \xi_{k+1,n} \right)^2 \right\}, \quad k = 1, \dots, n-1.$$

The resulting self-normalized test statistic for the AMOC problem is $S_n^{(1)}$, where

$$S_n^{(1)} = \sup_{k=1, \dots, n-1} S_n^{(1)}(k) \quad \text{and} \quad S_n^{(1)}(k) = C_n^2(k)/V_n(k). \quad (2.4)$$

Under [Assumption 2.1](#) and H_0 , the limiting distribution of $S_n^{(1)}$ is non-degenerate and pivotal. The nuisance parameter σ^2 is asymptotically cancelled out in the numerator $C_n^2(k)$ and the denominator $V_n(k)$ on the right hand side of [\(2.4\)](#). Moreover, since there is no CP in the intervals $[1, k_1]$ and $[k_1 + 1, n]$ under H_1 , the SN at the true CP, $V_n(k_1)$, is invariant to the change and therefore their proposed test does not suffer from the well-known non-monotonic power problem; see, e.g., [Vogelsang \(1999\)](#). However, this appealing feature no longer exists in the multiple-CP setting. [Zhang and Lavitas \(2018\)](#) improved by proposing a self-normalized multiple-CP test without specifying m . The test utilizes forward and backward scans to select two time intervals, $[1, k_1]$ and $[k_2, n]$ for $1 < k_1, k_2 < n$, and aims at detecting the largest change. Applying the SN in [Shao and Zhang \(2010\)](#) to each of these two subsamples, their test was proved to be consistent. However, the method tends to consider only the first and the last CPs. Thus, it affects power as will be shown in our simulation studies in [Section 6](#). In the next section, we propose a framework for extending a one-CP test to a valid multiple-CP self-normalized test. It is achieved by utilizing the localization idea.

3 Locally self-normalized statistic

We consider the multiple-CP testing problem, i.e., to test the H_0 in (2.1) against

$$H_{\geq 1} : \mu_1 = \cdots = \mu_{k_1} \neq \mu_{k_1+1} = \cdots = \mu_{k_2} \neq \cdots \neq \mu_{k_M+1} = \cdots = \mu_n, \quad (3.1)$$

for an unknown number of CPs $M \geq 1$, and unknown times $1 < k_1 < \cdots < k_M < n$. Also denote $\pi_j = k_j/n$ and $\Delta_j = \mu_{k_{j+1}} - \mu_{k_j}$ be the j th relative CP time and the corresponding mean change, respectively, for $j = 1, \dots, M$. Since M is usually unknown and possibly larger than one in practice, the multiple-change alternative (3.1) is more sensible than the one-change alternative (2.2). To improve the power of (2.3), we generalize the CUSUM process to a localized CUSUM statistic. Define it and its SN as

$$\begin{aligned} L_n^{(C)}(k | s, e) &:= (e - s + 1)^{-1/2} \sum_{i=s}^k \{X_i - (e - s + 1)^{-1} \xi_{s,e}\} \\ &= \left(\frac{n}{e - s + 1} \right)^{1/2} \left[C_n(k) - C_n(s-1) - \frac{k - s + 1}{e - s + 1} \{C_n(e) - C_n(s-1)\} \right], \end{aligned} \quad (3.2)$$

$$V_n^{(C)}(k | s, e) := \frac{k - s + 1}{(e - s + 1)^2} \sum_{j=s}^k L_n^{(C)}(j | s, k)^2 + \frac{e - k}{(e - s + 1)^2} \sum_{j=k+1}^e L_n^{(C)}(j | k + 1, e)^2, \quad (3.3)$$

respectively, where $1 \leq s \leq k \leq e \leq n$. The indices s and e denote the starting and ending times of a local subsample $\{X_s, \dots, X_e\}$, respectively. The statistic $L_n^{(C)}(k | s, e)$ is used to detect a local difference between $\{X_s, \dots, X_k\}$ and $\{X_{k+1}, \dots, X_e\}$. Indeed, (3.2) generalizes the global CUSUM process (2.3) because $C_n(k) \equiv L_n^{(C)}(k | 1, n)$. Moreover, according to (3.2), the localized CUSUM process allows fast recursive computation as it is a function of $C_n(\cdot)$. Consequently, the *locally self-normalized* (LSN) statistic is defined as

$$T_n^{(C)}(k | s, e) := \frac{L_n^{(C)}(k | s, e)^2}{V_n^{(C)}(k | s, e)}, \quad \text{for } 1 \leq s \leq k \leq e \leq n, \quad (3.4)$$

and $T_n^{(C)}(k | s, e) = 0$ otherwise; see Remark 3.1 for a non-SN approach. The LSN statistic generalizes Shao and Zhang (2010)'s proposal in the sense that $S_n^{(1)}(k) \equiv T_n^{(C)}(k | 1, n)$. To infer how likely k is a potential CP location, we consider all the symmetric local windows

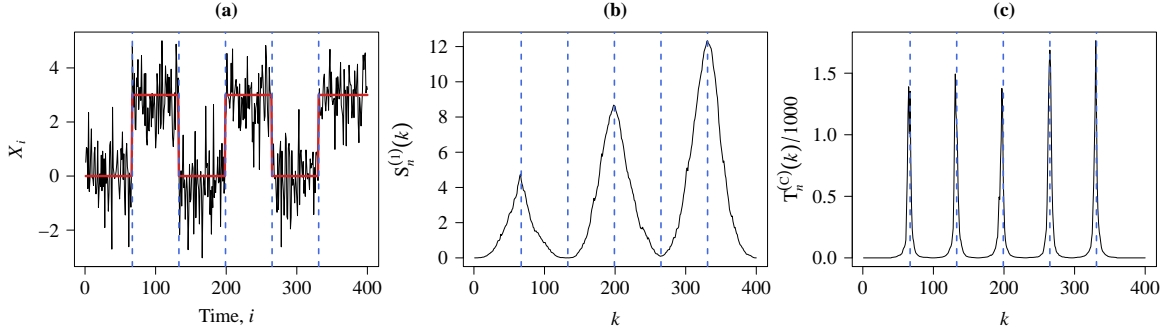


Figure 3.1: (a) A realization of time series (black solid line) with 5 CPs (blue dashed lines) and its mean function (red solid line). (b) The score function $S_n^{(1)}(k)$ employed by [Shao and Zhang \(2010\)](#). (c) The proposed score function $T_n^{(C)}(k)$.

that center at k . The resulting score function is

$$T_n^{(C)}(k) = \sup_{\lfloor n\epsilon \rfloor \leq d \leq n} T_n^{(C)}(k \mid k-d, k+1+d), \quad (3.5)$$

where $0 < \epsilon < 1/2$ is a fixed local tuning parameter, which is similarly used in, e.g., [Huang et al. \(2015\)](#) and [Zhang and Lavitas \(2018\)](#); see Remark 3.2 for discussing the choice of symmetric windows. In particular, they suggested to choose $\epsilon = 0.1$. This suggestion is followed throughout this article. In essence, (3.4) compares the local subsamples of length $d+1$ before and after time k , i.e., $\mathcal{S}_{\text{before}} = \{X_{k-d}, \dots, X_k\}$ and $\mathcal{S}_{\text{after}} = \{X_{k+1}, \dots, X_{k+1+d}\}$, for each possible width d that is not too small. The statistic $T_n^{(C)}(k)$ records the change corresponding to the most obvious d . We visualize our proposed score function $T_n^{(C)}(\cdot)$ and [Shao and Zhang \(2010\)](#) proposal $S_n^{(1)}(\cdot)$ defined in (2.4) in Figure 3.1 when they are applied to a time series with 5 CPs. [Zhang and Lavitas \(2018\)](#)'s method is not included because it does not map a time k to a score. Clearly, $T_n^{(C)}(\cdot)$ attains the local maxima near all true CP locations, while $S_n^{(1)}(\cdot)$ cannot. Possible reasons are reduced CP detection capacity of global CUSUM by other changes, non-monotonic CP configuration, and non-robust SN. By design, the score function can be extended to CP estimation; see Remark 3.3.

Finally, aggregating the scores $T_n^{(C)}(k)$ across k , we obtain the proposed test statistic:

$$T_n^{(C)} := \frac{1}{n - 2\lfloor \epsilon n \rfloor - 1} \sum_{k=\lfloor \epsilon n \rfloor + 1}^{n - \lfloor \epsilon n \rfloor - 1} T_n^{(C)}(k), \quad (3.6)$$

which captures the effects of all potential CPs instead of merely the first and the last CPs as in [Zhang and Lavitas \(2018\)](#). Hence, this statistic is potentially more powerful for testing multiple CPs than the existing state-of-the-art SN test ([Zhang and Lavitas, 2018](#)). Define $0 < \pi_1 < \dots < \pi_M < 1$ to be $M \geq 1$ relative CP times so the CP occurs at times $\lfloor n\pi_1 \rfloor, \dots, \lfloor n\pi_M \rfloor$. For convenience, denote $\pi_0 = 0$ and $\pi_{M+1} = 1$. [Theorem 3.1](#) below states the limiting distribution of $T_n^{(C)}$ and the consistency of the test.

Theorem 3.1 (Limiting distribution and consistency). *Suppose [Assumption 2.1](#) is satisfied. (i) Under H_0 , we have*

$$T_n^{(C)} \xrightarrow{d} \mathbb{T} := (1 - 2\epsilon)^{-1} \int_{\epsilon}^{1-\epsilon} \sup_{\delta > \epsilon} \frac{\mathbb{L}(t \mid t - \delta, t + \delta)^2}{\mathbb{V}(t \mid t - \delta, t + \delta)} dt, \quad (3.7)$$

for any $0 < \epsilon < 1/2$, where

$$\mathbb{V}(t \mid t - \delta, t + \delta) = \frac{1}{4\delta} \left\{ \int_{t-\delta}^t \mathbb{L}(\tau \mid t - \delta, t)^2 d\tau + \int_t^{t+\delta} \mathbb{L}(\tau \mid t, t + \delta)^2 d\tau \right\}, \quad (3.8)$$

$$\mathbb{L}(t \mid \tau_1, \tau_2) = \frac{1}{\sqrt{\tau_2 - \tau_1}} \left[\mathbb{B}(t) - \mathbb{B}(\tau_1) - \frac{t - \tau_1}{\tau_2 - \tau_1} \{ \mathbb{B}(\tau_2) - \mathbb{B}(\tau_1) \} \right]. \quad (3.9)$$

(ii) Under $H_{\geq 1}$, if there exist $j \in \{1, \dots, M\}$ and $C > 0$ such that the j th CP time satisfies $\epsilon < \min(\pi_j - \pi_{j-1}, \pi_{j+1} - \pi_j)$ and the j th change magnitude satisfies $|\Delta_j| = |\mu_{k_{j+1}} - \mu_{k_j}| > C$ as $n \rightarrow \infty$, then $\lim_{n \rightarrow \infty} T_n^{(C)} = \infty$ in probability.

Under H_0 , the test statistic $T_n^{(C)}$ has a pivotal limiting distribution, whose quantiles can be easily found by simulation; see [Table D.2](#) in the appendix and [Section 5](#) for more discussion. Under $H_{\geq 1}$, the test is of power 1 asymptotically when the change magnitude is at least a non-zero constant. Moreover, [Assumption 2.1](#) is satisfied by short-range dependent data. It can be generalized to handle long-range dependent data; see [Example 4.4](#). [Theorem 3.2](#) below concerns a local alternative hypothesis that contains CP having diminishing change magnitude. It states the regime of the size of CP at which our test remains powerful.

Theorem 3.2 (Local limiting power). *Under $H_{\geq 1}$, parametrize the j th change magnitude $|\Delta_j(n)| = |\mu_{k_{j+1}} - \mu_{k_j}|$ as a function of n . If there exist $j \in \{1, \dots, M\}$ and $0.5 < \kappa \leq 1$*

such that the j th CP satisfies $\epsilon < \min(\pi_j - \pi_{j-1}, \pi_{j+1} - \pi_j)$ and $|\Delta_j(n)| \asymp n^{\kappa-1}$ as $n \rightarrow \infty$, then $\lim_{n \rightarrow \infty} T_n^{(C)} = \infty$ in probability.

The smallest change magnitude so that the test remains powerful satisfies $\kappa > 0.5$. This result is in line with [Zhang and Lavitas \(2018\)](#). Indeed, from the proof of [Theorem 3.2](#), it is easy to see that CP tests based on the CUSUM process are of power one asymptotically only if the order of change magnitude is larger than $n^{-1/2}$. Therefore, our proposed test preserves the change detecting ability of the CUSUM process.

Remark 3.1 (Non-SN approach). Users may instead use a consistent estimator of the LRV, say $\hat{\sigma}_n^2$, to replace the SN [\(3.3\)](#), $V_n^{(C)}(k | k - d, k + 1 + d)$, for all k and d . The performance is expected to be affected by the robustness of CP estimators (if any) and bandwidth parameter as discussed in [Kiefer and Vogelsang \(2005\)](#). Alternatively, the LRV can be estimated robustly by splitting the dataset as in [\(3.3\)](#). However, the estimator of σ^2 will become very noisy due to small subsample sizes. This extra variability in estimating σ^2 may accumulate and eventually ruin the test statistic. Our approach takes the variability of $V_n^{(C)}(k | k - d, k + 1 + d)$ into account, thus, it is expected to perform better.

Remark 3.2 (Symmetric windows). Define the score function based on non-symmetric windows as

$$\tilde{T}_n^{(C)}(k) = \sup_{\lfloor \epsilon n \rfloor \leq d_0, d_1 \leq n} T_n^{(C)}(k | k - d_0, k + 1 + d_1). \quad (3.10)$$

The corresponding test statistic is $\tilde{T}_n^{(C)} = \sum_{k=\lfloor \epsilon n \rfloor+1}^{n-\lfloor \epsilon n \rfloor-1} \tilde{T}_n^{(C)}(k) / (n - 2\lfloor \epsilon n \rfloor - 1)$. To balance computational cost and power, we suggest using symmetric windows $T_n^{(C)}(k)$ instead of $\tilde{T}_n^{(C)}(k)$, and set the local subsamples before and after target time k , i.e., $\mathcal{S}_{\text{before}}$ and $\mathcal{S}_{\text{after}}$, to have the same width d . The test consistency only requires existence of one CP in the local windows. The change can still be captured under symmetric windows without significant power loss. Using non-symmetric windows significantly increases computational cost and is not expected to bring vast improvement in power. Some simulation evidence is provided in [Sections 5.1 and 6.4](#).

Remark 3.3 (CP time estimation). The score function $T_n^{(C)}(\cdot)$ in [\(3.5\)](#) can be used for CP estimation; see [Figure 3.1 \(c\)](#) for visualization. Motivated by the GOALS algorithm

(Jiang *et al.*, 2022+), the set of estimated CP times can be obtained by finding the local maximizers of the score functions:

$$\hat{\Pi} = \left\{ k \in \{\lfloor n\epsilon \rfloor, \dots, n - \lfloor n\epsilon \rfloor\} : T_n^{(C)}(k) = \max_{k - \lfloor n\epsilon \rfloor < j \leq k + \lfloor n\epsilon \rfloor} T_n^{(C)}(j) \text{ and } T_n^{(C)}(k) > \varrho \right\}, \quad (3.11)$$

where ϱ is the decision threshold that is of order $o(n)$. The estimation may be improved through integrating other screening algorithms to perform model selection in order to avoid overestimating the number of CPs. For example, the screening and ranking algorithm (SaRa) (Niu and Zhang, 2012) and the scanning procedure proposed by Yau and Zhao (2016). Alternatively, it is possible to apply our proposed test to stepwise estimation, for example, binary segmentation (BS) (Vostrikova, 1981), wild binary segmentation (Fryzlewicz, 2014), etc; see Section E in the appendix for the detail of integrating our proposed scanning procedure with SaRa and BS.

4 General framework for constructing LSN statistics

The proposed test statistic $T_n^{(C)}$ in (3.6) sheds light on how multiple-CP tests should be performed. In particular, we combine the advantages of localization and self-normalization. Although $T_n^{(C)}$ demonstrates to have appealing features as we see in Figure 3.1, it is not fully general in terms of two aspects to be stated below. In this section, we lay out the underlying principles to define a general class of statistics for testing multiple CPs.

First, $T_n^{(C)}$ is a functional of the global CUSUM process $C_n(\cdot)$. Thus, potential CPs are detected via differences between local averages of X_i 's, which however may not be the best choice, in particular for the data that have heavy-tailed distributions. Generally, one may consider any specific *global change detecting process* $\{D_n(\lfloor nt \rfloor)\}_{0 \leq t \leq 1}$ for the AMOC problem. Applying the localization trick (3.2) and the self-normalization trick (3.3) to $D_n(\cdot)$ instead of $C_n(\cdot)$, we obtain the generalized LSN statistic $T_n^{(D)}(k \mid s, e) = L_n^{(D)}(k \mid$

$s, e)^2/V_n^{(D)}(k | s, e)$, where

$$\begin{aligned} L_n^{(D)}(k | s, e) &= \left(\frac{n}{e-s+1} \right)^{1/2} \left[D_n(k) - D_n(s-1) - \frac{k-s+1}{e-s+1} \{D_n(e) - D_n(s-1)\} \right], \\ V_n^{(D)}(k | s, e) &= \frac{k-s+1}{(e-s+1)^2} \sum_{j=s}^k L_n^{(D)}(j | s, k)^2 + \frac{e-k}{(e-s+1)^2} \sum_{j=k+1}^e L_n^{(D)}(j | k+1, e)^2. \end{aligned}$$

If $D_n(\cdot)$ converges weakly in Skorokhod space to $\sigma_D \mathbb{D}(\cdot)$ for some $\sigma_D \in (0, \infty)$, where $\mathbb{D}(\cdot)$ is an empirical process whose distribution is pivotal, then $T_n^{(D)}(k | d)$ is asymptotically pivotal as in Theorem 3.1. Examples of $D_n(\cdot)$, based on Wilcoxon statistics, Hodges–Lehmann statistics, and influence functions, are provided in Examples 4.1–4.3. Extensions to long-range dependent and multivariate time series are provided in Examples 4.4 and 4.5, respectively.

Second, there are two free indices, d and k , in $T_n^{(D)}(k | k-d, k+1+d)$. The maximum operator in (3.5) and the mean operator in (3.6) are used to aggregate the indices d and k , respectively. The introduction of d is to let the data choose the window sizes. We remark that the performance of the MOSUM statistic, which is one special case of localized CUSUM with a fixed window size, depends critically on the window size (Eichinger and Kirch, 2018). Hence, they suggested to consider multiple window sizes for robustness. We follow their suggestion to improve performance by aggregating all possible window sizes. Generally, users may choose their preferred aggregation operators, e.g., median, trimmed mean, etc, for aggregation. Formally, for any finite set of indices $S \subset \mathbb{Z}$ having size $|S|$, we say that \mathcal{P} is an aggregation operator if $\mathcal{P}_{i \in S} a_i$ maps $\{a_i \in \mathbb{R} : i \in S\}$ to a real number, e.g., if $\mathcal{P} = \max$, $\mathcal{P}_{i \in S} a_i = \max_{i \in S} a_i$ gives the maximum; and if $\mathcal{P} = \text{mean}$, $\mathcal{P}_{i \in S} a_i = \sum_{i \in S} a_i / |S|$ gives the sample mean. Hence, the most general form of our proposed test statistic is

$$T_n^{(D)} = T_n^{(D)}[\mathcal{P}^{(1)}, \mathcal{P}^{(2)}] = \mathcal{P}_{\lfloor \epsilon n \rfloor < k < n - \lfloor \epsilon n \rfloor}^{(2)} \left[\mathcal{P}_{\lfloor n \epsilon \rfloor \leq d \leq n}^{(1)} \left\{ T_n^{(D)}(k | k-d, k+1+d) \right\} \right],$$

where $\mathcal{P}^{(1)}$ and $\mathcal{P}^{(2)}$ are some aggregation operators. In particular, $T_n^{(C)}[\max, \text{mean}]$ is

used in (3.6). It is practically convenient to use weighted sum and weighted average, i.e.,

$$\mathcal{P}_{\lfloor n\epsilon \rfloor \leq d \leq n}^{(1)} a_d = \max_{\lfloor n\epsilon \rfloor \leq d \leq n} w_d^{(1)} a_d \quad \text{and} \quad \mathcal{P}_{\lfloor \epsilon n \rfloor < k < n - \lfloor \epsilon n \rfloor}^{(2)} a_k = \frac{\sum_{\lfloor \epsilon n \rfloor < k < n - \lfloor \epsilon n \rfloor} w_k^{(2)} a_k}{\sum_{\lfloor \epsilon n \rfloor < k < n - \lfloor \epsilon n \rfloor} w_k^{(2)}},$$

where $w_d^{(1)}$'s and $w_k^{(2)}$'s are some constants specified by users. The weights guarantee the local intervals are not too small in order to avoid degeneracy of the SN. They are also used to reflect user's prior beliefs on k and d . We propose to use $\mathcal{P}^{(2)} = \text{mean}$ instead of $\mathcal{P}^{(2)} = \text{max}$ for better empirical performance. By construction, our proposed LSN statistics remain large over the neighborhoods of the true CPs. Thus, the averaged score capture evidence contributed by all CPs and their neighborhoods, whereas the maximum score can only capture evidence contributed by one single CP corresponding to the highest score. In this sense, $\mathcal{P}^{(2)} = \text{mean}$ is more suitable for multiple-CP testing.

Our approach is more flexible as it supports a general CP detecting process $D_n(\cdot)$ and general aggregation operators $\mathcal{P}^{(1)}$ and $\mathcal{P}^{(2)}$. Moreover, our proposed LSN statistic is a function of the supplied global CP detecting process. Therefore, recursive computation of the LSN statistics, regardless of the supplied global change detecting process, is possible for our approach. It results in lower computational cost; see Section F in the appendix. In a nutshell, our framework is an automatic procedure for generalizing any one-CP detecting statistic $D_n(\cdot)$ to a multiple-CP detecting statistic $T_n^{(D)}$. We demonstrate it via following examples.

Example 4.1 (Wilcoxon rank statistics). An outlier-robust non-parametric CP test can be constructed by using the Wilcoxon two-sample statistic. The corresponding global change detecting process is

$$W_n(\lfloor nt \rfloor) = \frac{1}{n^{3/2}} \sum_{i=1}^{\lfloor nt \rfloor} \sum_{j=\lfloor nt \rfloor+1}^n \left(\mathbb{1}_{\{X_i \leq X_j\}} - \frac{1}{2} \right) = n^{-3/2} \left(\sum_{i=1}^{\lfloor nt \rfloor} R_i - \frac{\lfloor nt \rfloor}{n} \sum_{i'=1}^n R_{i'} \right), \quad (4.1)$$

for $t \in [0, 1]$, where $R_i = \sum_{j=1}^n \mathbb{1}_{\{X_j \leq X_i\}}$ is the rank of X_i when there is no tie in X_1, \dots, X_n . Assuming that the data is weakly dependent and can be represented as a functional of an absolutely regular process. Under some mixing conditions, we have

$W_n(\lfloor nt \rfloor) \xrightarrow{d} \sigma_W \{\mathbb{B}(t) - t\mathbb{B}(1)\}$, where $\sigma_W^2 = \sum_{k \in \mathbb{Z}} \text{Cov}\{F(X_0), F(X_k)\}$ and $F(\cdot)$ is the distribution function of X_1 with a bounded density; see Theorem 3.1 in [Dehling et al. \(2015\)](#). Using the principles in Section 4, we may use (4.1) to construct a self-normalized multiple-CP Wilcoxon test and eliminate the nuisance parameter σ_W by using the test statistic $T_n^W := T_n^W[\max, \text{mean}]$, whose limiting distribution is stated as follows.

Corollary 4.1 (Limiting distribution of T_n^W). *Under the RCs in Theorem 3.1 of [Dehling et al. \(2015\)](#) and H_0 , $T_n^{(W)} \xrightarrow{d} \mathbb{T}$.*

Example 4.2 (Hodges–Lehmann order statistics). Hodges–Lehmann statistic is another popular alternative to the CUSUM statistic in (2.3). Its global change detecting process is

$$H_n(\lfloor nt \rfloor) = n^{-3/2} \lfloor nt \rfloor (n - \lfloor nt \rfloor) \text{median} \{(X_i - X_j) : 1 \leq i \leq \lfloor nt \rfloor < j \leq n\}, \quad (4.2)$$

for $t \in [0, 1]$, where $\text{median}(\mathcal{S})$ denotes the sample median of a set \mathcal{S} . It has a better performance than the CUSUM test under skewed and heavy-tailed distributions. Under the regularity conditions in [Dehling et al. \(2020\)](#), we have $H_n(\lfloor nt \rfloor) \xrightarrow{d} \sigma_H u(0)^{-1} \{\mathbb{B}(t) - t\mathbb{B}(1)\}$, where $u(x) = \int_{\mathbb{R}} f(y) f(x + y) dy$, $\sigma_H^2 = \sum_{k \in \mathbb{Z}} \text{Cov}\{F(X_0), F(X_k)\}$, f is the density of X_1 , and F is the distribution function of X_1 . Similarly, we can apply the Hodges–Lehmann statistic to test for multiple CPs. The test statistic is $T_n^{(H)} = T_n^{(H)}[\max, \text{mean}]$, whose limiting distribution is stated below. To our best knowledge, there is no existing self-normalized test that uses the Hodges–Lehmann statistic. It is included for detecting CP in heavy-tailed data and showing the generality of our proposed self-normalization framework.

Corollary 4.2 (Limiting distribution of $T_n^{(H)}$). *Under the RCs in Theorem 1 of [Dehling et al. \(2020\)](#) and H_0 , $T_n^{(H)} \xrightarrow{d} \mathbb{T}$.*

Example 4.3 (Influence functions for testing general parameters). Instead of testing changes in mean, one may be interested in other quantities, e.g., variances, quantiles and model parameters. Let $\theta_i = P(F_i^{(h)})$, where $h \in \mathbb{N}$, $P(\cdot)$ is a functional, and $F_i^{(h)}$ is the joint distribution function of $Y_i := (X_i, \dots, X_{i+h-1})^\top$ for $i = 1, \dots, n - h + 1$. For example,

for $h = 1$, $\mu_i = \int_{-\infty}^{\infty} x dF_i^{(1)}(x)$ and $\sigma_i^2 = \int_{\mathbb{R}} x^2 dF_i^{(1)}(x) - \{\int_{\mathbb{R}} x dF_i^{(1)}(x)\}^2$ are the marginal mean and variance at time i respectively. For $h = 2$, the lag-1 autocovariance at time i is $\gamma_i(1) = \int_{\mathbb{R}^2} (x_i - \mu_i)(x_{i-1} - \mu_{i-1}) dF_i^{(2)}(x_{i-1}, x_i)$. The hypotheses in (2.1) and (3.1) are redefined by replacing μ_i 's by θ_i 's. A possible global change detecting process is

$$G_n(\lfloor nt \rfloor) = \frac{\lfloor nt \rfloor (n - \lfloor nt \rfloor)}{n^{3/2}} \left(\widehat{\theta}_{1, \lfloor nt \rfloor} - \widehat{\theta}_{\lfloor nt \rfloor + 1, n} \right), \quad (4.3)$$

for $t \in [0, 1]$; see, e.g., Shao (2010), Shao and Zhang (2010) and Shao (2015). We remark that $\widehat{\theta}$ is allowed to be of dimension $q > 1$; see Example 4.5 for the construction of the corresponding global change detecting process. Clearly, if $\widehat{\theta}_{i,j} = (j - i + 1)^{-1} \sum_{t=i}^j X_t$, then $G_n(\cdot) = C_n(\cdot)$. So, (4.3) generalizes (2.3) from testing changes in μ_i 's to testing changes in θ_i 's. The final test statistic is $T_n^{(G)} := T_n^{(G)}[\max, \text{mean}]$.

The limiting distribution of (4.3) requires some standard regularity conditions in handling statistical functionals. Define the empirical distribution of Y_i 's based on the sample Y_s, \dots, Y_e by $\widehat{F}_{s,e}^{(h)} = (e - s + 1)^{-1} \sum_{i=s}^e \delta_{Y_i}$, where δ_y is a point mass at $y \in \mathbb{R}^h$. Assume that $\widehat{\theta}_{s,e} := P(\widehat{F}_{s,e}^{(h)})$ is asymptotically linear in the following sense, as $e - s \rightarrow \infty$:

$$P(\widehat{F}_{s,e}^{(h)}) = P(F^{(h)}) + (e - s + 1)^{-1} \sum_{i=s}^e \text{IF}(Y_i | P, F^{(h)}) + R_{s,e}, \quad (4.4)$$

where $R_{s,e}$ is a remainder term, $F^{(h)} = F_s^{(h)} = \dots = F_e^{(h)}$, and $\text{IF}(y | P, F^h) = \lim_{\epsilon \rightarrow 0} \{P((1 - \epsilon)F^h + \epsilon \delta_y) - P(F^h)\} / \epsilon$ is the influence function; see Section 2.3 of Wasserman (2006). The asymptotic linear representation (4.4) is known as a nonparametric delta method.

Corollary 4.3 (Limiting distribution of $T_n^{(G)}$). *Under H_0 , $I_n(\lfloor nt \rfloor) := n^{-1/2} \sum_{i=1}^{\lfloor nt \rfloor} \text{IF}(Y_i | P, F^{(h)})$ for $t \in [0, 1]$ and $h \in \mathbb{N}$, where $F^{(h)} = F_1^{(h)} = \dots = F_{n-h+1}^{(h)}$. Suppose that (i) $\mathbb{E}\{\text{IF}(Y_i | P, F^h)\} = 0$ for all i , (ii) $\{I_n(t) : t \in [0, 1]\} \Rightarrow \{\sigma_G \mathbb{B}(t) : t \in [0, 1]\}$ for some $0 < \sigma_G < \infty$, and (iii) $\sup_{k=1, \dots, n-1} |R_{1:k}| + |R_{(k+1):n}| = o_p(n^{-1/2})$. Then $T_n^{(G)} \xrightarrow{d} \mathbb{T}$.*

Example 4.4 (Long-range dependent time series). Long-range dependence (LRD) is widely used for modeling time series data in, e.g., earth sciences, econometrics and traffic systems;

see [Palma \(2007\)](#) for a review. The time series is of LRD if the autocovariances satisfy

$$\gamma(k) \sim |k|^{-D}\phi(k), \quad (4.5)$$

as $k \rightarrow \infty$, where $D \in (0, 1)$ is the LRD parameter, $\phi(\cdot)$ is a slowly varying function at infinity; see, e.g., [Pipiras and Taqqu \(2017\)](#). In this section, we discuss two possible change detecting processes for handling LRD.

First, the global CUSUM process (2.3) with suitable normalization converges under the LRD setting. Specifically, by Theorem 5.1 in [Taqqu \(1975\)](#), the scaled CUSUM process satisfies

$$C_n^*(\lfloor nt \rfloor) := (\sqrt{n}/d_n)C_n(\lfloor nt \rfloor) \xrightarrow{d} \sigma_{C^*} \{\mathbb{B}_H(t) - t\mathbb{B}_H(1)\},$$

where $d_n^2 \sim 2n^{2-D}\phi(n)/\{(1-D)(2-D)\}$, σ_{C^*} is a positive constant and $\mathbb{B}_H(\cdot)$ is a standard fractional Brownian motion with a Hurst parameter $H = 1 - D/2$. Therefore, $C_n^*(\cdot)$ can be used in our framework and the resulting test statistic is $T_n^{(C^*)} = T_n^{(C^*)}[\max, \text{mean}]$. Second, since the Wilcoxon statistic is a partial sum of ranks, the invariance principle still holds under suitable normalization and some regularity conditions. By Theorem 2 in [Dehling et al. \(2013\)](#),

$$W_n^*(\lfloor nt \rfloor) := (\sqrt{n}/d_n)W_n(\lfloor nt \rfloor) \xrightarrow{d} (2\sqrt{\pi})^{-1} \{\mathbb{B}_H(t) - t\mathbb{B}_H(1)\}.$$

The resulting test statistic is $T_n^{(W^*)} := T_n^{(W^*)}[\max, \text{mean}]$. Note that users do not need to specify the unknown sequence d_n since it is cancelled out by our SN. Thus, $T_n^{(C^*)} = T_n^{(C)}$ and $T_n^{(W^*)} = T_n^{(W)}$. However, by Corollary 4.4 below, the limiting distribution is a function of a fractional Brownian motion instead of a Brownian motion. Note that [Shao \(2011\)](#) and [Betken \(2016\)](#) proposed global self-normalized test for the AMOC problem under long-range dependent time series. Our approach contributes by further extending it to the multiple-CP testing.

Corollary 4.4 (Limiting distribution of $T_n^{(C^*)}$ and $T_n^{(W^*)}$). *Let $X_i = \mu_i + h(U_i)$, where $\{U_i\}$ is a stationary zero-mean standard Gaussian process and its autocovariances satisfy (4.5), and h is a measurable strictly monotone function such that $\mathbb{E}\{h(U_i)\} = 0$. Under*

H_0 , we have $T_n^{(C^*)} \xrightarrow{d} \mathbb{T}_H$ and $T_n^{(W^*)} \xrightarrow{d} \mathbb{T}_H$, where

$$\mathbb{T}_H := (1 - 2\epsilon)^{-1} \int_{\epsilon}^{1-\epsilon} \sup_{\delta > \epsilon} \frac{\mathbb{L}_H(t | t - \delta, t + \delta)^2}{\mathbb{V}_H(t | t - \delta, t + \delta)} dt,$$

for any $0 < \epsilon < 1/2$, where \mathbb{L}_H is defined as \mathbb{L} in (3.9) but with $\mathbb{B}(\cdot)$ being replaced by $\mathbb{B}_H(\cdot)$; and \mathbb{V}_H is defined as \mathbb{V} in (3.9) but with $\mathbb{L}(\cdot | \cdot, \cdot)$ being replaced by $\mathbb{L}_H(\cdot | \cdot, \cdot)$.

In practice, the unknown parameter H can be consistently estimated through regression in the spectral domain (Palma, 2007) by, e.g., the local Whittle method (Künsch, 1987). Shao and Wu (2007) showed the consistency of the local Whittle estimator.

Example 4.5 (Multi-dimensional parameter). Our approach extends to the multivariate case naturally. Let $\{\mathbf{Q}_n(\lfloor nt \rfloor)\}_{0 \leq t \leq 1}$ be a q -dimensional CP detecting process under the AMOC problem, where $q \in \mathbb{N}$. For example for testing changes in q -dimensional parameter Θ , we can use a multivariate version of (4.3):

$$\mathbf{Q}_n(\lfloor nt \rfloor) = \frac{\lfloor nt \rfloor (n - \lfloor nt \rfloor)}{n^{3/2}} \left(\widehat{\Theta}_{1, \lfloor nt \rfloor} - \widehat{\Theta}_{\lfloor nt \rfloor + 1, n} \right), \quad (4.6)$$

where $\widehat{\Theta}_{s,e}$ is the estimator for Θ using the subsample $\{X_s, \dots, X_e\}$. We define the corresponding LSN statistic as $T_n^{(Q)}(k | s, e) = L_n^{(Q)}(k | s, e)^T V_n^{(Q)}(k | s, e)^{-1} L_n^{(Q)}(k | s, e)$, where

$$L_n^{(Q)}(k | s, e) = \left(\frac{n}{e - s + 1} \right)^{1/2} \left[\mathbf{Q}_n(k) - \mathbf{Q}_n(s - 1) - \frac{k - s + 1}{e - s + 1} \{ \mathbf{Q}_n(e) - \mathbf{Q}_n(s - 1) \} \right],$$

$$V_n^{(Q)}(k | s, e) = \frac{k - s + 1}{(e - s + 1)^2} \sum_{j=s}^k L_n^{(Q)}(j | s, k)^{\otimes 2} + \frac{e - k}{(e - s + 1)^2} \sum_{j=k+1}^e L_n^{(Q)}(j | k + 1, e)^{\otimes 2},$$

and $A^{\otimes 2} = AA^T$ for any matrix A . Aggregating $T_n^{(Q)}(k | s, e)$ as in (3.5) and (3.6), we obtain the test statistic $T_n^{(Q)} := T_n^{(Q)}[\max, \text{mean}]$. Its limiting distribution is stated as follows.

Corollary 4.5 (Limiting distribution of $T_n^{(Q)}$). *Assume $\{\mathbf{Q}_n(\lfloor nt \rfloor) : t \in [0, 1]\} \Rightarrow \{\Sigma_Q^{1/2} \{\mathbb{B}^{(q)}(t) - t\mathbb{B}^{(q)}(1)\} : t \in [0, 1]\}$ for some unknown positive definite matrix $\Sigma_Q^{1/2} \in \mathbb{R}^{q \times q}$, and $\mathbb{B}^{(q)}(\cdot)$*

is q -dimensional standard Brownian motion. Under H_0 , we have $\mathbb{T}_n^{(Q)} \xrightarrow{d} \mathbb{T}^{(q)}$ for any $0 < \epsilon < 1/2$, where

$$\mathbb{T}^{(q)} := (1 - 2\epsilon)^{-1} \int_{\epsilon}^{1-\epsilon} \sup_{\delta > \epsilon} \mathbb{L}^{(q)}(t | t - \delta, t + \delta)^T \mathbb{V}^{(q)}(t | t - \delta, t + \delta)^{-1} \mathbb{L}^{(q)}(t | t - \delta, t + \delta) dt,$$

where $\mathbb{L}^{(q)}$ is defined as \mathbb{L} in (3.9) but with $\mathbb{B}(\cdot)$ being replaced by $\mathbb{B}^{(q)}(\cdot)$; and $\mathbb{V}^{(q)}$ is defined as \mathbb{V} in (3.9) but with $\mathbb{L}(\cdot | \cdot, \cdot)^2$ being replaced by $\mathbb{L}^{(q)}(\cdot | \cdot, \cdot)^{\otimes 2}$.

Shao and Zhang (2010) proposed a general AMOC self-normalized change point test for the mean of multivariate time series. Our approach localizes their proposed CP detecting process and self normalizer for multiple-CP detection. Note that their proposed SN requires repeated calculation of the quantities of interest for each subsample while our SN reuses the global change detecting process which allows faster computation.

Remark 4.1. If the dimension q increases with respect to the sample size n , then the proposed self normalizer $V_n^{(Q)}(\cdot)$ may not be invertible. To overcome the issue, Zhang *et al.* (2022+) and Wang *et al.* (2022) proposed univariate change detecting processes based on U-statistic for testing existence of CPs in the mean of high dimensional independent data. Wang *et al.* (2022) further integrated their proposal into Zhang and Lavitas (2018)'s framework and the test was shown to preserve power in the multiple-CP setting. By applying their proposal into our framework, the non-invertible issue can be avoided. Note that Wang *et al.* (2022) proposed a change detecting process that converges to a function of a centered Gaussian process. Thus, their test statistic is asymptotically pivotal. The critical values can be found through Monte Carlo simulation. The performance of the test is left for further investigation.

5 Discussion and Implementation

5.1 Comparison with existing methods

Shao and Zhang (2010) extended the self-normalized one-CP test (2.4) to a “supervised”

multiple-CP test tailored for testing m CPs, where m is pre-specified. The test statistic is

$$S_n^{(m)} = \sup_{(k_1, \dots, k_m) \in \Omega_n^{(m)}(\epsilon)} \sum_{j=1}^m T_n^{(C)}(k_1 | k_{j-1}, k_{j+1}), \quad (5.1)$$

where $1 = k_0 < k_1 < \dots < k_m < k_{m+1} = n$, and

$$\Omega_n^{(m)}(\epsilon) = \{k_1, \dots, k_m : \forall j \in \{1, \dots, m\}, \lfloor \epsilon n \rfloor \leq \min(k_j - k_{j-1}, k_{j+1} - k_j)\}.$$

The trimmed region $\Omega_n^{(m)}(\epsilon)$ prevents computing estimates by too few observations. [Zhang and Lavitas \(2018\)](#) later proposed a “unsupervised” self-normalized multiple-CP test which does not require specifying m and defined as,

$$Z_n = \sup_{(k_1, k_2) \in \Omega_n^{(2)}(\epsilon)} T_n^{(C)}(k_1 | 1, k_2) + \sup_{(k_1, k_2) \in \Omega_n^{(2)}(\epsilon)} T_n^{(C)}(k_2 | k_1, n). \quad (5.2)$$

Although both $S_n^{(m)}$, Z_n and $T_n^{(C)}$ use the LSN CUSUM statistics, i.e., $T_n^{(C)}(k | s, e)$ defined in (3.4), as building blocks, they have different restrictions on the local windows and aggregate the LSN statistics in different ways.

[Shao and Zhang \(2010\)](#)’s test statistic is the maximum of sum of LSN statistics calculated on m local windows with target time points k_1, \dots, k_m , i.e., $[1, k_2], \dots, [k_{m-1}, n]$. This approach is also used by [Antoch and Jarušková \(2013\)](#) for constructing a non-self-normalized multiple-CP test. It has a strict control on the m local windows since the boundaries of a window relate to previous and next windows. If the number of CPs M is misspecified, some of the windows may not contain only one CP. If $m < M$, the self normalizers are not robust to the changes. If $m > M$, some degree of freedom is wasted to detect CPs that do not exist. Both two cases may lead to a huge loss in power.

[Zhang and Lavitas \(2018\)](#)’s approach sets the left end of the window to be 1 in the forward scan, and the right end to be n in the backward scan. So, their approach tends to scan for the first CP $k_1 \in [1, e]$, and the last CP $k_M \in [s, n]$ for some e, s ; see Section 6.4. In contrast, our approach scans for all possible CPs. We also allow the windows to start and end at any times instead of restricting them to start at time 1 or end at time n .

Besides, [Jiang *et al.* \(2022+\)](#) recently considered a self-normalized CP estimation problem for a quantile regression model, while we consider a general CP testing problem. Since we solve different inference problems, the results are not directly comparable. So, we only compare the self normalizers in these two approaches. First, their self normalizer is specifically designed for quantile regression model, but ours is built on a general framework, which supports any global change detecting process; see Section 4. One of our major contributions is to extend any one-CP test to multiple-CP self normalized test. Second, computing their self normalizer requires fitting the quantile regression model $O(n^2)$ times on all possible local subsamples. In contrast, our self normalizer is a function of a global change detecting process, which can be computed by fitting the models on $O(n)$ local subsamples. It significantly reduces computational burden. Although we focus on different problems, our proposed test statistic can be integrated into the first step of their algorithm. The fused algorithm has a potential of further enhancing generality and computational flexibility. We leave it for further study.

Computational efficiency is usually a major concern in constructing multiple-CP tests. Table 5.1 and Figure 5.1(a) present the average computational times for the test statistics KS_n , $\text{S}_n^{(1)}$, $\text{S}_n^{(m)}$, Z_n , $\text{T}_n^{(C)}$, $\text{T}_n^{(W)}$ and $\text{T}_n^{(H)}$. The computational cost of KS_n and $\text{S}_n^{(1)}$ is the least since they are tailor-made for the AMOC problem and have the simplest forms. Moreover, the computational cost of $\text{S}_n^{(m)}$ is scaled exponentially with m . Among the self-normalized multiple-CP tests, $\text{S}_n^{(2)}$, Z_n , $\text{T}_n^{(C)}$ and $\text{T}_n^{(W)}$ have the same computational complexity. Moreover, our framework allows fast recursive computation. It further reduces the computational time of $\text{T}_n^{(C)}$ and $\text{T}_n^{(W)}$; see Section F in the appendix. The higher time cost required by $\text{T}_n^{(H)}$ is solely due to higher time cost of computing the global Hodges–Lehmann change detecting statistic (4.2). Figure 5.1(b) shows that the computational cost of using nonsymmetric window in $\tilde{\text{T}}_n^{(C)}$ is significantly larger than that of $\text{T}_n^{(C)}$ because of the larger feasible set in computing the score function (3.10). However, the gain in power is insignificant; see Section 6.4. The incremental power improvement does not justify the huge additional time cost. Therefore, using symmetric windows is recommended.

Table 5.1: Comparisons among different CP tests in terms of (a) finite-sample size accuracy with respect to the nominal type-I error rate; (b) powerfulness under different actual numbers of CP M ; (c) time complexity of computing the test statistics based on a sample of size n ; (d) robustness against outliers; and (e) requirements of computing a LRV estimate $\hat{\sigma}_n^2$ and specifying a target number of CPs m . The comparisons in (a) and (b) are based on our simulation results in Section 6 and the appendix.

		(a) size accuracy		(b) powerfulness		(c) time complexity	(d) robustness	(e) requirement	
				$M = 1$	$M > 1$			$\hat{\sigma}_n^2$	m
KS_n	low	high	low			$O(n)$	low	yes	no
$S_n^{(1)}$	high	high	low			$O(n)$	low	no	yes
$S_n^{(m)}$	medium	medium	depends on m			$O(n^m)$	low	no	yes
Z_n	medium	medium	medium			$O(n^2)$	low	no	no
$T_n^{(C)}$	high	high	high			$O(n^2)$	low	no	no
$T_n^{(W)}$	high	high	high			$O(n^2)$	high	no	no
$T_n^{(H)}$	high	high	high			$O(n^3 \log n)$	high	no	no

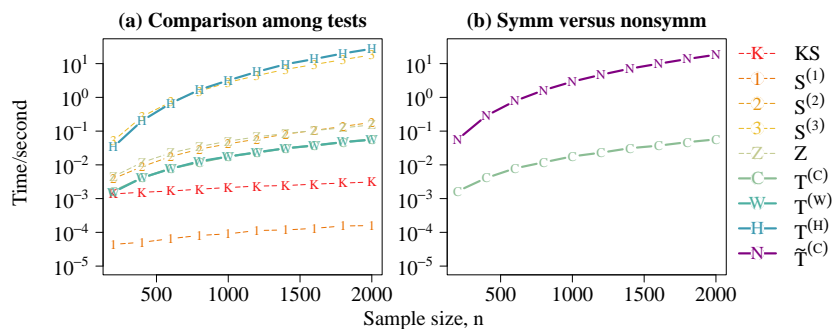


Figure 5.1: Average computation times of (a) test statistics considered (including KS_n , $S_n^{(1)}$, $S_n^{(2)}$, $S_n^{(3)}$, Z , $T_n^{(C)}$, $T_n^{(W)}$, $T_n^{(H)}$) and (b) proposed CUSUM test using symmetric windows (symm) $T_n^{(C)}$ versus nonsymmetric windows (nonsymm) $\tilde{T}_n^{(C)}$. All experiments are performed in R 4.1.0 on Intel Core i9-10900 CPU @ 2.8 GHz, and 64-bit operating system.

5.2 Finite- n adjusted critical values

In the time series context, the accuracy of the invariance principle (i.e., Assumption 2.1) may deteriorate when the sample size is small (Kiefer and Vogelsang, 2005). Therefore, the asymptotic theory in, e.g., Theorem 3.1, may not kick in. It may lead to severe size distortion. To mitigate this problem, finite-sample adjusted critical values can be used. We propose to compute a critical value $c_\alpha(n, \rho)$ by matching the autocorrelation function (ACF) at lag one ρ and n for different specified level of significance $\alpha \in (0, 1)$. The values of $c_\alpha(n, \rho)$ are tabulated in Section D of the appendix for $\alpha \in \{0.01, 0.05, 0.1\}$, $n \in \{100, 200, \dots, 1000, 2000, 3000, \dots, 10000\}$, and $\rho \in \{0, \pm 0.1, \dots, \pm 0.9\}$. The testing procedure is outlined as follows.

1. Compute the sample lag-1 ACF $\hat{\rho}$ of $\{X_{i+\lfloor n^{1/3} \rfloor} - X_i\}_{i=1}^{n-\lfloor n^{1/3} \rfloor}$.
2. Obtain the critical value $c_\alpha(n, \hat{\rho})$. Use interpolation if necessary.
3. Reject the null if $T_n^{(\aleph)} > c_\alpha(n, \hat{\rho})$, where $\aleph \in \{C, W, H, G\}$.

The limiting critical value is approximated by using finite- n critical value with $n = 10000$. Since $\hat{\rho}$ relies on the differenced data with a suitable lag, the change points (if any) have negligible effect on $\hat{\rho}$. The consistency of $\hat{\rho}$ is developed on the following framework. Let $X_i = \mu_i + Z_i$, where μ_i 's are deterministic and Z_i 's are zero-mean stationary noises. Define $Z_i = g(\dots, \varepsilon_{i-1}, \varepsilon_i)$, where ε_i 's are independent and identical (IID) random variables and g is some measurable function. Let ε'_i be IID copy of ε_i and $Z'_i = g(\dots, \varepsilon_{-1}, \varepsilon'_0, \varepsilon_1, \dots, \varepsilon_i)$. For $p > 1$ and $\|Z_i\|_p < \infty$, the physical dependence measure (Wu, 2011) is defined as $\lambda_p(i) = \|Z_i - Z'_i\|_p$, where $\|\cdot\|_p = (\mathbf{E}|\cdot|^p)^{1/p}$. Theorem 5.1 below states that $\hat{\rho}$ is a consistent estimator of $\rho := \gamma(1)/\gamma(0)$ even there exist a large number (M) of CPs, where $\gamma(k) = \mathbf{E}(Z_1 Z_{1+k})$.

Theorem 5.1. *Assume $\mathbf{E}(Z_1^4) < \infty$ and $\sum_{i=1}^{\infty} \lambda_4(i) < \infty$. Define $|\Delta_*| = \sup_{1 \leq j \leq M} |\Delta_j|$. Let $b = b_n$ be an \mathbb{N} -valued sequence. If $b/n + 1/b + (bM/n)\Delta_*^2 \rightarrow 0$ as $n \rightarrow \infty$, then $\hat{\rho} \xrightarrow{\text{pr}} \rho$.*

In particular, if $b = \lfloor n^{1/3} \rfloor$ and $|\Delta_*| < \infty$, then Theorem 5.1 guarantees that $\hat{\rho}$ is consistent for ρ provided that the actual number of CPs satisfies $M = o(n^{2/3})$. This testing procedure does not assume any parametric structure as we only intend to match the sample ACF at lag one. Although it is possible to further match ACF at a higher lag, the proposal is to balance the accuracy and the computational cost. Simulation result shows that the tests have accurate size under the above critical value adjustment procedure. We emphasize that this adjustment only affects the finite-sample performance because the critical value $c_\alpha(n, \rho)$ is a constant as a function of ρ when $n \rightarrow \infty$.

6 Simulation experiments

6.1 Setting and overview

Throughout Section 6, the experiments are designed as follows. The time series is generated from a signal-plus-noise model: $X_i = \mu_i + Z_i$. The values of μ_i 's will be specified in Sections 6.2 and 6.3. The zero-mean noises Z_i 's are simulated from a stationary bilinear autoregressive (BAR) model: $Z_i = (\varpi + \vartheta \varepsilon_i)Z_{i-1} + \varepsilon_i$ for $i = 1, \dots, n$, where ε_i 's are independent standard normal random variables, and $\varpi, \vartheta \in \mathbb{R}$ such that $\varpi^2 + \vartheta^2 < 1$. Similar conclusions are obtained under other noise models, including autoregressive-moving-average model, threshold AR model, and absolute value nonlinear AR model. Due to space constraint, their results are deferred to the appendix. The critical value is chosen according to the adjustment procedure described in Section 5.2.

6.2 Size and power

In this subsection, we examine the size and power of different CP tests when there exist various numbers of CPs. Following the suggestion of Huang *et al.* (2015) and Zhang and Lavitas (2018), we choose $\epsilon = 0.1$ in $S_n^{(2)}$, $S_n^{(3)}$, Z_n and our proposals in order to have a fair comparison. Suppose that the CPs are evenly spaced and the mean change directions are alternating (increasing or decreasing):

$$\mu_i = \Delta \sum_{j=1}^M (-1)^{j+1} \mathbb{1}_{\{i/n > j/(M+1)\}}, \quad (6.1)$$

where $M \in \{1, \dots, 6\}$ denotes the number of CPs, and $\Delta \in \mathbb{R}$ controls the magnitude of the mean changes. Clearly, $\mu_i \equiv 0$ under H_0 .

All tests are computed at nominal size $\alpha = 5\%$. The null rejection rates $\hat{\alpha}$, for sample sizes $n \in \{200, 400\}$, are presented in Table 6.1. To summarize the result, we further report the sample root mean squared error (RMSE) of $\hat{\alpha}$ over all cases of ϑ and ϖ for each test and each n . The self-normalized tests generally have more accurate size than the non-self-normalized test KS_n . The finding agrees with Shao (2015). The self-normalized approach

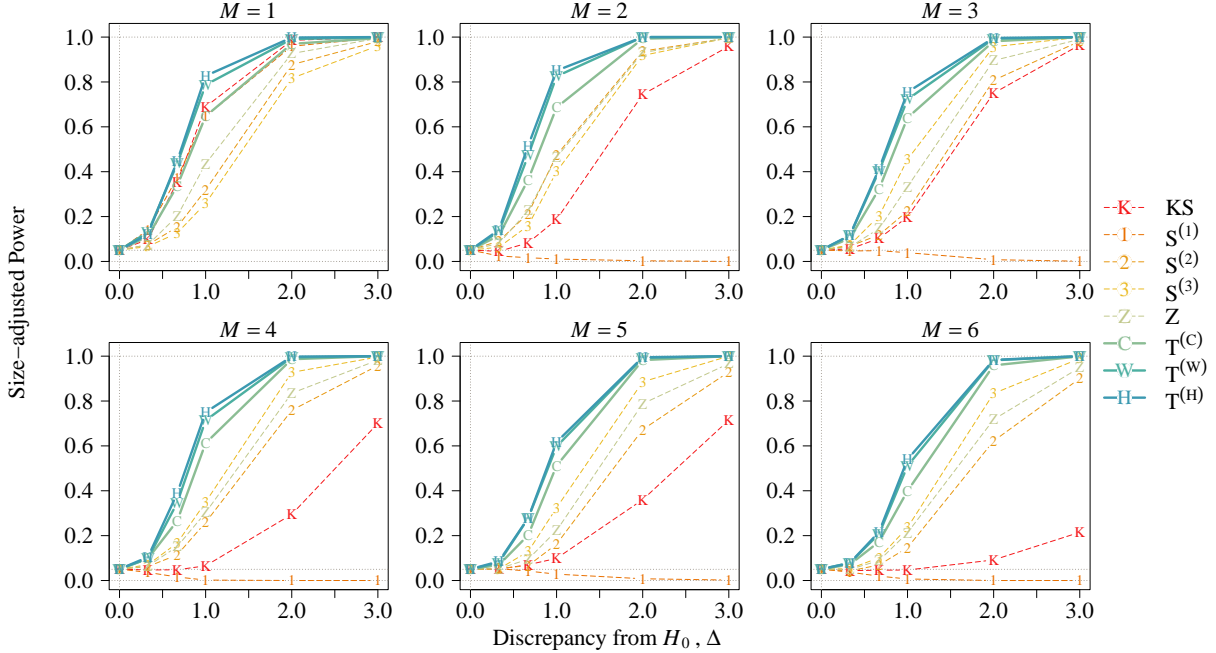


Figure 6.1: Size-adjusted power under BAR model with $\varpi = \vartheta = 0.5$, $n = 200$ and mean function (6.1).

is a special case of the fixed bandwidth approach with the largest possible bandwidth and thus achieves the smallest size distortion according to Kiefer and Vogelsang (2002). In comparison among the self-normalized tests, $T_n^{(W)}$ and $T_n^{(H)}$ control the size most accurately. In particular, our proposed tests have the least severe under-size problem, which is observed in the existing self-normalized tests (i.e., $S_n^{(1)}$, $S_n^{(2)}$, $S_n^{(3)}$, and Z_n) when $\varpi < 0$. Moreover, Shao and Zhang (2010)'s proposal $S_n^{(m)}$ suffers from an increasing size distortion as m increases. This finding is in line with Zhang and Lavitas (2018). The outperformance of $T_n^{(W)}$ and $T_n^{(H)}$ over $T_n^{(C)}$ can be attributed to the outlier robustness achieved by rank and order statistics. This advantage is particularly obvious in bilinear time series as this model is well known to produce sudden high amplitude oscillations to mimic structures in, e.g., explosion and earthquake data in seismology; see Section 5.2 of Rao and Gabr (1984). However, in the more standard ARMA models, $T_n^{(C)}$ performs as well as $T_n^{(W)}$ and $T_n^{(H)}$; see the appendix for the detailed results.

The power curve against Δ is computed at 5% nominal size by using 2^{10} replications with $n = 200$. Figure 6.1 shows the size-adjusted power when $\varpi = \vartheta = 0.5$. The (unadjusted)

Table 6.1: Null rejection rates $\hat{\alpha}$ at nominal size $\alpha = 5\%$ under BAR model and mean function (6.1). The sample RMSE of $\hat{\alpha}$ over all cases of ϑ and ϖ is computed for each test and each n . The values of $\hat{\alpha}$ and RMSE are expressed in percentage. The smaller the RMSE, the better is the test in controlling the type-I error.

ϑ	ϖ	$n = 200$								$n = 400$							
		KS $_n$	S $_n^{(1)}$	S $_n^{(2)}$	S $_n^{(3)}$	Z $_n$	T $_n^{(C)}$	T $_n^{(W)}$	T $_n^{(H)}$	KS $_n$	S $_n^{(1)}$	S $_n^{(2)}$	S $_n^{(3)}$	Z $_n$	T $_n^{(C)}$	T $_n^{(W)}$	T $_n^{(H)}$
0.8	0.5	14.4	7.5	9.6	5.3	7.6	1.1	4.0	3.4	11.3	5.3	5.3	3.1	5.4	0.8	3.8	3.3
	0.3	13.5	5.6	5.8	3.1	5.1	1.2	4.5	3.4	10.7	4.9	4.5	2.7	4.5	1.3	4.0	3.4
	0	15.4	4.7	2.8	1.3	2.4	2.3	5.6	4.6	10.6	4.8	3.7	1.9	3.0	2.1	4.1	3.7
	-0.3	23.9	4.6	1.7	0.4	1.5	2.1	7.8	6.3	15.6	3.9	2.1	0.8	1.9	2.1	5.6	5.0
	-0.5	31.2	3.9	1.6	0.4	1.2	2.0	7.7	7.1	25.6	4.5	1.4	0.3	1.4	1.4	6.4	6.3
0.5	0.8	31.8	11.9	26.1	27.2	27.1	3.6	11.0	9.0	31.8	8.0	14.9	12.8	14.3	2.2	5.7	3.6
	0.5	13.7	6.5	9.5	8.8	8.1	2.1	4.5	3.9	10.0	6.0	6.6	6.1	6.4	2.1	3.9	3.5
	0.3	11.0	5.1	5.5	4.9	5.6	3.0	5.0	4.6	7.6	4.8	5.7	4.1	5.2	2.7	4.5	4.1
	0	9.4	3.9	3.8	2.0	2.7	3.8	6.5	6.1	6.6	4.8	4.1	3.1	3.8	3.2	4.3	4.4
	-0.3	17.9	3.5	1.7	0.4	1.5	4.3	6.3	5.9	10.0	4.2	3.2	1.8	2.5	3.1	5.3	4.8
	-0.5	29.8	3.1	1.0	0.0	0.8	4.1	7.2	6.0	19.8	3.9	2.7	1.5	2.0	3.3	6.0	6.0
	-0.8	44.1	2.6	0.2	0.0	0.1	4.3	8.7	7.3	37.3	2.9	0.9	0.1	0.4	3.2	6.9	6.5
-0.5	0.8	29.8	10.1	24.0	27.7	24.8	2.8	11.4	8.5	29.3	8.2	11.9	9.6	12.4	1.6	4.9	3.6
	0.5	12.2	5.6	8.6	7.1	9.0	1.7	3.4	2.6	10.0	5.1	5.4	4.4	5.9	2.3	4.0	3.4
	0.3	9.3	4.9	6.3	3.6	5.8	2.4	3.7	3.4	7.4	4.3	5.3	3.7	4.6	3.2	4.1	3.6
	0	9.1	5.1	3.4	2.1	3.0	3.6	4.7	4.3	6.4	4.8	4.4	3.2	4.0	3.3	5.8	5.3
	-0.3	15.8	3.9	1.6	1.0	1.8	3.1	6.1	5.2	10.1	4.6	3.7	2.0	3.0	3.8	5.3	5.0
	-0.5	27.9	3.6	1.0	0.6	1.1	4.3	6.2	6.0	19.5	4.4	3.1	1.6	3.0	4.3	5.4	5.1
	-0.8	44.0	1.8	0.7	0.0	0.3	4.7	6.3	6.3	38.7	3.5	1.0	0.2	0.9	3.1	6.1	5.6
-0.8	0.5	13.6	7.4	7.4	4.5	6.3	0.8	3.1	2.5	11.0	6.2	4.5	2.8	3.9	1.1	3.2	2.5
	0.3	13.2	5.9	4.6	2.3	3.6	1.0	3.2	2.7	9.1	5.7	3.3	2.1	2.7	1.9	4.2	3.4
	0	14.4	5.1	2.6	1.1	2.4	1.3	4.1	3.2	11.2	4.5	3.6	1.6	3.1	2.4	5.8	5.1
	-0.3	21.1	5.4	1.9	0.5	1.3	1.6	6.3	4.7	17.9	4.9	2.4	1.0	1.8	2.7	6.8	5.5
	-0.5	31.4	5.2	1.3	0.2	1.3	1.9	8.3	7.0	28.2	5.6	1.9	0.5	1.4	2.1	6.0	5.2
	RMSE	18.9	2.2	6.5	7.4	6.8	2.7	2.5	1.8	15.1	1.2	3.2	3.6	3.3	2.7	1.0	1.2

power are presented in appendix. We also repeat the experiments with different values of ϖ and ϑ . The results are similar, thus, they are deferred to the appendix. In general, $T_n^{(W)}$ and $T_n^{(H)}$ have the highest power for all the cases. Their outperformance in power over $T_n^{(C)}$ is again attributed to the robustness against outliers. If only CUSUM-type tests are considered, the non-self-normalized test KS_n performs better than self-normalized tests when $M = 1$, however, it seriously under-performs when $M > 1$ as KS_n is tailor-made for the one-CP alternative (2.2). Although $S_n^{(1)}$ has the highest power among the self-normalized CUSUM tests when $M = 1$, it suffers from the notorious non-monotonic power issue (with respect to Δ) when $M > 1$. It is because its SN is not robust to the multiple CPs. Thus, $S_n^{(1)}$ is no longer a consistent test when $M > 1$.

It is surprising that our proposal $T_n^{(C)}$ outperforms [Shao and Zhang \(2010\)](#)'s test $S_n^{(m)}$ even when the number of CPs is well-specified, i.e., $M = m$. The message behind this observation is that knowing the true number of CP does not give advantage because one can identify a structural change by observing the data around it without looking at the whole segmented series. It, indeed, partially motivates our localized framework. Moreover, as we discussed in [Section 5.1](#), $S_n^{(m)}$ defines the local windows restrictively. It accumulates errors if the boundaries of the local windows are off from the actual CPs. It is also interesting to see that, compared with $S_n^{(1)}$, the tests $S_n^{(2)}$ and $S_n^{(3)}$ are less sensitive to misspecification of M although they are still less powerful than our proposals.

6.3 Ability to capture effects of all changes

This subsection investigates why our proposed tests have a higher power in a broader CP structures than the existing unsupervised multiple-CP test Z_n . Consider the 3-CP setting with the magnitudes of changes at the first and the last CPs are only half of the second CP. Specifically, we consider two mean functions:

- (Case 1) equal magnitude: $\mu_i = \Delta \{ \mathbb{1}_{\{i > \lfloor n/4 \rfloor\}} - \mathbb{1}_{\{i > \lfloor 2n/4 \rfloor\}} + \mathbb{1}_{\{i > \lfloor 3n/4 \rfloor\}} \}$; and
- (Case 2) unequal magnitude: $\mu_i = \Delta \{ \frac{1}{2} \cdot \mathbb{1}_{\{i > \lfloor n/4 \rfloor\}} - \mathbb{1}_{\{i > \lfloor 2n/4 \rfloor\}} + \frac{1}{2} \cdot \mathbb{1}_{\{i > \lfloor 3n/4 \rfloor\}} \}$.

[Figure 6.2](#) shows the result when $\varpi = \vartheta = 0.5$. The result under other time series models is provided in the appendix. Compared to Case 1, Z_n and $S_n^{(2)}$ lose roughly half of the power in Case 2. In contrast, the power of our tests only reduces by 1/3 when $\Delta \leq 1$ while remains about the same when $\Delta \geq 2$. Therefore, our tests are more powerful and are more robust to mean change structures than Z_n . It is because our proposals are able to capture all change structures whereas Z_n only takes the first and the last CPs into account; see [\(5.2\)](#).

6.4 Tradeoff of using symmetric windows

To balance computational cost and power, we propose to use symmetric windows when constructing the LSN statistic; see [Remark 3.2](#). Intuitively, changes can still be detected

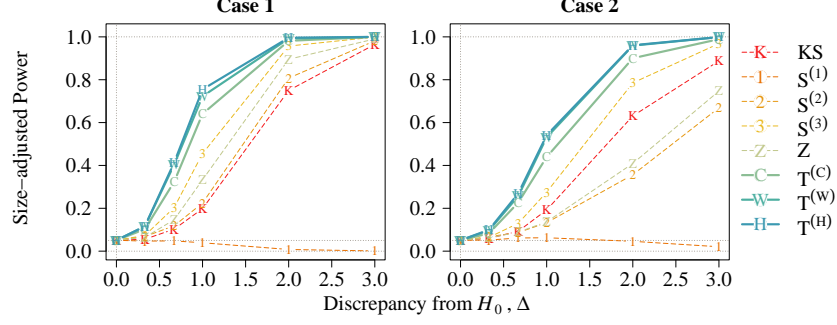


Figure 6.2: Size-adjusted power under BAR model with $\varpi = \vartheta = 0.5$, $n = 200$ and mean functions in Cases 1 and 2.

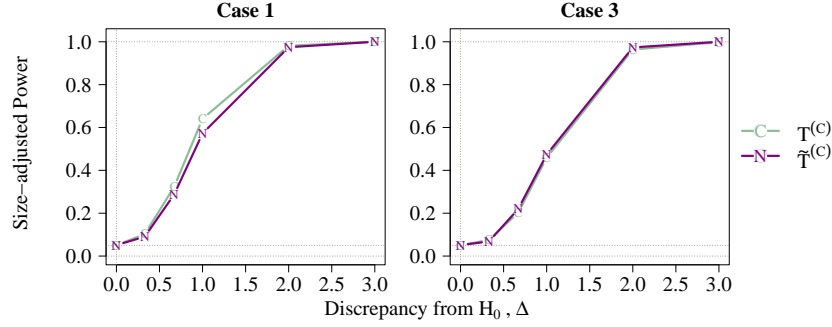


Figure 6.3: Size-adjusted power under BAR model with $\varpi = \vartheta = 0.5$, $n = 200$ and mean functions in Cases 1 and 3.

by the contrast between samples of the same size. In this subsection, we study the power loss of $T_n^{(C)}$ due to the use of symmetric windows. We consider three-CP alternative with changes even and unevenly spaced in order to compare $T_n^{(C)}$ and $\tilde{T}_n^{(C)}$. Specifically, let the mean function with changes evenly spaced be Case 1 defined in Section 6.3, while the unevenly spaced CP model is defined as

- (Case 3) unevenly spaced CPs: $\mu_i = \Delta \{ \mathbb{1}_{\{i > [0.15n]\}} - \mathbb{1}_{\{i > [0.3n]\}} + \mathbb{1}_{\{i > [0.85n]\}} \}$.

Figure 6.3 presents the size-adjusted power of $T_n^{(C)}$ and $\tilde{T}_n^{(C)}$ when $\varpi = \vartheta = 0.5$. More simulation result is provided in the appendix. In both cases, $T_n^{(C)}$ performs similar to $\tilde{T}_n^{(C)}$. This indicates that using nonsymmetric windows does not bring significant advantage in power while it drastically increases computational burden; see Section 5.1. Therefore, we recommend symmetric windows to balance the power and the computational cost.

7 Real data analysis

7.1 NASDAQ call option volume

We perform CP analysis for the Bloomberg’s NASDAQ call option volume index (Bloomberg code: OPCVNQC index) from 24 March 2017 to 21 March 2022 ($n = 1259$). The data are retrieved from Bloomberg¹. Researchers and practitioners are interested in using the option volume to analyze the stock market. Pan and Poteshman (2006) investigated the market price adjustment and identified strong evidence of informed trading in the option market. Johnson and So (2012) found that option-to-stock-volume (O/S) ratio is significant in predicting the magnitude and sign of abnormal return resulting from earning surprises. It is consistent to the finding that the option volume reflects private information. Further divided the option volume into categories, Ge *et al.* (2016) founded that higher O/S ratio in general predicts lower stock return since more components of option volume negatively predict return.

Since the option volume is a significant factor of the market analysis, CP analysis on the constant mean option volume is thus of direct interest. The test statistics and p -values are presented in Table 7.1. Since the result of our proposed tests reveal strong evidence against the hypothesis that no CPs exist, we further conduct mean change point location estimation, defined in (3.11), of which the estimates are indicated by red vertical lines in Figure 7.1. Using the CUSUM process, the estimated CP dates are 27 November 2017, 30 January 2020, and 2 November 2020. The test using Wilcoxon statistics lead to similar results, while the test using Hodges–Lehmann statistics does not detect the first CP. The most dominant CP is the second CP at the end of January 2020. Studies have found a surge in trading activities worldwide and observed the trading from home effect (Chiah and Zhong, 2020; Ortmann *et al.*, 2020). Chiah and Zhong (2020) explained the sudden growth of trading activities could be attributed to some retail investors regarded the stock market as gambling substitute. The jump in trading volume may also result from changing growth expectation and reaction to the post COVID-19 stimulus policies from the investors

¹<https://www.bloomberg.com/professional/product/market-data/>

Table 7.1: Multiple-CP test on the mean of the NASDAQ Call Option Volume.

	KS_n	$S_n^{(1)}$	$S_n^{(2)}$	$S_n^{(3)}$	Z_n	$T_n^{(C)}$	$T_n^{(W)}$	$T_n^{(H)}$
Test statistic	25.24	460.06	467.18	25.03	910.33	44.94	52.67	31.46
p -value	$\leq 10^{-3}$	$\leq 10^{-3}$	$\leq 10^{-3}$	$\leq 10^{-3}$	$\leq 10^{-3}$	$\leq 10^{-3}$	$\leq 10^{-3}$	$\leq 10^{-3}$

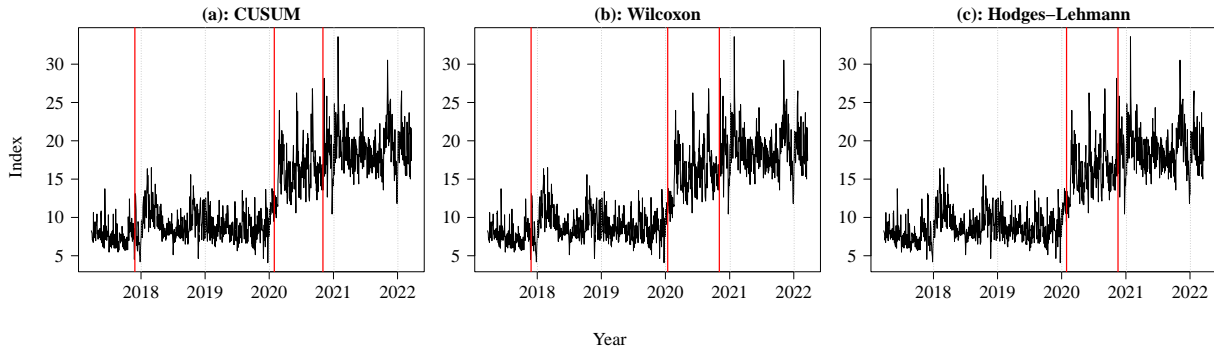


Figure 7.1: Estimated change point locations are indicated by red vertical lines by using (a) CUSUM process, (b) Wilcoxon statistics and (c) Hodges–Lehmann statistics. Data retrieved from Bloomberg

(Gormsen and Koijen, 2020).

7.2 Shanghai-Hong Kong Stock Connect turnover

We apply our proposed method to perform CP analysis for the Shanghai-Hong Kong Stock Connect Southbound Turnover index (Bloomberg code: AHXHT index) from 23 March 2017 to 22 March 2022 ($n = 1232$). The turnover index is based on the Hang Seng Stock Connect China AH (H) index which composites the most liquid shares eligible for the trading mechanism and listed in Hong Kong. The data are also retrieved from Bloomberg. The Stock Connect is a channel that allows both Mainland China and Hong Kong investors to access other stock markets mutually. The southbound is the direction for Shanghai investors to invest in Hong Kong stock market. Studies have shown that the Stock Connect improves mutual markets liquidity and capital market liberalization (Bai and Chow, 2017; Huo and Ahmed, 2017; Xu *et al.*, 2020). Recently, the effect of the Stock Connect on the market risk and volatility has caught attention. Ruan *et al.* (2018) found an increasing cross correlation between Shanghai and Hong Kong stock markets, suggesting higher risks after the implementation of the Stock Connect. Huo and Ahmed (2017) also studied that

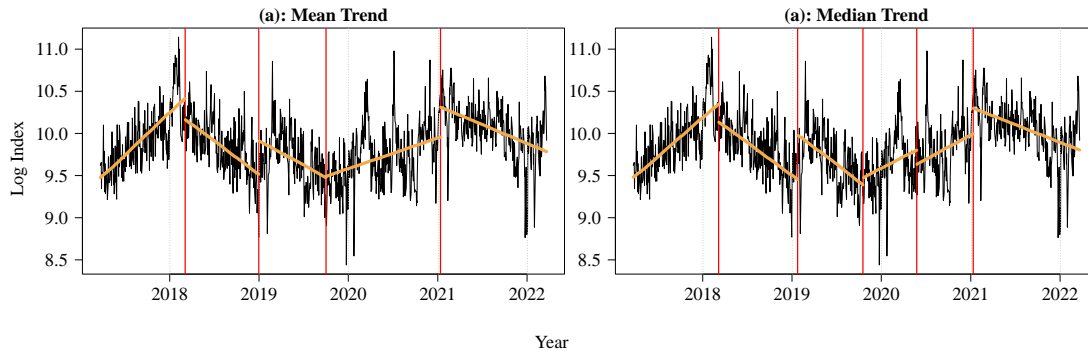


Figure 7.2: Estimated (a) mean trend and (b) median trend CPs are indicated by red vertical lines. The orange lines indicate the fitted regression lines within each region separated by the estimated CPs. Data are retrieved from Bloomberg.

the cointegration between the stock markets and concluded that volatility spillover effect is strengthened. The result from [Chan *et al.* \(2018\)](#) further supported that the Stock Connect turnover is significant to the market volatility. As an indicator of foreign investment, the Stock Connect turnover is important for market volatility modeling. Therefore, we study whether CP exists in the Stock Connect Southbound daily turnover.

We investigate whether changes in trend exist in the log daily turnovers. Under our framework, it suffices to define a global change detecting process. It is, therefore, straightforward for practitioners. We consider the global change detecting process defined in (4.3) with two possible choices of $\hat{\theta}_{1:k}$ and $\hat{\theta}_{k+1:n}$ specified below.

1. (Mean trend model) For each fixed $1 \leq k \leq n$, let $\mathbf{E}X_i = (\alpha_k^- + \beta_k^- \frac{i}{n}) \mathbb{1}_{\{i \leq k\}} + (\alpha_k^+ + \beta_k^+ \frac{i}{n}) \mathbb{1}_{\{i > k\}}$ for $i = 1, \dots, n$, where $\alpha_k^-, \beta_k^- \in \mathbb{R}$ are the intercept and slope of the mean trend at or before time k , respectively, whereas $\alpha_k^+, \beta_k^+ \in \mathbb{R}$ are corresponding values after time k . Then $\hat{\theta}_{1:k}$ and $\hat{\theta}_{k+1:n}$ are defined as the ordinary least-squares estimators of β_k^- and β_k^+ , respectively.
2. (Median trend model) For each fixed $1 \leq k \leq n$, let $\text{median}(X_i) = (\alpha_k^- + \beta_k^- \frac{i}{n}) \mathbb{1}_{\{i \leq k\}} + (\alpha_k^+ + \beta_k^+ \frac{i}{n}) \mathbb{1}_{\{i > k\}}$ for $i = 1, \dots, n$, where $\alpha_k^-, \beta_k^-, \alpha_k^+, \beta_k^+ \in \mathbb{R}$ are similarly interpreted as in the mean trend model. Then $\hat{\theta}_{1:k}$ and $\hat{\theta}_{k+1:n}$ are estimators of β_k^- and β_k^+ , respectively; see the modified Barrodale and Roberts algorithm ([Koenker and d'Orey, 1987](#)). The estimators are computed by the R package "quantreg".

The resulting test statistics are 47.46 and 40.64. Both p -values are less than 1%. The

trend change point location estimates are indicated by red vertical lines in Figure 7.2. The mean and median trend analysis agree on four estimated CPs, which are estimated on 7 March 2018, 24 January 2019, 2 October 2019 and 12 January 2021 under the median trend analysis. In same time, it further detects one CP on 25 May 2020. The first CP is likely to be the China-United States trade war. After the trade war began in January 2018, the Stock Connect turnover became downtrend. Until the COVID-19 events, an uptrend is detected after the end of 2019. Similar to the finding in the NASDAQ call option volume, the trading from home effect is observed. The uptrend stopped after the beginning of 2021.

8 Conclusion

Our proposed method improves existing CP tests and brings several advantages: (i) it has high power and controls size well, (ii) neither specification of number of CPs nor consistent estimation of nuisance parameters is required, (iii) change point location estimate can be naturally produced, (iv) general change detecting statistics, e.g., rank and order statistics, are allowed to enhance robustness (v) it is capable to test change in general parameter of interest other than mean; and (vi) both short-range and long-range dependence are supported. Table 5.1 summarizes the properties of the proposed tests. Besides, our proposal is driven by intuitive principles, so that as long as a one-change detecting statistic is provided, our proposal can generalize it to a multiple-change detecting statistic. We anticipate that our framework can be applied to non-time-series data, e.g., spatial data and spatial-temporal data, in future work.

A Proofs of theorems

Proof of Theorems 3.1 and 3.2. (i) Under H_0 and by continuous mapping theorem, Assumption 2.1 implies that $\{C_n(\lfloor nt \rfloor) : t \in [0, 1]\} \Rightarrow \{\sigma(\mathbb{B}(t) - t\mathbb{B}(1)) : t \in [0, 1]\}$. Note that $\mathbb{T}_n^{(C)}$ is a composite function of $C_n(\cdot)$ via (3.2), (3.3), (3.4), (3.5), and (3.6), each of which is a continuous and measurable map. By continuous mapping theorem, we obtain $\mathbb{T}_n^{(C)} \xrightarrow{d} \mathbb{T}$ in (3.7). The limiting distribution \mathbb{T} is well-defined because $V_n^{(C)}(k \mid k - d, k + 1 + d)$

converges to a non-negative and non-degenerate distribution for any $\lfloor n\epsilon \rfloor \leq d \leq n$ and $\lfloor \epsilon n \rfloor + 1 \leq k \leq n - \lfloor \epsilon n \rfloor - 1$, provided that $\epsilon > 0$.

(ii) For consistency, we consider the j th relative CP time π_j such that the corresponding change magnitude satisfies $|\Delta_j| \asymp n^{\kappa-1}$, where $0.5 < \kappa \leq 1$. Denote $\Delta_* = \Delta_j$ and $k_* = \lfloor n\pi_j \rfloor$. Under the assumption, there exist $c \in \mathbb{R}^+$ and $3/2 - \kappa \leq \Upsilon < 1$ such that $\epsilon + \lfloor cn^\Upsilon \rfloor / n < \min(\pi_j - \pi_{j-1}, \pi_{j+1} - \pi_j)$ is satisfied for a large enough n . Therefore, there is only one CP in the interval $k_* \pm (\lfloor \epsilon n \rfloor + \lfloor cn^\Upsilon \rfloor)$. It suffices to consider $d = \lfloor \epsilon n \rfloor$. For all k such that $|k - k_*| \leq \lfloor bn^\Upsilon \rfloor$ where $0 < b < c$, we can decompose

$$\begin{aligned} \mathbb{L}_n^{(C)}(k \mid k-d, k+d+1)^2 &= \frac{d+1}{8} (\bar{X}_{(k-d):k} - \bar{X}_{(k+1):(k+d+1)})^2 \\ &= \frac{d+1}{8} \left(\{ \bar{Z}_{(k-d):k} - \bar{Z}_{(k+1):(k+d+1)} \} - \left\{ 1 - \frac{|k_* - k|}{d+1} \right\} \Delta_* \right)^2 \\ &= \frac{1}{8} \left[\left(\sqrt{d+1} \{ \bar{Z}_{(k-d):k} - \bar{Z}_{(k+1):(k+d+1)} \} \right) - \left\{ \sqrt{d+1} - \frac{\lfloor bn^\Upsilon \rfloor}{\sqrt{d+1}} \right\} \Delta_* \right]^2 \\ &\geq \{O_p(1) + \Xi_{1,n}\}^2, \end{aligned} \tag{A.1}$$

where $|\Xi_{1,n}| \asymp n^{\kappa-1/2}$. Next, for the SN $V_n^{(C)}(k \mid k-d, k+d+1)$, we consider two cases: $k \geq k_*$ and $k < k_*$. If $k \geq k_*$, there is only one CP in the interval $[k-d, k]$. Following similar calculations as in (A.1), we know that $\mathbb{L}_n^{(C)}(j \mid k-d, k)^2 \leq \mathbb{L}_n^{(C)}(k_* \mid k-d, k)$ for all $j = k-d, \dots, k$, provided that n is large enough. Moreover, since there is no CP in the interval $[k+1, k+1+d]$, $\mathbb{L}_n^{(C)}(j \mid k+1, k+1+d)^2 = O_p(1)$ for all $j = k+1, \dots, k+1+d$. Therefore,

$$\begin{aligned} V_n^{(C)}(k \mid k-d, k+d+1) &= \frac{1}{4(d+1)} \left\{ \sum_{j=k-d}^k \mathbb{L}_n^{(C)}(j \mid k-d, k)^2 + \sum_{j=k+1}^{k+1+d} \mathbb{L}_n^{(C)}(j \mid k+1, k+1+d)^2 \right\} \\ &\leq \frac{1}{4} \mathbb{L}_n^{(C)}(k_* \mid k-d, k)^2 + O_p(1) \\ &= \frac{(d+1 - \lfloor bn^\Upsilon \rfloor)^2 (\lfloor bn^\Upsilon \rfloor)^2}{2(d+1)^3} \{ \bar{Z}_{(k-d):k_*} - \bar{Z}_{k_*:k} - \Delta_* \}^2 + O_p(1) \\ &\leq \{O_p(1) + \Xi_{2,n}\}^2, \end{aligned}$$

where $|\Xi_{2,n}| \asymp n^{\Upsilon+\kappa-3/2}$. For the case when $k < k_*$, the analysis is similar and $V_n^{(C)}$ are of

the same order. From above, there exists a constant $c' \neq 0$ such that

$$\mathbb{T}_n^{(C)}(k) \geq \left\{ \frac{O_p(1) + \Xi_{1,n}}{O_p(1) + \Xi_{2,n}} \right\}^2 = \{o_p(1) + c'n^{1-\Upsilon}\}^2,$$

for all $k = k_* - \lfloor bn^\Upsilon \rfloor, \dots, k_* + \lfloor bn^\Upsilon \rfloor$. Since $\mathbb{T}_n^{(C)}(k) \geq 0$ for all k , we have

$$\mathbb{T}_n^{(C)} \geq n^{-1} \sum_{k=k_*-\lfloor bn^\Upsilon \rfloor}^{k_*+\lfloor bn^\Upsilon \rfloor} \mathbb{T}_n^{(C)}(k) = c''n^{1-\Upsilon} \{o_p(1) + 1\}^2, \quad (\text{A.2})$$

for a large enough n , where $c'' > 0$ is a constant. Consequently, $\mathbb{T}_n^{(C)} \rightarrow \infty$ in probability as $n \rightarrow \infty$ because $\Upsilon < 1$. \square

Proof of Theorem 5.1. Define $D_t = (X_{t+b} - X_t)/\sqrt{2}$ for $t = 1, \dots, N$, where $N = n - b + 1$. The ACF estimator at lag 1 based on $\{D_t\}$ is $\hat{\rho} = \hat{\gamma}(1)/\hat{\gamma}(0)$, where $\hat{\gamma}(k) = \sum_{t=1}^{N-k} (D_t - \bar{D})(D_{t+k} - \bar{D})/N$ for $k = 0, 1$, and $\bar{D} = N^{-1} \sum_{t=1}^N D_t$. Define $M_t^{(\alpha)} = \alpha_{t+b} - \alpha_t - (\bar{\alpha}_{1+b, N+b} - \bar{\alpha}_{1, N})$ for $\alpha \in \{\mu, Z\}$, where $\bar{\alpha}_{s,e} = (e - s + 1)^{-1} \sum_{i=s}^e \alpha_i$. Then, we rewrite

$$\hat{\gamma}(1) = \frac{1}{2N} \sum_{t=1}^{N-1} (M_t^{(Z)} + M_t^{(\mu)})(M_{t+1}^{(Z)} + M_{t+1}^{(\mu)}) = \frac{1}{2} (\hat{\gamma}_N^{(ZZ)} + \hat{\gamma}_N^{(\mu Z)} + \hat{\gamma}_N^{(Z\mu)} + \hat{\gamma}_N^{(\mu\mu)}), \quad (\text{A.3})$$

where $\hat{\gamma}_N^{(\alpha\beta)} = N^{-1} \sum_{t=1}^{N-1} M_t^{(\alpha)} M_{t+1}^{(\beta)}$ and $\alpha, \beta \in \{\mu, Z\}$. We derive the probability limits of $\hat{\gamma}_N^{(ZZ)}$, $\hat{\gamma}_N^{(\mu Z)}$, $\hat{\gamma}_N^{(Z\mu)}$ and $\hat{\gamma}_N^{(\mu\mu)}$ one by one. First, for $\hat{\gamma}_N^{(ZZ)}$, we have

$$\begin{aligned} \hat{\gamma}_N^{(ZZ)} &= \frac{1}{N} \sum_{t=1}^{N-1} (Z_{t+b} - \bar{Z}_{1+b, N+b})(Z_{t+b+1} - \bar{Z}_{1+b, N+b}) - \frac{1}{N} \sum_{t=1}^{N-1} (Z_{t+b} - \bar{Z}_{1+b, N+b})(Z_{t+1} - \bar{Z}_{1, N}) \\ &\quad - \frac{1}{N} \sum_{t=1}^{N-1} (Z_t - \bar{Z}_{1, N})(Z_{t+b+1} - \bar{Z}_{1+b, N+b}) + \frac{1}{N} \sum_{t=1}^{N-1} (Z_t - \bar{Z}_{1, N})(Z_{t+1} - \bar{Z}_{1, N}) \\ &=: \hat{\gamma}_{N,1}^{(ZZ)} - \hat{\gamma}_{N,2}^{(ZZ)} - \hat{\gamma}_{N,3}^{(ZZ)} + \hat{\gamma}_{N,4}^{(ZZ)}. \end{aligned}$$

Note that $\sum_{i=1}^{\infty} \lambda_4(i) < \infty$ implies $\sum_{k=1}^{\infty} |\gamma(k)| < \infty$. By Theorem 7 in Wu (2011), ergodic

theorem and Slutsky's lemma,

$$\widehat{\gamma}_{N,1}^{(ZZ)} = \frac{1}{N} \sum_{t=1}^{N-1} Z_{t+b} Z_{t+b+1} - \bar{Z}_{1+b,N+b} \left\{ \frac{1}{N} \sum_{t=1}^{N-1} (Z_{t+b} + Z_{t+1+b}) - \left(1 - \frac{1}{N}\right) \bar{Z}_{1+b,N+b} \right\} \xrightarrow{\text{Pr}} \gamma(1),$$

where “ $\xrightarrow{\text{Pr}}$ ” denotes convergence in probability. Similarly, we have $\widehat{\gamma}_{N,4}^{(ZZ)} \xrightarrow{\text{Pr}} \gamma(1)$. The asymptotic behavior for sample autocovariance function at a divergent lag is different to that at a fixed lag. Nevertheless, by Theorem 8 in Wu (2011), ergodic theorem and Slutsky's lemma, we have $\widehat{\gamma}_{N,2}^{(ZZ)} - \gamma(b-1) \xrightarrow{\text{Pr}} 0$ and $\widehat{\gamma}_{N,3}^{(ZZ)} - \gamma(b+1) \xrightarrow{\text{Pr}} 0$. By Slutsky's lemma again, we have $\widehat{\gamma}_N^{(ZZ)} \xrightarrow{\text{Pr}} 2\gamma(1)$. Next, we consider $\widehat{\gamma}_N^{(\mu Z)}$ and $\widehat{\gamma}_N^{(Z\mu)}$. Note that $M_t^{(\mu)}$ is deterministic and by Markov inequality. So, for all $\epsilon > 0$, we have

$$\mathbf{P}(|\widehat{\gamma}_n^{(\mu Z)}| > \epsilon) \leq \frac{\mathbf{E}(|\widehat{\gamma}_n^{(\mu Z)}|)}{\epsilon} \leq \frac{1}{2N\epsilon} \sum_{t=1}^{N-1} [(M_t^{(\mu)})^2 + \mathbf{E}\{(M_{t+1}^{(Z)})^2\}].$$

Since $\{\mu_{t+b} - \mu_t\}_{1 \leq t \leq N}$ has at most bM non-zero elements, we have

$$0 \leq \frac{1}{N} \sum_{t=1}^{N-1} (M_t^{(\mu)})^2 \leq \frac{1}{N} \sum_{t=1}^N (\mu_{t+b} - \mu_t)^2 \leq \frac{bM}{N} \Delta^2 \rightarrow 0. \quad (\text{A.4})$$

Moreover, expanding $\sum_{t=1}^{N-1} \mathbf{E}\{(M_{t+1}^{(Z)})^2\}/N$, we have

$$\frac{2}{N^2} \sum_{t=2}^N \sum_{i=1}^N \{\gamma(|t+b-i|) + \gamma(|t-b-i|)\} - \frac{2N-2}{N} \left\{ \gamma(b) + \frac{1}{N^2} \sum_{i,j=1}^N \gamma(|i-j-b|) \right\},$$

which converges to 0 in probability by the absolute summability of $\gamma(k)$. Therefore, we have $\widehat{\gamma}_N^{(\mu Z)} \xrightarrow{\text{Pr}} 0$. By similar arguments, we also have $\widehat{\gamma}_N^{(Z\mu)} \xrightarrow{\text{Pr}} 0$. Then, we consider $\widehat{\gamma}_N^{(\mu\mu)}$. By the result in (A.4), we have $0 \leq \widehat{\gamma}_N^{(\mu\mu)} \leq \sum_{t=1}^{N-1} \{(M_t^{(\mu)})^2 + (M_{t+1}^{(\mu)})^2\}/N \rightarrow 0$. Putting all these results back to (A.3), we obtain $\widehat{\gamma}(1) \xrightarrow{\text{Pr}} \gamma(1)$. For $\widehat{\gamma}(0)$, we have

$$\widehat{\gamma}(0) = \frac{1}{2N} \sum_{t=1}^N \{(M_t^{(Z)})^2 + (M_t^{(\mu)})^2 + 2M_t^{(Z)} M_t^{(\mu)}\}. \quad (\text{A.5})$$

Consider the first term of (A.5), we have, by Theorems 7 and 8 in Wu (2011), that

$$\frac{1}{N} \sum_{t=1}^N (M_t^{(Z)})^2 = \frac{\sum_{t=1}^N (Z_{t+b}^2 + Z_t^2 - 2Z_{t+b}Z_t)}{N} - (\bar{Z}_{1+b, N+b} - \bar{Z}_{1, N})^2 \xrightarrow{\text{pr}} 2\gamma(0).$$

By similar arguments as above, we also have $N^{-1} \sum_{t=1}^N (M_t^{(\mu)})^2 \rightarrow 0$ and $N^{-1} \sum_{t=1}^N M_t^{(Z)} M_t^{(\mu)} \xrightarrow{\text{pr}} 0$ as $b \rightarrow \infty$. Therefore, $\hat{\gamma}(0) \xrightarrow{\text{pr}} \gamma(0)$ as $b \rightarrow \infty$. Hence, we have $\hat{\rho} \xrightarrow{\text{pr}} \gamma(1)/\gamma(0) = \rho$. \square

B Proofs of Corollaries

Proof of Corollaries 4.1 and 4.2. The proof is similar to the CUSUM case and we highlight the difference. By Theorem 3.1 in Dehling *et al.* (2015), we have $W_n(\lfloor nt \rfloor) \xrightarrow{d} \sigma_W^2 \{\mathbb{B}(t) - t\mathbb{B}(1)\}$. Moreover by Theorem 1 in Dehling *et al.* (2020), we have $\{\mathbb{H}_n(\lfloor nt \rfloor) : t \in [0, 1]\} \xrightarrow{d} \{(\sigma_H/u(0))(\mathbb{B}(t) - t\mathbb{B}(1)) : t \in [0, 1]\}$. The result follows by using similar argument as in the proof of Theorem 3.1 and replacing σ by σ_W^2 for $T_n^{(W)}$ and $\sigma_H/u(0)$ for $T_n^{(H)}$. \square

Proof of Corollary 4.3. Using (4.4), we can rewrite

$$G_n(k) = \frac{k(n-k)}{n^{3/2}} (\hat{\theta}_{1:k} - \hat{\theta}_{k+1:n}) = I_n(t) - \frac{k}{n} I_n(1) + \frac{k(n-k)}{n^{3/2}} (R_{1:k} - R_{k+1:n}).$$

The last term vanishes uniformly over k as $n \rightarrow \infty$ since $\sup_{k=1, \dots, n-1} |R_{1:k}| + |R_{k+1:n}| = o_p(n^{-1/2})$. Therefore, $\{G_n(\lfloor nt \rfloor) : t \in [0, 1]\} \xrightarrow{d} \{\sigma(\mathbb{B}(t) - t\mathbb{B}(1)) : t \in [0, 1]\}$ by the continuous mapping theorem. The result follows by using similar arguments as in the proof of Theorem 3.1. \square

Proof of Corollaries 4.4 and 4.5. Note that $\{C_n^*(\lfloor nt \rfloor) : t \in [0, 1]\} \Rightarrow \{\sigma_{C^*} \mathbb{B}_H(t) - t\mathbb{B}_H(1) : t \in [0, 1]\}$ and $\{W_n^*(\lfloor nt \rfloor) : t \in [0, 1]\} \Rightarrow \{(2\sqrt{\pi})^{-1} \mathbb{B}_H(t) - t\mathbb{B}_H(1) : t \in [0, 1]\}$. Moreover, $T_n^{(C^*)}$ and $T_n^{(W^*)}$ is a continuous and measurable function of $C_n^*(\cdot)$ and $W_n^*(\cdot)$ respectively. The above arguments also apply and the limiting distribution is a functional of standard fractional Brownian motion $\mathbb{B}_H(t)$ instead of the standard Brownian motion $\mathbb{B}(t)$.

Regarding to $T_n^{(Q)}$, since $\{Q_n(\lfloor nt \rfloor) : t \in [0, 1]\} \Rightarrow \{\sigma_Q \{\mathbb{B}^q(t) - t\mathbb{B}^q(1)\} : t \in [0, 1]\}$ and $T_n^{(Q)}$ is a continuous and measurable function of $Q_n(\cdot)$, we have the result by continuous

mapping theorem. □

C Supplementary Simulation Result

C.1 Setting

In this session, the size and power of our proposed tests ($T_n^{(C)}$, $T_n^{(W)}$ and $T_n^{(H)}$), [Shao and Zhang \(2010\)](#) proposed tests ($S_n^{(1)}$, $S_n^{(2)}$ and $S_n^{(3)}$) as well as [Zhang and Lavitas \(2018\)](#) proposed test (Z_n) are further investigated under the standard autoregressive (AR) model, autoregressive-moving-average (ARMA) model, threshold AR (TAR) model and absolute value nonlinear AR (NAR) model in Sections [C.2](#), [C.3](#), [C.4](#) and [C.5](#) respectively. Extra results under the bilinear AR (BAR) model are also provided in [C.6](#). The performance for the tests under non-Gaussian time series is investigated in Section [C.7](#). The power comparison between all the test concerned when the magnitudes of changes are not equal is reported in Section [C.8](#). Last but not least, the power comparison after the use of nonsymmetric windows is presented in Section [C.9](#). All results are obtained using 2^{10} replications and the nominal size is 5%. The sample size is $n = 200$ unless specified. We define ε_i to be independent standard normal random variables for $i = 1, \dots, n$. We again consider the signal-plus-noise model, $X_i = \mu_i + Z_i$, and let μ_i to be the signal, specified in equation [\(6.1\)](#) from the main article, i.e.,

$$\mu_i = \Delta \sum_{j=1}^M (-1)^{j+1} \mathbb{1}_{\{i/n \geq j/(M+1)\}}, \quad (\text{C.1})$$

where $M \in \{1, \dots, 6\}$ denotes the number of CPs, and $\Delta \in \mathbb{R}$ is the magnitude of the mean changes.

C.2 AR Model

In this subsection, we investigate the performance under the AR(1) model. Specifically, the data has the form $X_i - \mu_i = \varpi(X_{i-1} - \mu_{i-1}) + \varepsilon_i$, where the AR parameter $|\varpi| < 1$. The null rejection rates are documented in [Table C.1](#). Our proposed tests have accurate size in

Table C.1: Null rejection rates (%) at 5% nominal size under AR model and mean function (C.1).

ϖ	$n = 200$								$n = 400$							
	KS $_n$	S $_n^{(1)}$	S $_n^{(2)}$	S $_n^{(3)}$	Z $_n$	T $_n^{(C)}$	T $_n^{(W)}$	T $_n^{(H)}$	KS $_n$	S $_n^{(1)}$	S $_n^{(2)}$	S $_n^{(3)}$	Z $_n$	T $_n^{(C)}$	T $_n^{(W)}$	T $_n^{(H)}$
0.8	53.6	9.0	25.9	43.3	27.2	16.1	23.9	21.8	52.6	6.0	12.9	23.4	14.6	9.3	12.7	12.1
0.5	13.7	5.7	9.8	10.9	10.4	5.5	7.3	6.5	9.4	4.5	5.7	8.3	5.4	5.1	5.5	5.1
0.3	10.1	5.4	6.7	5.6	6.8	4.5	5.3	5.4	7.7	4.2	5.0	5.8	4.8	5.2	5.0	4.8
0	7.4	5.2	3.5	2.5	3.1	4.1	4.7	4.6	5.0	4.2	4.5	4.6	3.8	5.2	4.7	4.2
-0.3	13.0	4.3	2.5	0.8	2.2	4.4	5.3	4.7	6.6	3.3	2.8	3.0	2.5	5.4	4.7	4.9
-0.5	23.7	3.7	1.5	0.4	1.4	5.0	5.8	5.3	14.7	3.1	2.1	1.9	2.1	5.0	4.4	4.8
-0.8	46.0	2.4	0.5	0.1	0.1	7.8	9.2	9.3	38.9	2.3	1.0	0.1	1.0	6.6	7.7	7.3

most cases. Although $S_n^{(1)}$ has more accurate size when $\varpi = 0.8$, our tests are not severely under-sized when $\varpi < 0$ as observed in other self-normalized tests. The non-self-normalized Kolmogorov–Smirnov (KS) test has larger size distortion than the self-normalized tests.

Figures C.1 and C.2 present the power while Figures C.3 and C.4 present the size-adjusted power. In the single CP case, our proposed tests lose the least power among multiple-CP tests comparing to $S_n^{(1)}$ and KS_n , which are tailored for the at-most-one-change (AMOC) problem. However, $S_n^{(1)}$ suffers non-monotonic power in multiple-CP case. The issue is also observed in the KS test when $\varpi = -0.5$, yet it does not appear in the unadjusted power. Under multiple-CP case, our proposed tests have the largest power. In particular, $S_n^{(2)}$ and $S_n^{(3)}$ have lower power than our proposed tests even the number of CP is well-specified.

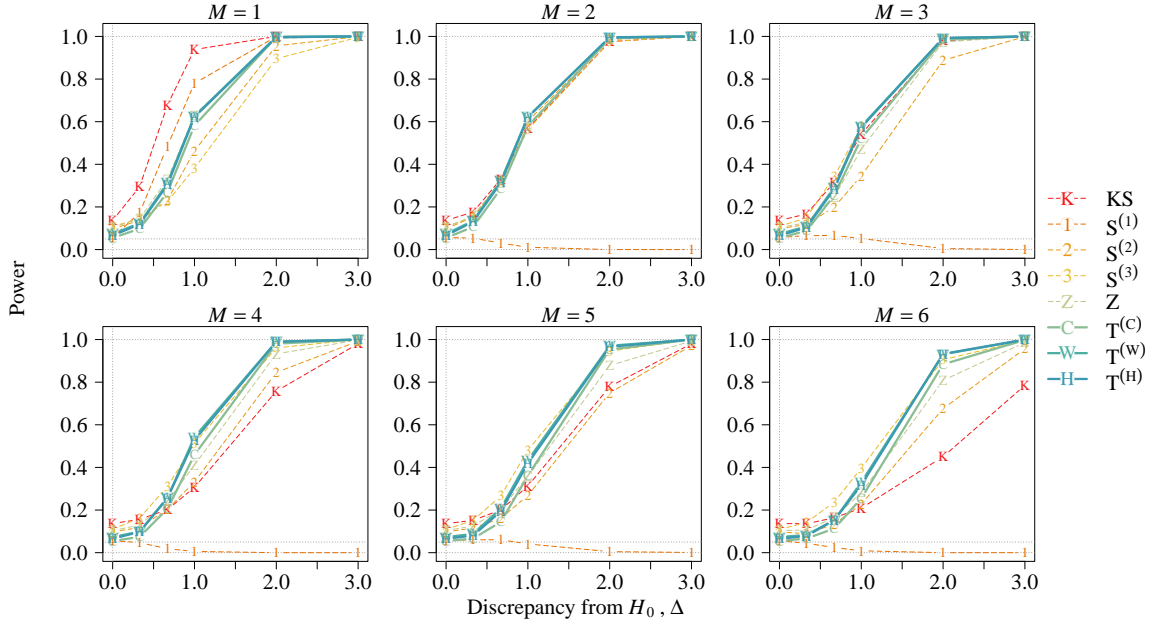


Figure C.1: Power under AR model with $\varpi = 0.5$ and mean function (C.1).

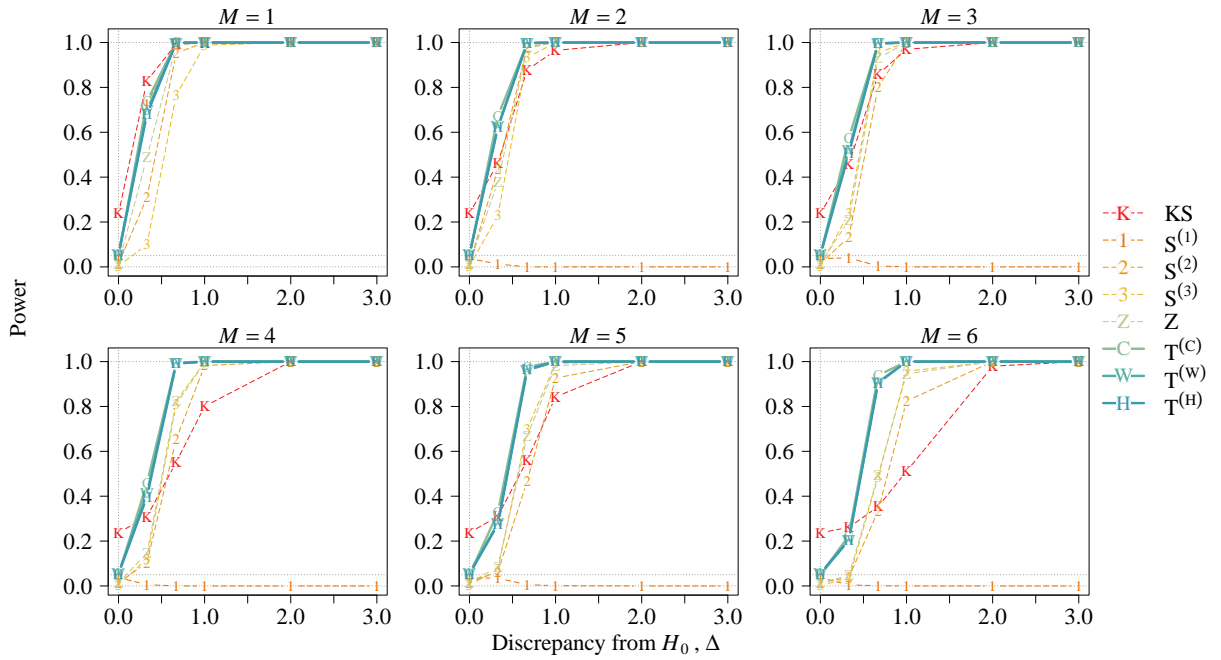


Figure C.2: Power under AR model with $\varpi = -0.5$ and mean function (C.1).

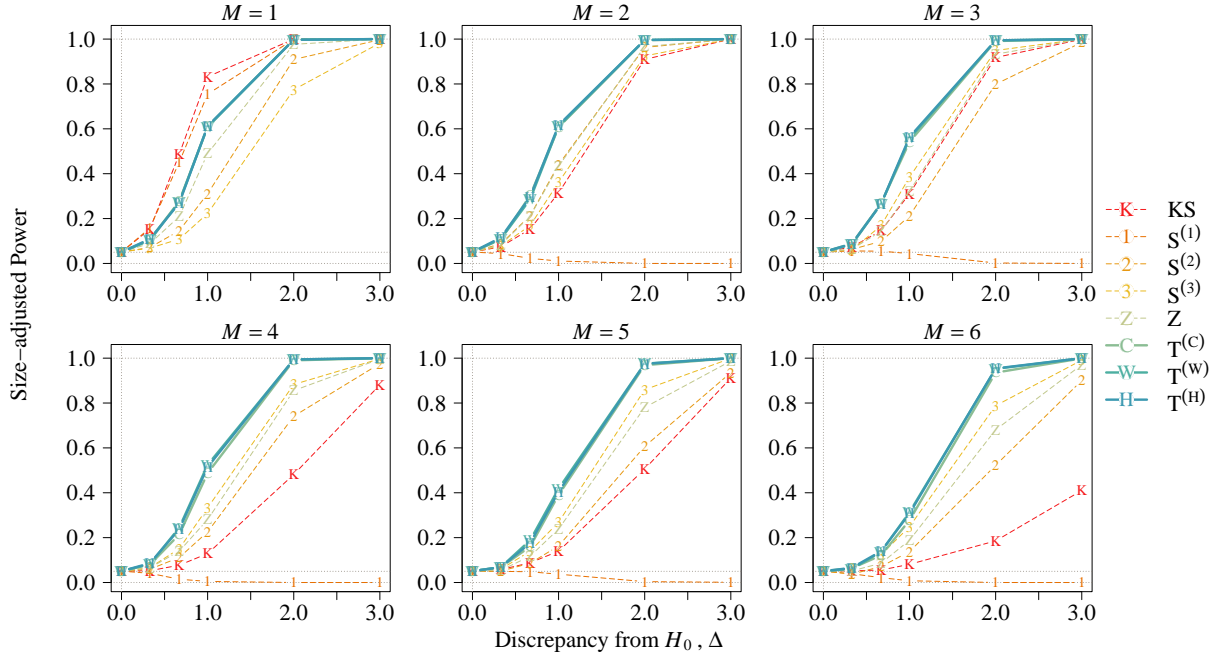


Figure C.3: Size-adjusted power under AR model with $\varpi = 0.5$ and mean function (C.1).

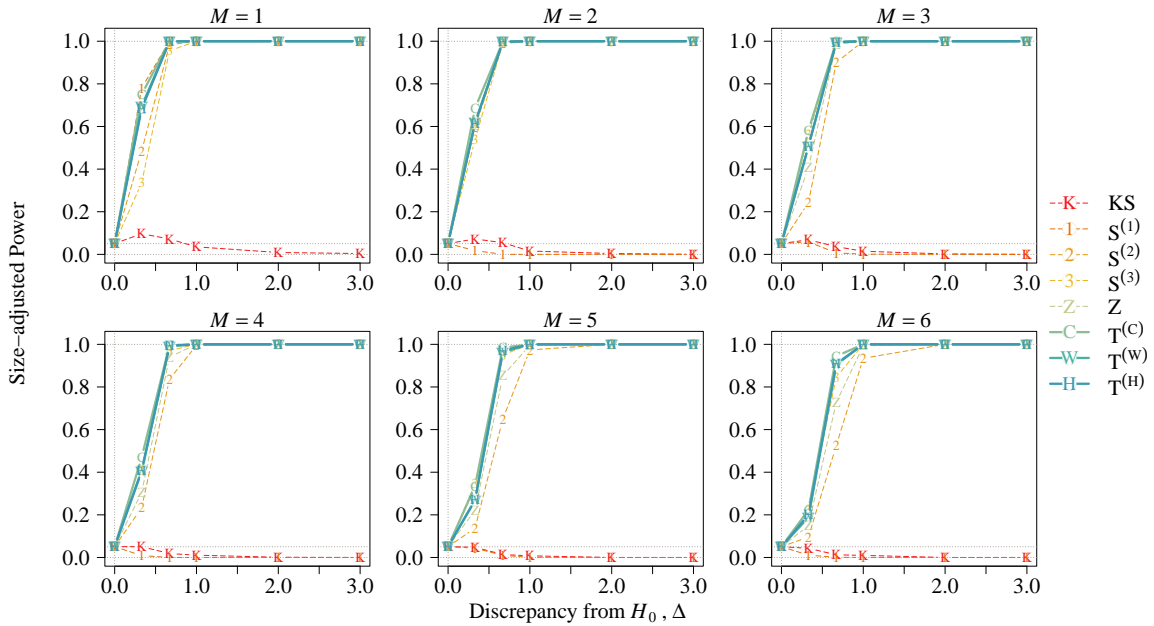


Figure C.4: Size-adjusted power under AR model with $\varpi = -0.5$ and mean function (C.1).

C.3 ARMA model

The ARMA model is defined as $X_i - \mu_i = \varpi(X_{i-1} - \mu_{i-1}) + \varepsilon_i + \varphi\varepsilon_{i-1}$, where $\varpi, \varphi \in (-1, 1)$. The size accuracy is reported in Table C.2. The self-normalized approach generally has more accurate size than the non-self-normalized approach. Roughly speaking, KS_n is seriously over-sized in most cases, while the self-normalized tests are under-sized in some cases. Overall, $S_n^{(1)}$ has the most accurate size, but the size distortion of $S_n^{(m)}$ is increasing with m . The size performance of self-normalized multiple-CP tests is mixed. Our proposed tests in general are under-sized while other multiple-CP tests, i.e., $S_n^{(2)}$, $S_n^{(3)}$ and Z_n , are over-sized when both φ and ϖ are positive. Consider when $\varpi = 0.8$. Our proposed tests have significantly smaller size distortion than other multiple-CP tests when φ is positive. Except when $\varphi = -0.5$, our proposed tests have larger size distortion, but nevertheless all multiple-CP tests are seriously over-sized. When both ϖ and φ are negative, self-normalized tests commit lower type-I error than the nominal size while non-self-normalized KS_n commits higher type-I error.

Figures C.5–C.8 present the power. A similar conclusion in Section C.2 is drawn. Our proposed tests have largest size-adjusted power in the multiple-CP case and lose the least power comparing to AMOC type tests, i.e., $S_n^{(1)}$ and KS_n , in the one-CP case.

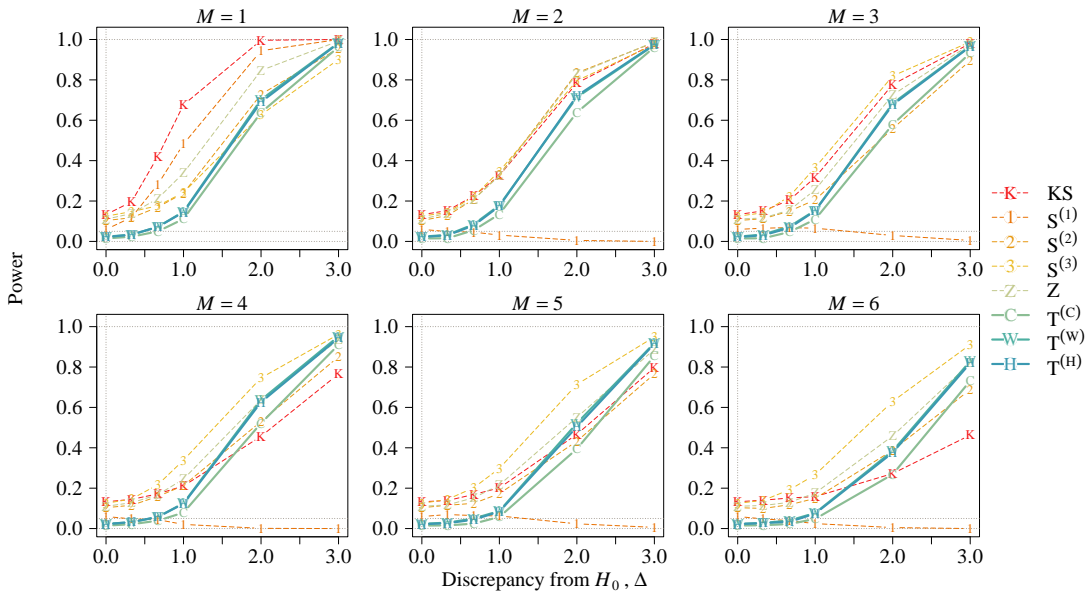


Figure C.5: Power under ARMA model with $\varpi = \varphi = 0.5$ and mean function (C.1).

Table C.2: Null rejection rates (%) at 5% nominal size under ARMA model and mean function (C.1).

φ	ϖ	$n = 200$									$n = 400$								
		KS _n	S _n ⁽¹⁾	S _n ⁽²⁾	S _n ⁽³⁾	Z _n	T _n ^(C)	T _n ^(W)	T _n ^(H)	KS _n	S _n ⁽¹⁾	S _n ⁽²⁾	S _n ⁽³⁾	Z _n	T _n ^(C)	T _n ^(W)	T _n ^(H)		
0.8	0.8	54.5	9.0	26.0	44.4	27.8	2.6	7.5	7.3	53.6	6.1	13.0	23.4	14.4	1.7	3.5	3.0		
	0.5	13.5	6.1	10.4	13.0	11.3	0.8	1.9	1.6	9.0	4.6	5.9	8.8	5.8	1.6	2.4	2.5		
	0.3	11.7	5.5	7.8	8.1	8.1	0.8	1.7	1.4	7.8	4.5	5.3	6.5	5.2	2.6	2.9	2.7		
	0	7.4	5.2	3.5	2.5	3.1	4.1	4.7	4.6	5.0	4.2	4.5	4.6	3.8	5.2	4.7	4.2		
	-0.3	8.7	5.1	5.1	3.7	5.2	2.1	2.7	2.6	5.8	4.1	4.0	4.9	3.9	4.0	4.2	4.2		
	-0.5	7.8	4.6	5.1	3.8	5.2	3.0	2.9	3.2	5.4	4.0	4.2	4.7	3.6	4.5	4.3	4.2		
0.5	0.8	54.6	9.0	26.1	44.3	28.2	4.1	10.1	9.7	53.7	6.1	13.1	23.5	14.5	2.6	4.5	4.5		
	0.5	13.3	6.0	10.4	12.5	11.0	1.5	2.3	2.1	9.0	4.5	5.7	8.7	6.0	2.1	3.0	3.1		
	0.3	11.7	5.4	7.7	7.8	7.8	1.4	2.2	2.4	7.4	4.5	5.1	6.4	5.2	3.2	3.7	3.1		
	0	7.4	5.2	3.5	2.5	3.1	4.1	4.7	4.6	5.0	4.2	4.5	4.6	3.8	5.2	4.7	4.2		
	-0.3	8.1	4.9	4.5	3.2	5.1	3.3	3.7	3.6	5.1	3.9	3.8	4.7	3.9	4.4	4.5	4.7		
	-0.8	10.2	4.4	3.3	1.5	2.5	8.4	9.0	8.7	6.1	4.0	3.4	3.1	2.6	6.7	6.6	6.4		
-0.5	0.8	43.7	8.6	20.3	29.9	22.5	32.4	37.8	36.6	43.5	6.0	12.3	19.7	14.0	17.5	20.3	20.7		
	0.3	11.8	3.6	1.4	0.4	1.4	1.5	2.1	2.2	6.3	2.9	2.0	1.6	2.1	2.7	2.7	2.9		
	0	7.4	5.2	3.5	2.5	3.1	4.1	4.7	4.6	5.0	4.2	4.5	4.6	3.8	5.2	4.7	4.2		
	-0.3	43.9	0.9	0.0	0.0	0.0	0.2	0.2	0.1	40.0	1.8	0.1	0.0	0.3	0.2	0.9	0.9		
	-0.5	53.3	1.0	0.0	0.0	0.0	0.1	0.4	0.2	50.7	1.0	0.1	0.0	0.0	0.0	0.4	0.2		
	-0.8	51.6	0.0	0.0	0.0	0.0	0.0	0.2	0.0	53.2	0.2	0.0	0.0	0.0	0.0	0.1	0.1		
-0.8	0.5	24.2	1.2	0.1	0.0	0.0	0.0	0.1	0.0	20.3	1.3	0.0	0.0	0.0	0.0	0.1	0.1		
	0.3	38.7	0.4	0.0	0.0	0.0	0.0	0.0	0.0	35.3	0.7	0.0	0.0	0.0	0.0	0.0	0.0		
	0	7.4	5.2	3.5	2.5	3.1	4.1	4.7	4.6	5.0	4.2	4.5	4.6	3.8	5.2	4.7	4.2		
	-0.3	55.8	0.0	0.0	0.0	0.0	0.0	0.0	0.0	52.8	0.0	0.0	0.0	0.0	0.0	0.0	0.0		
	-0.5	57.9	0.0	0.0	0.0	0.0	0.0	0.0	0.0	60.0	0.0	0.0	0.0	0.0	0.0	0.0	0.0		
	-0.8	52.1	0.0	0.0	0.0	0.0	0.0	0.0	0.0	54.6	0.0	0.0	0.0	0.0	0.0	0.0	0.0		

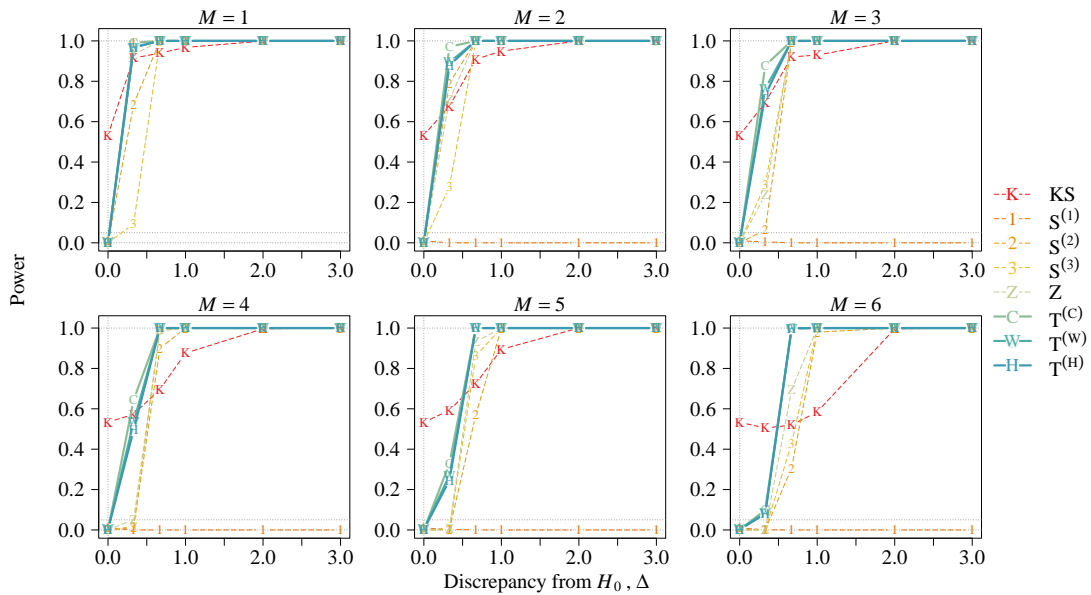


Figure C.6: Power under ARMA model with $\varpi = \varphi = -0.5$ and mean function (C.1).

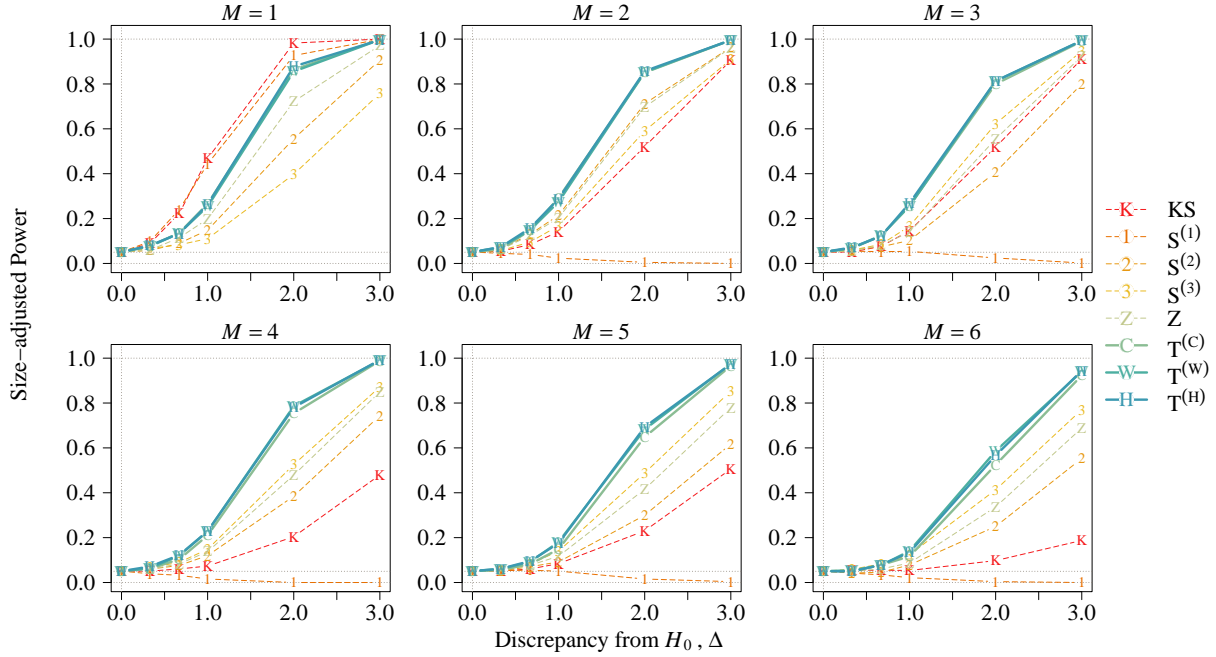


Figure C.7: Size-adjusted power under ARMA model with $\varpi = \varphi = 0.5$ and mean function (C.1).

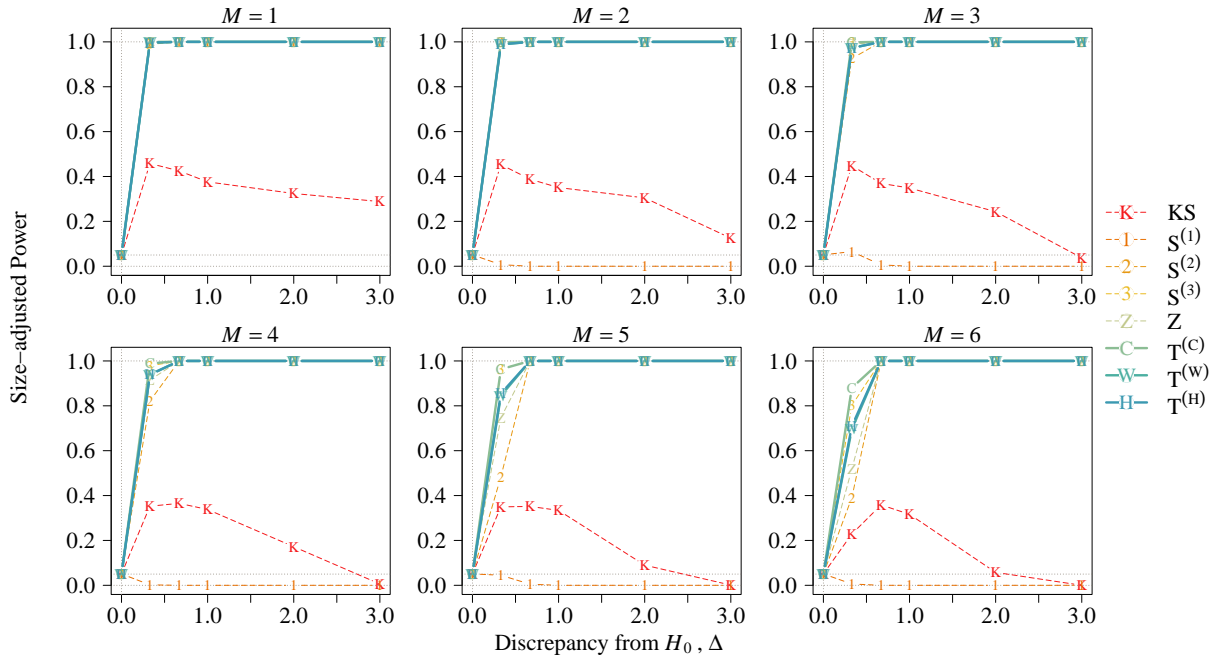


Figure C.8: Size-adjusted power under ARMA model with $\varpi = \varphi = -0.5$ and mean function (C.1).

C.4 TAR Model

The threshold AR model is defined to be

$$X_i - \mu_i = \{\varpi_1 I_{i-1} + \varpi_2(1 - I_{i-1})\}(X_{i-1} - \mu_{i-1}) + \varepsilon_i,$$

where $I_i = \mathbb{1}_{\{X_i - \mu_i \geq 0\}}$ and $\varpi_1, \varpi_2 \in (-1, 1)$. In this subsection, we report the performance under different choices of ϖ_1 and ϖ_2 . Table C.3 tabulates the null rejection rates. Similar to Section C.2, KS_n has larger size distortion than the self-normalized tests. Our proposed tests have more accurate size in general. Although our tests have larger size distortion than $S_n^{(1)}$ when $\varpi_1 = 0.8$, our proposed tests have accurate size while other self-normalized tests are seriously under-sized when both ϖ_1 and ϖ_2 are negative. In contrast to the result in BAR model, $T_n^{(C)}$ has more accurate size than $T_n^{(W)}$ and $T_n^{(H)}$ in general. A similar result in power is also observed in Figures C.9–C.16. Our proposed tests perform the best under multiple-CP case but they slightly underperform $S_n^{(1)}$ and KS_n under the single CP case.

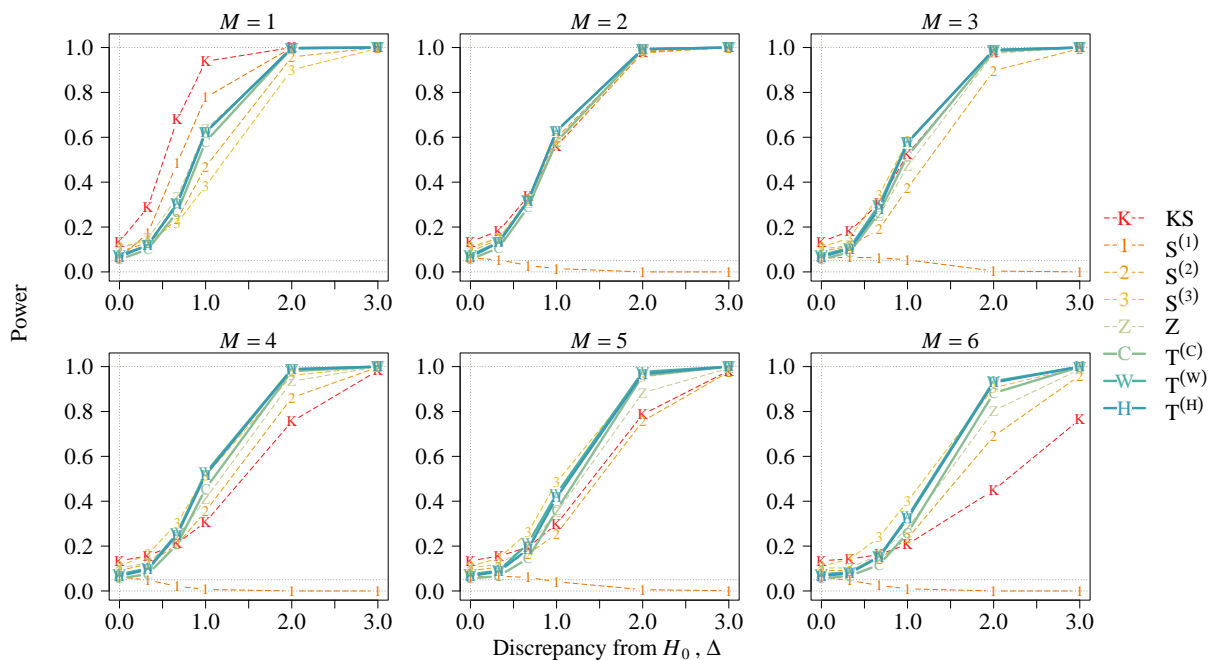


Figure C.9: Power under TAR model with $\varpi_1 = \varpi_2 = 0.5$ and mean function (C.1).

Table C.3: Null rejection rates (%) at 5% nominal size under TAR model and mean function (C.1).

		$n = 200$									$n = 400$							
ϖ_2	ϖ_1	KS _n	S _n ⁽¹⁾	S _n ⁽²⁾	S _n ⁽³⁾	Z _n	T _n ^(C)	T _n ^(W)	T _n ^(H)	KS _n	S _n ⁽¹⁾	S _n ⁽²⁾	S _n ⁽³⁾	Z _n	T _n ^(C)	T _n ^(W)	T _n ^(H)	
0.8	0.8	52.0	8.7	27.1	43.0	30.9	15.0	23.6	21.6	52.8	6.2	14.1	23.3	14.5	9.6	13.1	12.2	
	0.5	30.5	7.2	18.8	29.7	19.6	10.0	15.7	14.6	26.7	5.0	11.7	14.8	11.9	7.0	9.1	8.8	
	0.3	26.4	6.9	17.2	27.1	18.1	8.9	14.1	12.6	23.7	5.2	11.6	14.3	11.6	6.3	8.3	7.9	
	0	23.6	6.8	16.1	24.5	17.3	8.3	12.4	11.8	20.2	5.4	11.5	12.8	11.4	5.8	8.4	7.9	
	-0.3	21.1	6.7	14.5	22.6	15.7	7.7	11.6	11.4	18.5	5.3	10.8	12.4	10.4	6.0	8.1	8.2	
	-0.5	20.0	6.7	14.3	21.1	14.5	7.3	10.5	10.6	17.2	5.7	10.0	12.0	10.2	6.0	8.0	7.7	
	-0.8	18.2	6.4	13.4	18.7	14.4	6.4	10.3	9.9	16.3	5.4	9.3	10.6	9.5	6.0	7.1	6.9	
0.5	0.8	30.2	7.1	18.8	28.9	22.0	10.9	14.6	14.9	27.8	5.6	10.1	16.7	9.8	7.2	8.3	9.0	
	0.5	13.5	6.3	9.1	11.0	10.3	5.6	7.4	6.6	9.5	4.4	5.5	8.1	5.7	5.1	5.4	5.2	
	0.3	11.7	5.5	7.9	9.0	8.5	4.7	5.8	5.9	9.0	4.6	4.8	6.9	5.5	5.4	5.0	5.4	
	0	10.6	5.4	6.8	7.0	7.6	4.3	5.4	5.3	8.2	4.3	5.3	6.9	5.1	5.1	4.8	5.1	
	-0.3	8.5	5.0	5.9	5.7	5.9	4.1	4.9	5.2	7.5	4.9	5.2	5.9	4.4	5.1	4.6	5.2	
	-0.5	8.3	4.9	5.4	5.3	5.1	4.2	4.8	5.1	6.5	5.2	5.2	5.8	4.2	5.5	4.9	5.1	
	-0.8	7.3	4.3	4.8	4.1	4.2	4.1	4.9	4.8	5.1	5.4	4.8	4.8	3.8	5.0	4.8	4.8	
-0.5	0.8	19.8	6.9	14.7	21.0	14.8	8.3	10.7	10.4	16.4	5.3	7.7	10.4	9.0	5.1	7.1	6.7	
	0.5	8.2	4.3	5.8	4.4	5.3	4.1	5.2	4.5	6.3	3.9	4.1	4.6	3.8	4.4	5.0	4.9	
	0.3	7.6	4.2	3.5	2.4	3.7	4.0	4.5	4.6	5.4	4.0	3.6	3.5	3.2	4.5	4.8	4.6	
	0	10.3	4.4	2.4	1.4	2.0	4.1	4.7	4.3	5.9	3.8	2.7	2.8	2.7	5.3	4.8	5.0	
	-0.3	16.6	4.2	1.9	0.6	1.4	4.1	5.1	5.1	9.5	3.3	2.6	2.7	2.2	5.6	5.0	5.0	
	-0.5	24.4	3.5	1.4	0.5	1.3	4.8	5.6	5.6	14.4	3.1	2.3	2.0	2.1	5.1	4.6	4.9	
	-0.8	36.6	3.4	0.9	0.2	0.5	6.0	6.4	6.3	28.4	4.1	1.6	0.9	1.4	5.2	4.3	4.8	
-0.8	0.8	17.9	6.5	13.1	19.4	14.1	7.6	10.2	9.6	16.1	4.9	7.1	9.6	7.5	4.8	7.1	6.4	
	0.5	8.5	4.8	4.7	4.3	4.8	3.9	4.5	4.3	5.9	4.2	3.4	4.3	3.3	4.2	4.7	4.9	
	0.3	8.4	4.3	3.5	2.2	3.3	3.6	4.0	4.8	5.9	3.9	3.5	2.8	2.8	4.3	4.3	4.4	
	0	14.6	4.3	1.8	0.9	1.8	3.9	4.3	4.2	7.3	4.1	2.9	2.1	2.5	4.8	4.9	5.2	
	-0.3	26.6	3.4	1.4	0.4	1.1	4.3	5.4	5.1	17.0	3.1	2.1	2.0	2.1	5.0	4.6	4.7	
	-0.5	36.7	3.1	1.2	0.3	0.9	5.6	6.3	5.8	27.1	3.2	2.1	1.1	1.4	5.4	5.0	5.2	
	-0.8	43.7	2.1	0.4	0.1	0.2	8.3	9.5	8.8	39.0	2.4	0.9	0.2	0.6	7.2	7.7	6.9	

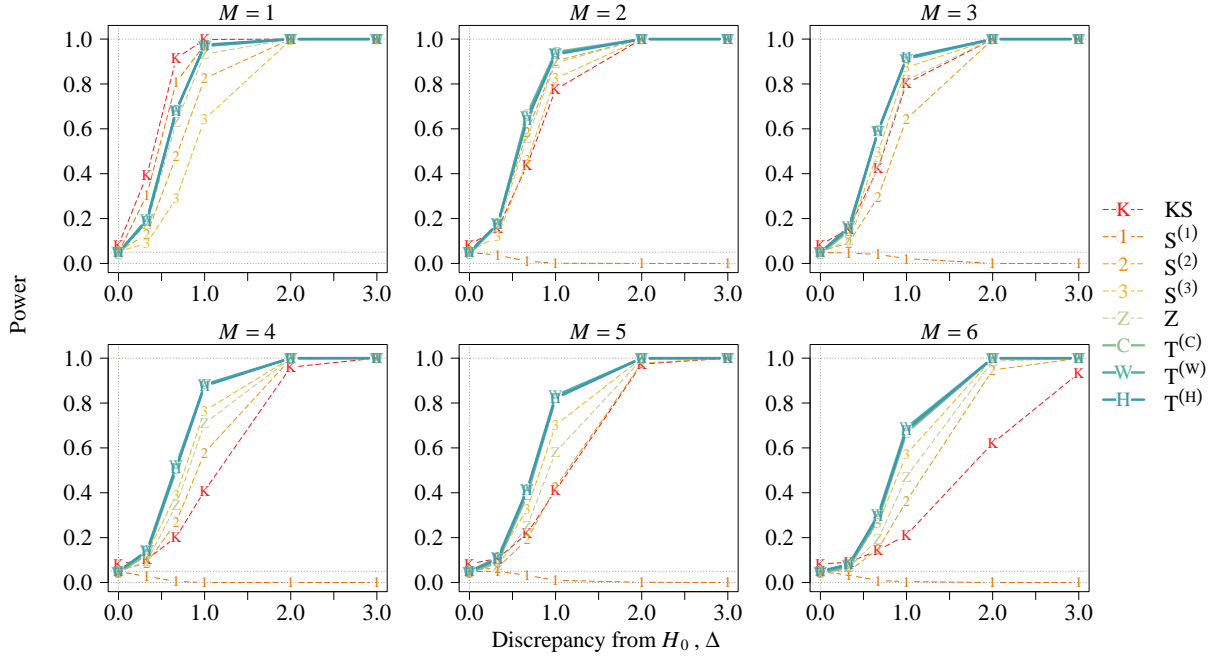


Figure C.10: Power under TAR model with $-\varphi_1 = \varphi_2 = 0.5$ and mean function (C.1).

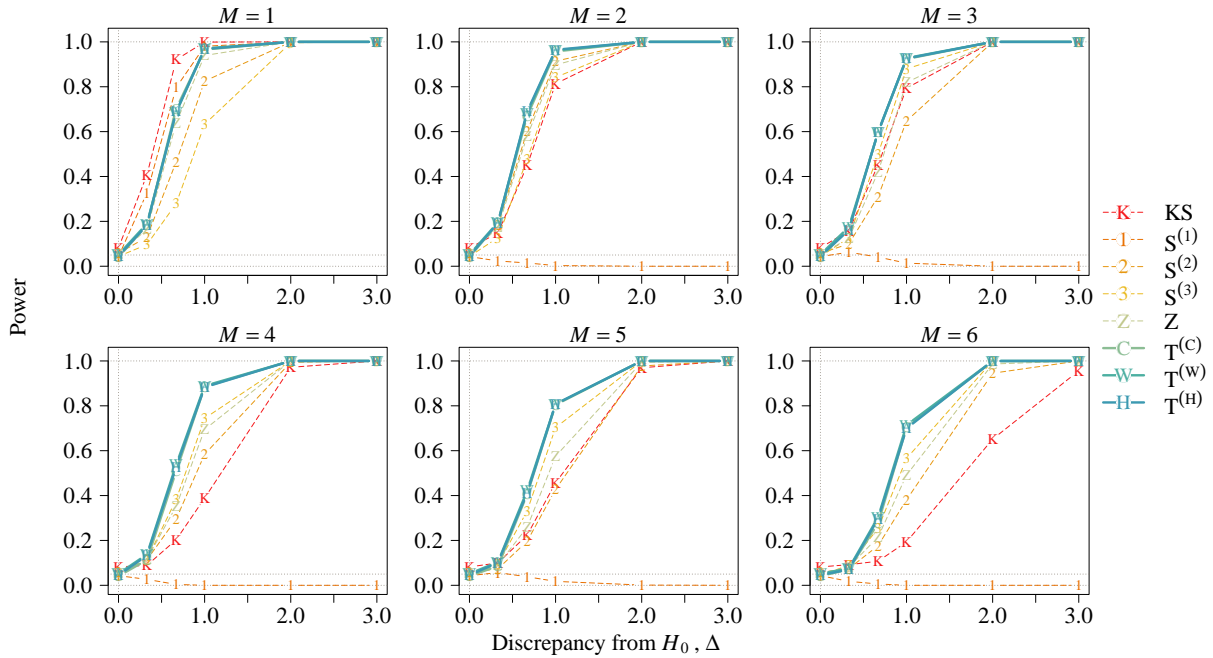


Figure C.11: Power under TAR model with $\varphi_1 = -\varphi_2 = 0.5$ and mean function (C.1).

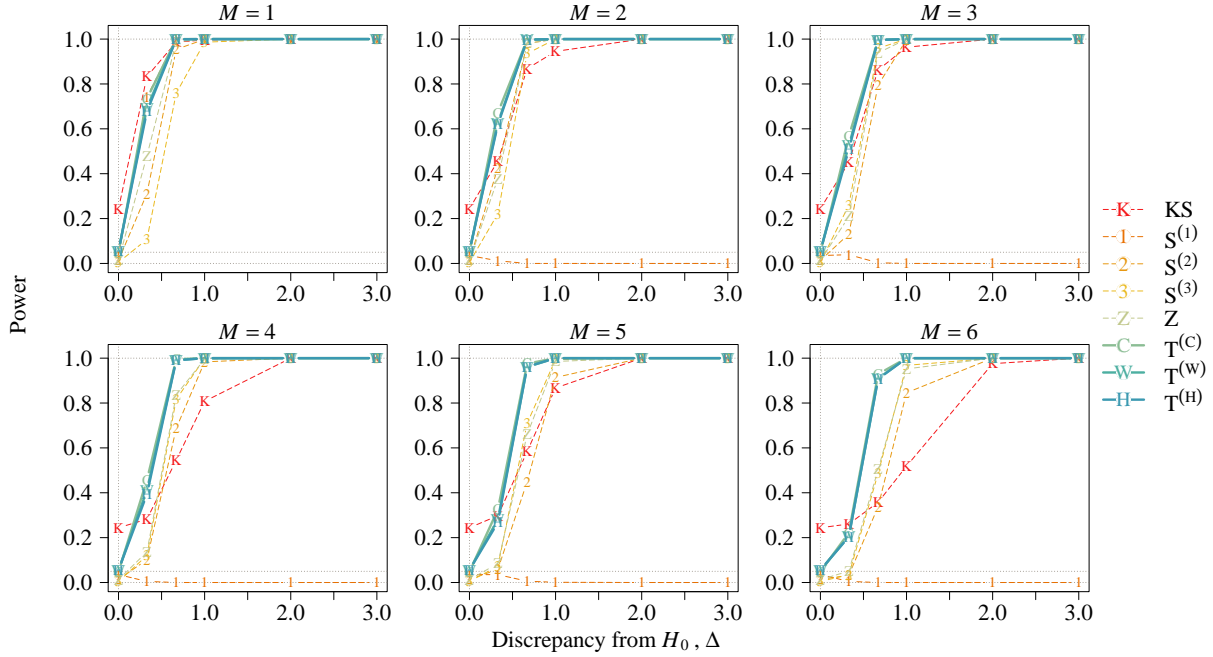


Figure C.12: Power under TAR model with $\varpi_1 = \varpi_2 = -0.5$ and mean function (C.1).

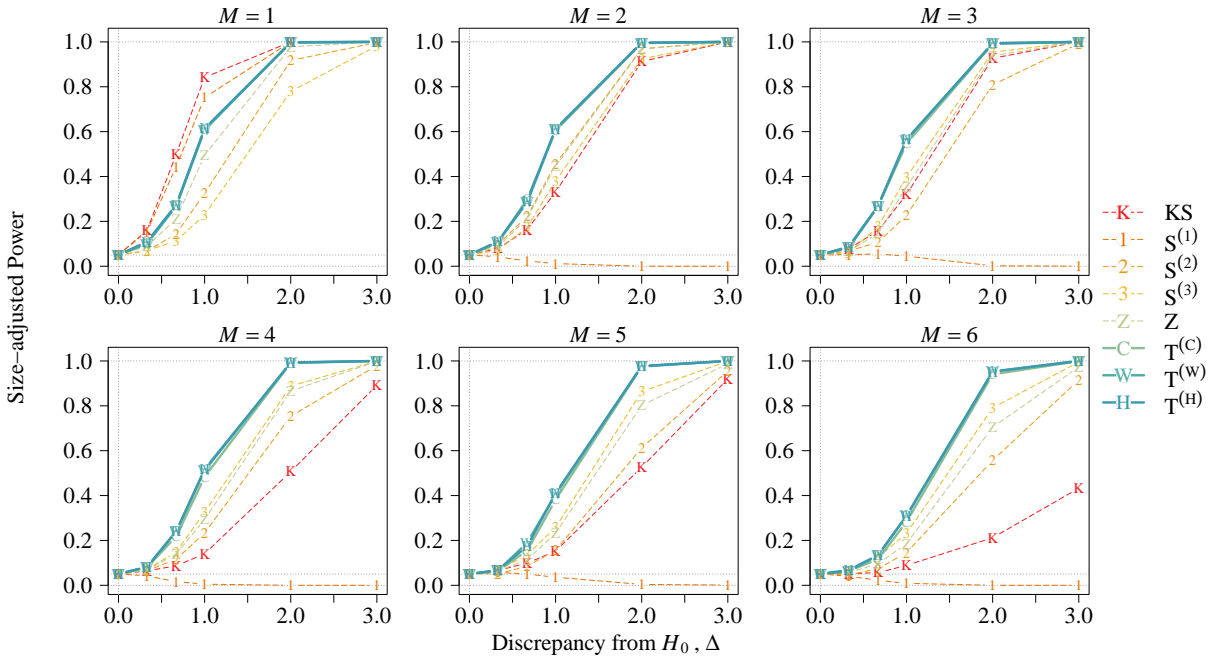


Figure C.13: Size-adjusted power under TAR model with $\varpi_1 = \varpi_2 = 0.5$ and mean function (C.1).

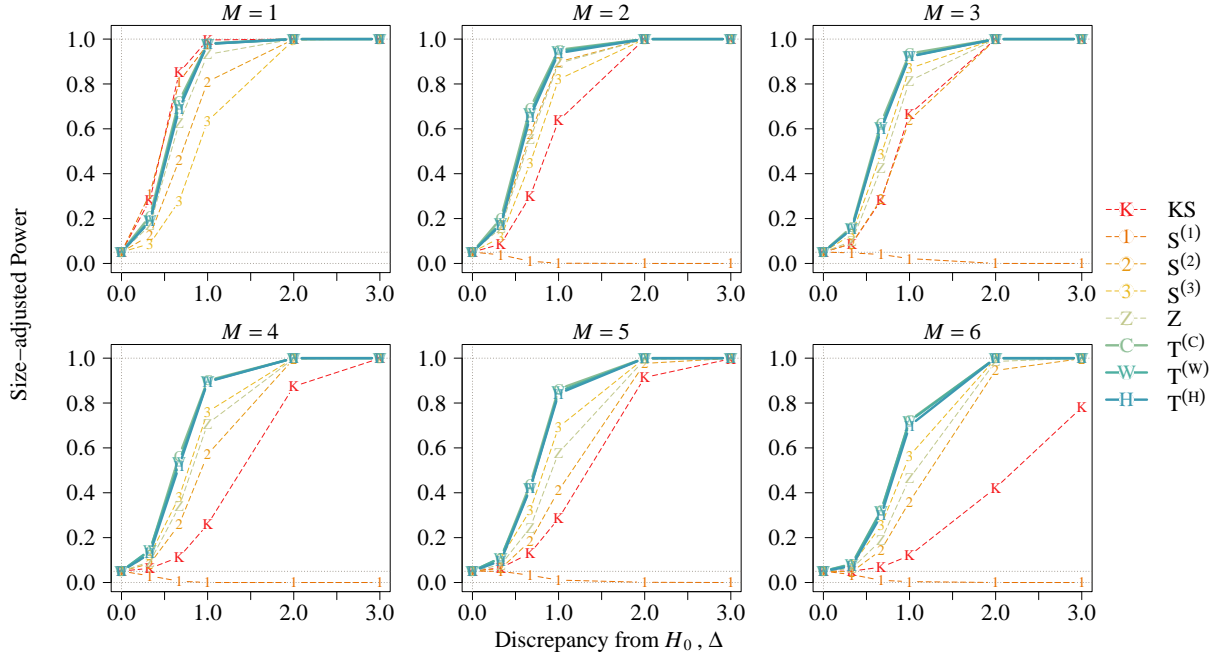


Figure C.14: Size-adjusted power under TAR model with $-\varpi_1 = \varpi_2 = 0.5$ and mean function (C.1).

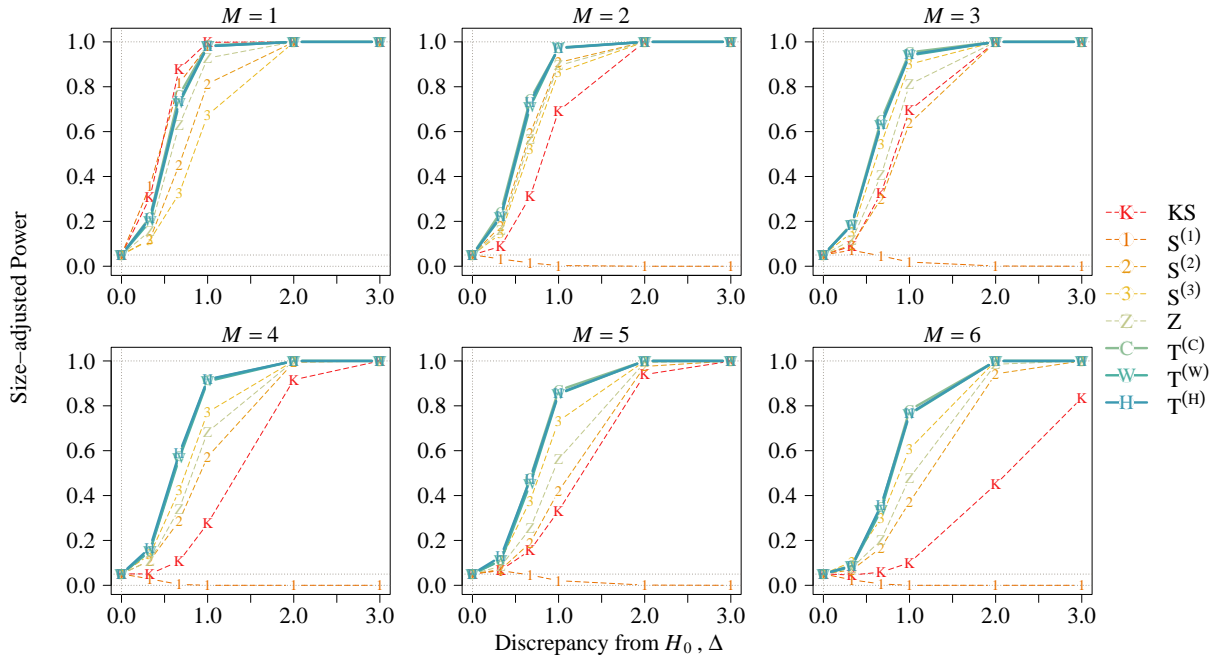


Figure C.15: Size-adjusted power under TAR model with $\varpi_1 = -\varpi_2 = 0.5$ and mean function (C.1).

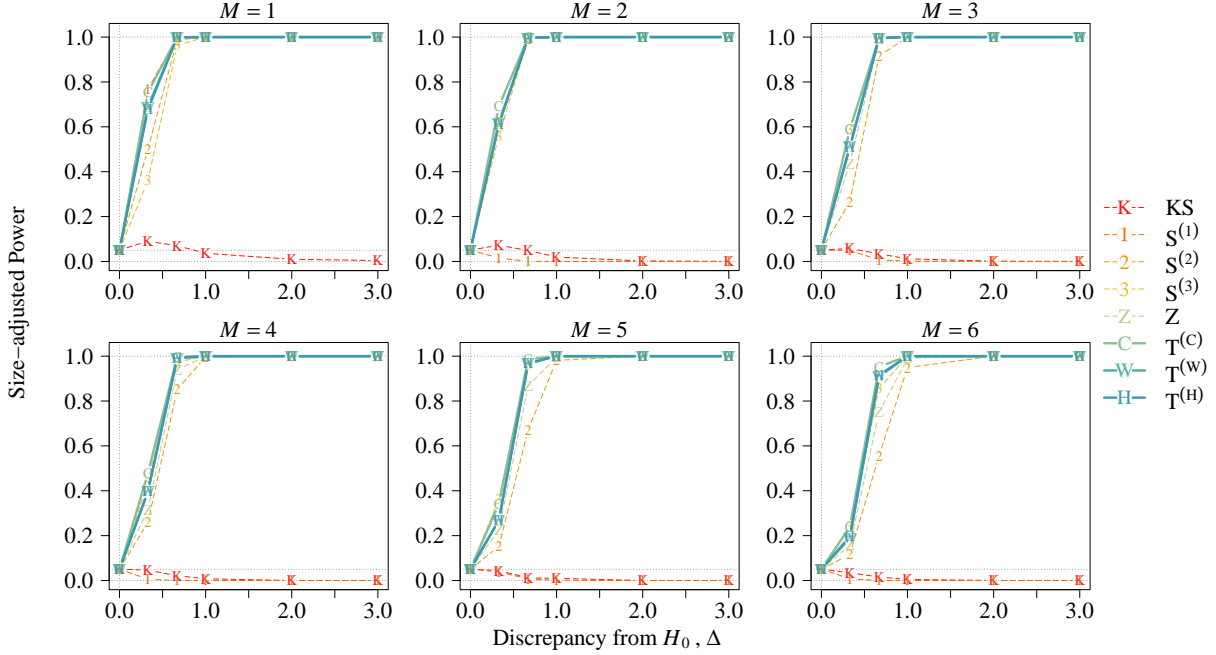


Figure C.16: Size-adjusted power under TAR model with $\varpi_1 = \varpi_2 = -0.5$ and mean function (C.1).

C.5 NAR Model

The data under the NAR model has form $X_i - \mu_i = \varpi |X_{i-1} - \mu_{i-1}| + \varepsilon_i \sqrt{1 - \varpi^2}$, where $\varpi \in (0, 1)$. From Table C.4, the self-normalized tests have similar size distortion when $|\varpi| \leq 0.5$, while KS_n has slightly larger size. When $|\varpi| = 0.8$, $S_n^{(1)}$ and $T_n^{(C)}$ are more accurate than other tests while $T_n^{(W)}$ and $T_n^{(H)}$ are less size distorted comparing to $S_n^{(2)}$, $S_n^{(3)}$ and Z_n . A similar result regarding to the power is observed in Figures C.17–C.20. After adjusting the size, our proposed tests have the highest power in the multiple-CP case and lose the least power among the multiple-CP tests in the single CP case.

Table C.4: Null rejection rates (%) at 5% nominal size under NAR model and mean function (C.1).

ϖ	$n = 200$								$n = 400$							
	KS _n	S _n ⁽¹⁾	S _n ⁽²⁾	S _n ⁽³⁾	Z _n	T _n ^(C)	T _n ^(W)	T _n ^(H)	KS _n	S _n ⁽¹⁾	S _n ⁽²⁾	S _n ⁽³⁾	Z _n	T _n ^(C)	T _n ^(W)	T _n ^(H)
0.8	18.1	6.4	13.1	19.3	14.2	7.6	10.2	9.6	16.0	4.9	7.2	9.5	7.6	4.8	7.1	6.4
0.5	8.2	4.3	5.8	4.4	5.3	4.1	5.2	4.5	6.3	3.9	4.1	4.6	3.8	4.4	5.0	4.9
0.3	7.2	4.7	4.0	3.1	3.9	4.1	4.6	4.7	5.7	4.2	3.4	4.4	3.3	5.0	4.8	4.7
0	7.3	4.8	4.4	2.5	3.3	4.1	5.0	4.9	5.0	3.9	3.2	4.8	3.3	5.1	4.6	4.5
-0.3	7.0	5.1	4.7	3.1	4.6	4.3	4.5	4.7	4.5	4.2	4.1	4.6	3.7	4.8	4.0	4.3
-0.5	8.3	4.9	5.4	5.3	5.1	4.2	4.8	5.1	6.5	5.2	5.2	5.8	4.2	5.5	4.9	5.1
-0.8	18.4	6.3	13.2	18.7	14.2	6.4	10.4	9.9	16.4	5.4	9.3	10.6	9.5	6.0	7.1	6.8

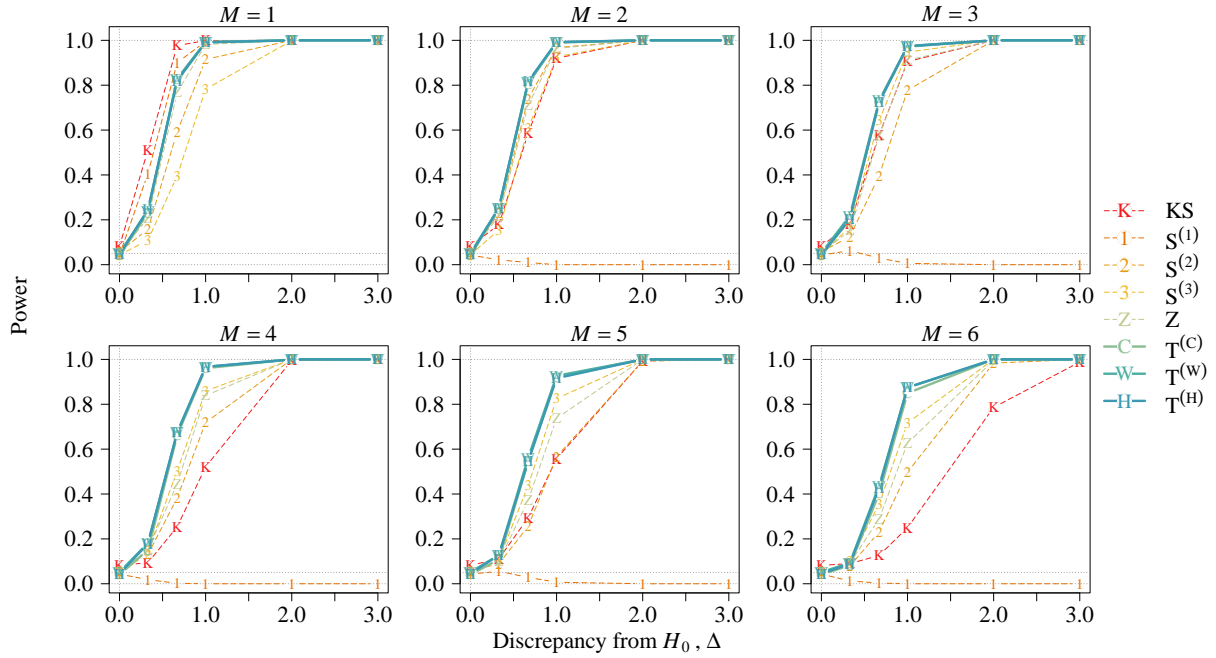
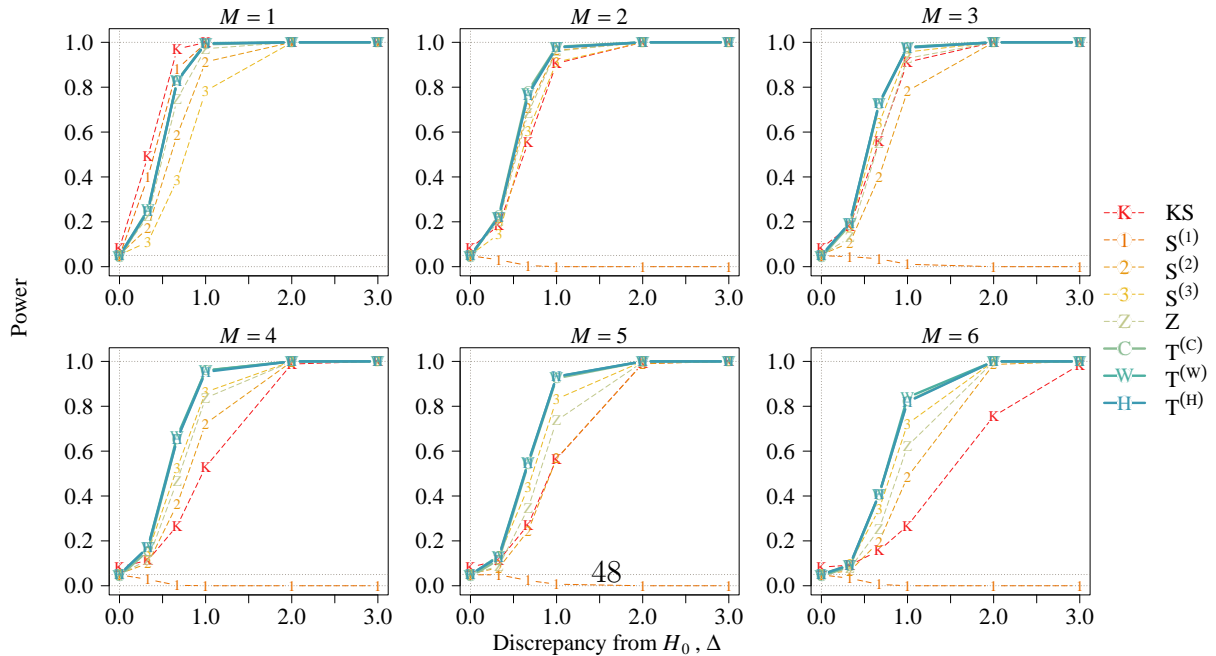


Figure C.17: Power under NAR model with $\varpi = 0.5$ and mean function (C.1).



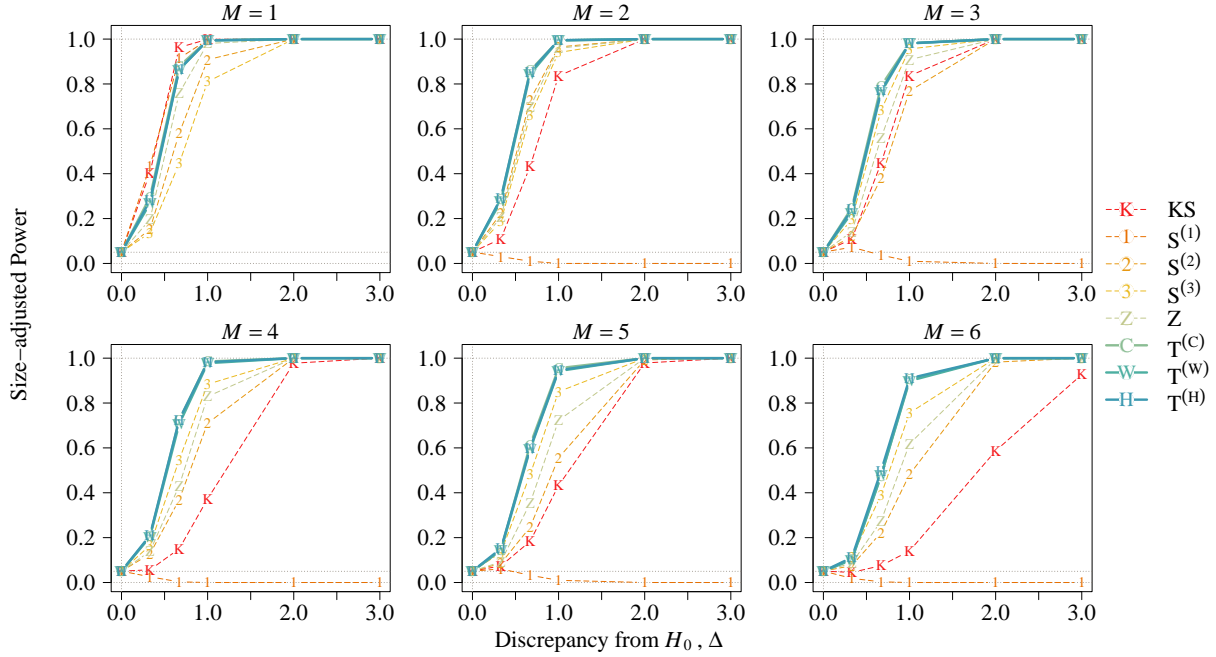


Figure C.19: Size-adjusted power under NAR model with $\varpi = 0.5$ and mean function (C.1).

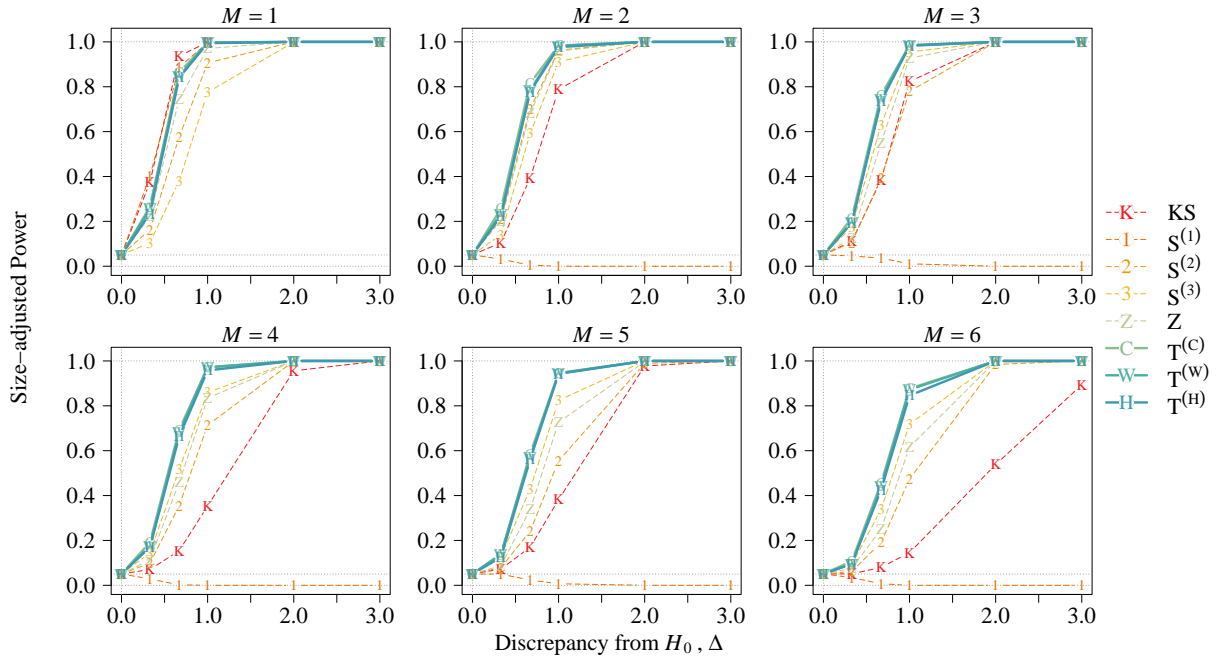


Figure C.20: Size-adjusted power under NAR model with $\varpi = -0.5$ and mean function (C.1).

C.6 BAR Model

Supplementing the result in the main text, we further report the power when $\vartheta = 0.8, -0.8$.

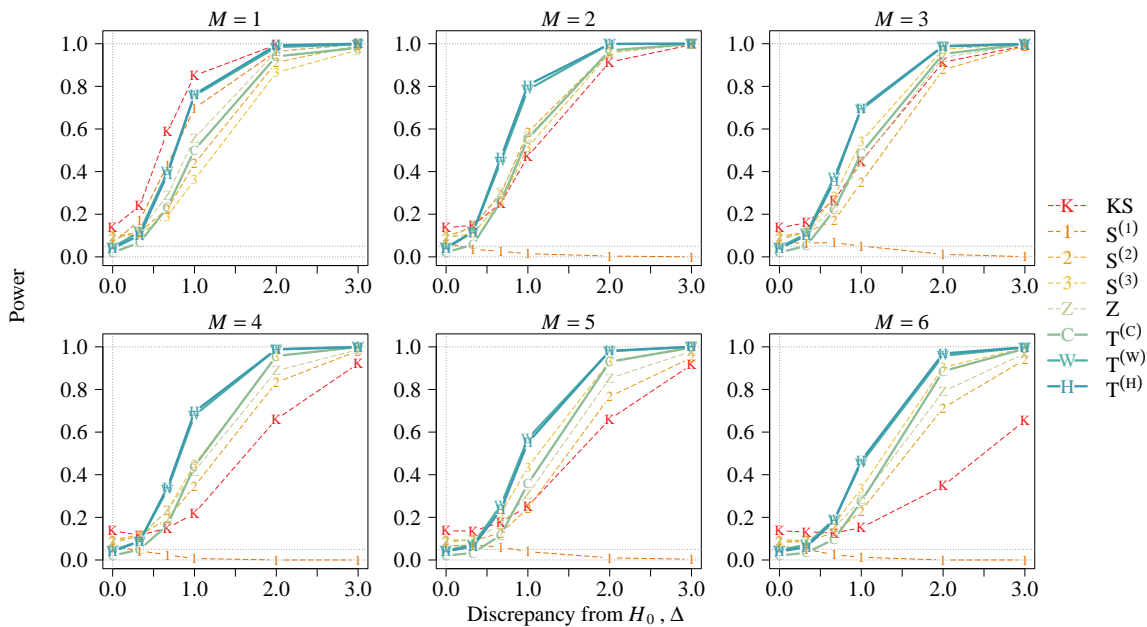


Figure C.21: Power under BAR model with $\varpi = \vartheta = 0.5$ and mean function (C.1).

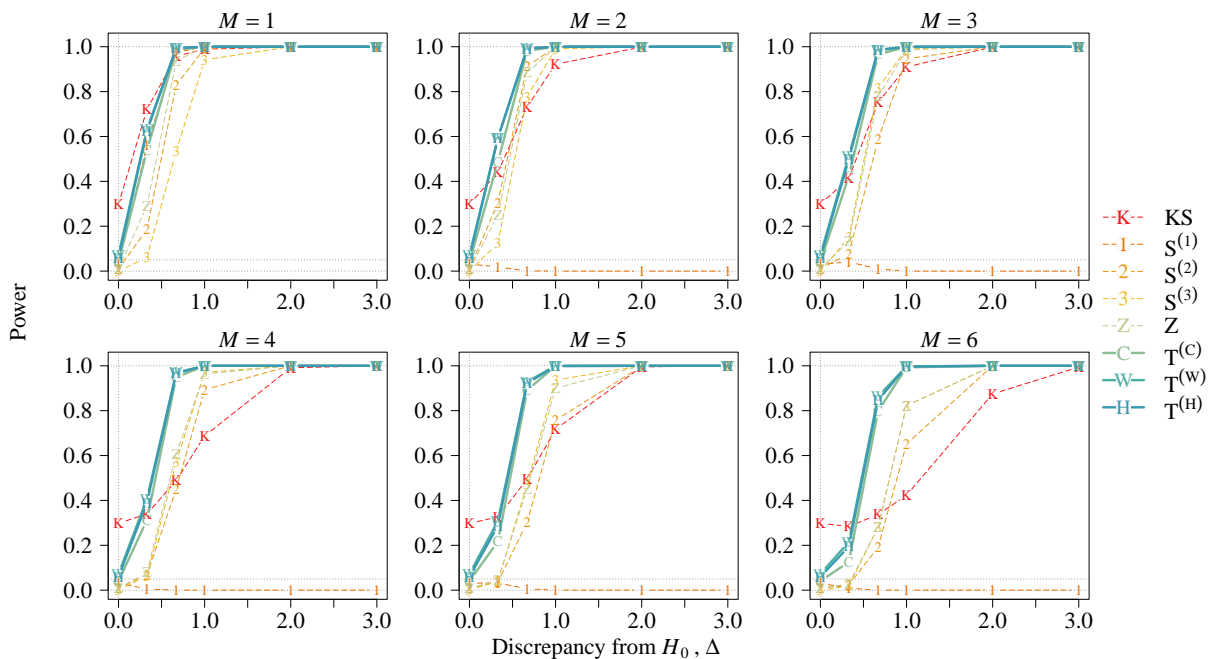


Figure C.22: Power under BAR model with $-\varpi = \vartheta = 0.5$ and mean function (C.1).

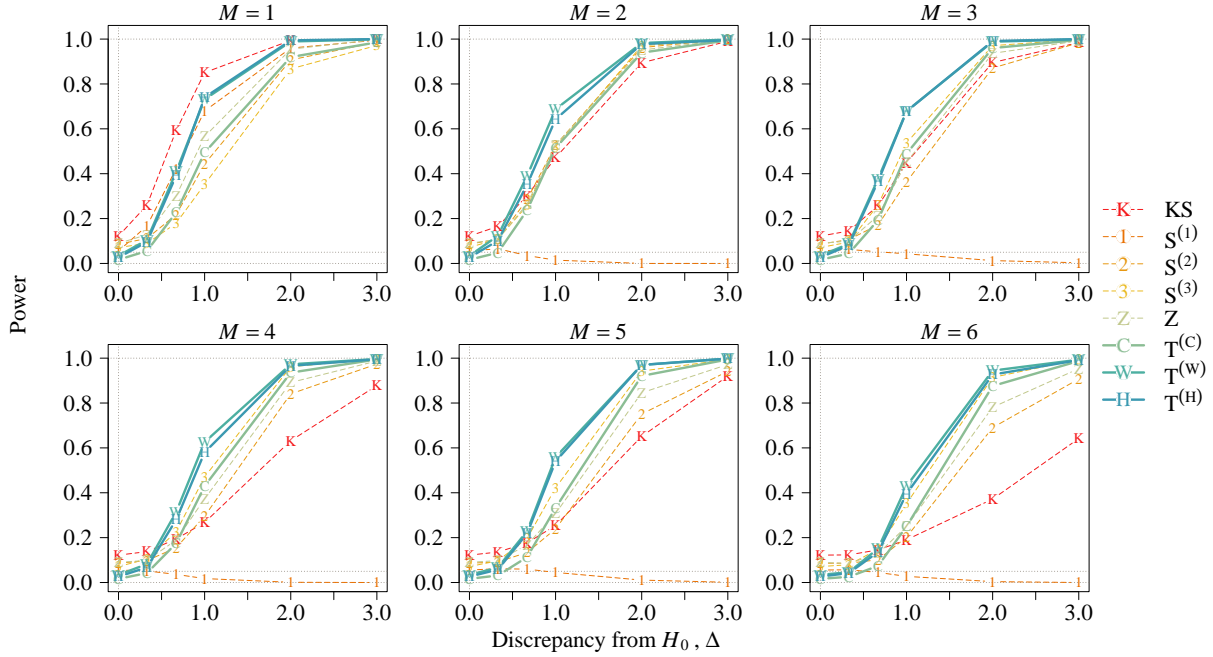


Figure C.23: Power under BAR model with $\varpi = -\vartheta = 0.5$ and mean function (C.1).

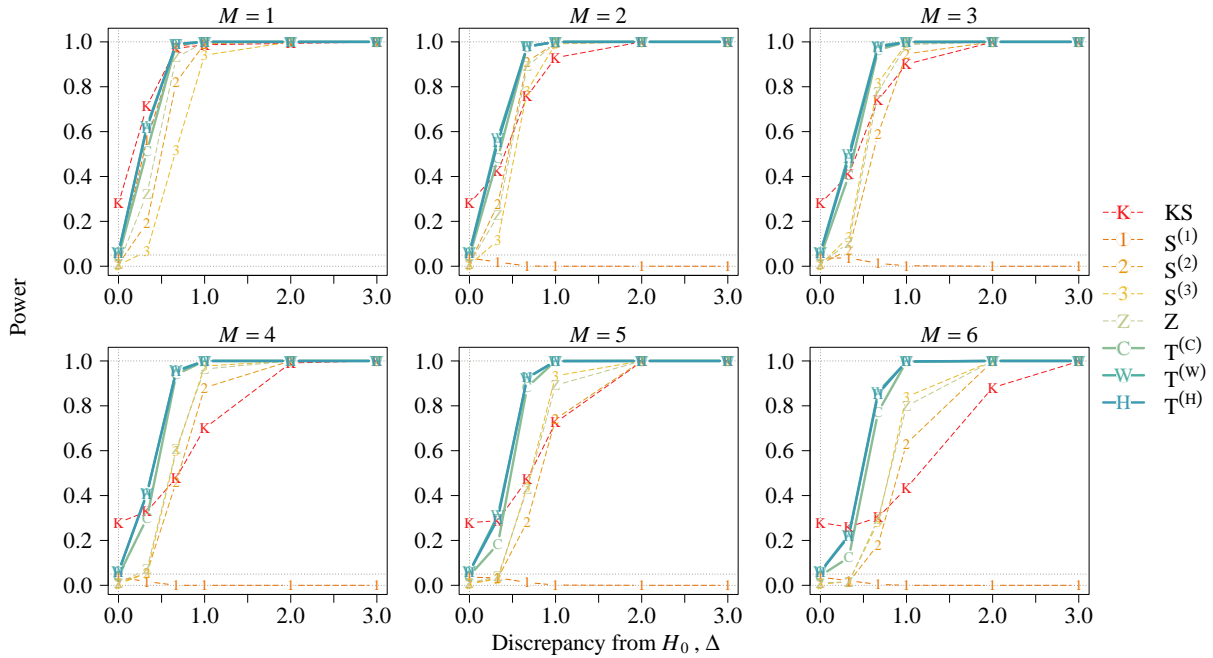


Figure C.24: Power under BAR model with $\varpi = \vartheta = -0.5$ and mean function (C.1).

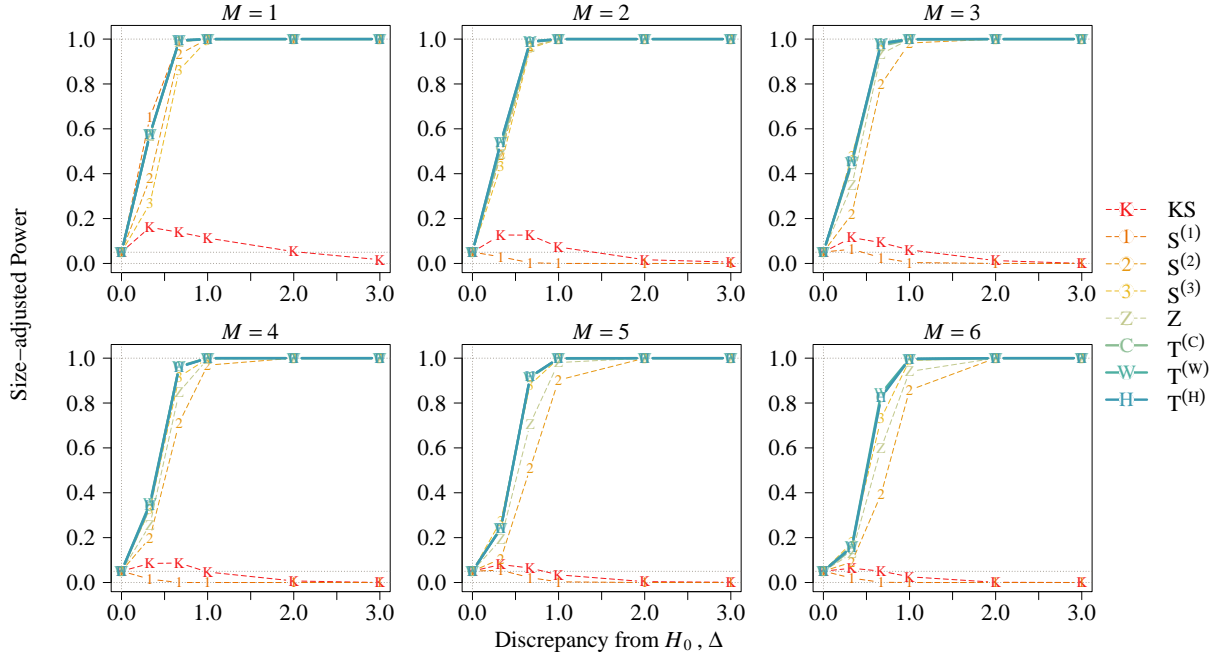


Figure C.25: Size-adjusted power under BAR model with $-\varpi = \vartheta = 0.5$ and mean function (C.1).

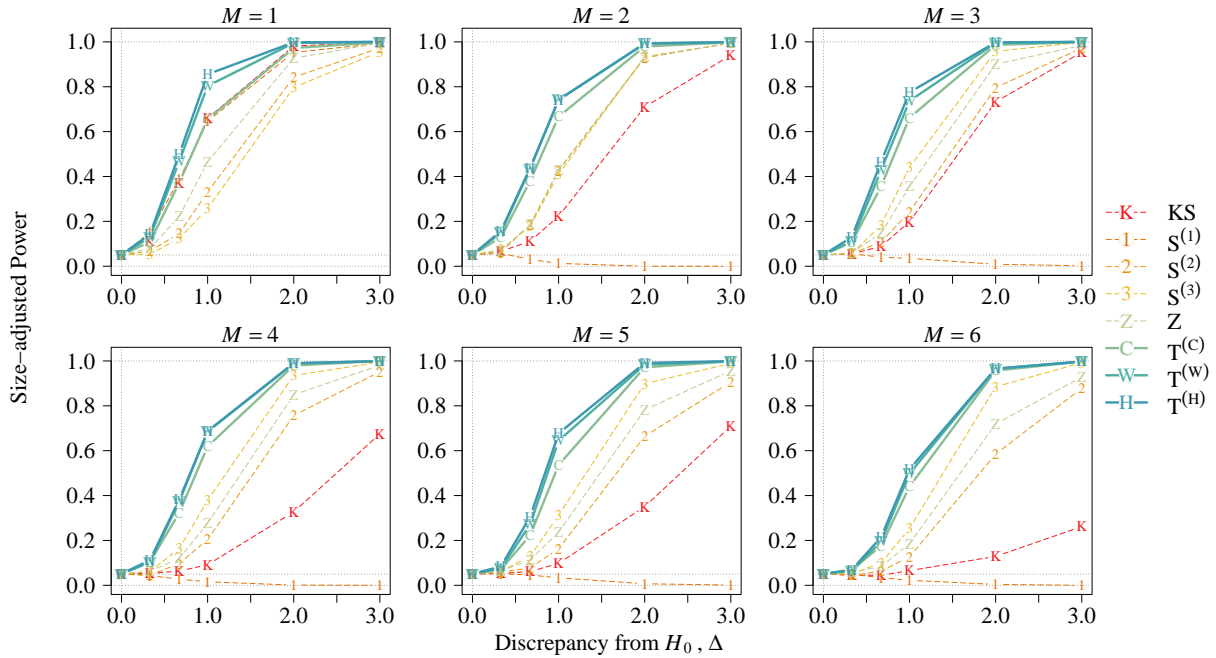


Figure C.26: Size-adjusted power under BAR model with $\varpi = -\vartheta = 0.5$ and mean function (C.1).

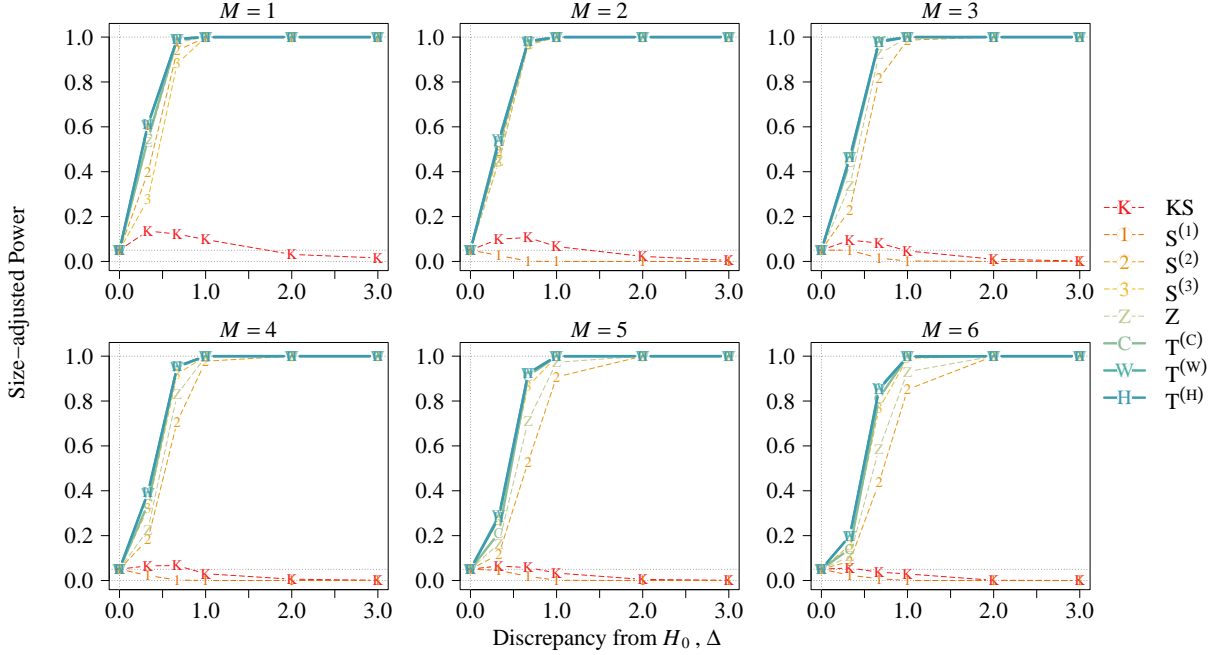


Figure C.27: Size-adjusted power under BAR model with $\varpi = \vartheta = -0.5$ and mean function (C.1).

C.7 Non-Gaussian time series

Consider again the signal-plus-noise model, we further investigate the performance under the AR model and the BAR model if the innovations ε follow the t -distribution with degree of freedom 5 instead of the standard normal distribution. Tables C.5 and C.6 present the size under the AR model and the BAR model respectively. Figures C.28–C.31 and Figures C.32–C.35 present the power under the AR model and the BAR model respectively. Similar result is also observed. Our proposed tests, $T_n^{(C)}$, $T_n^{(W)}$ and $T_n^{(H)}$, have higher size accuracy than other multiple-CP tests. Moreover, our tests have the largest power under multiple-CP case while lose the least power among the multiple-CP tests comparing to AMOC tests KS_n and $S_n^{(1)}$ in single CP case.

Table C.5: Null rejection rates (%) at 5% nominal size under AR model with innovations following t -distribution.

ϖ	$n = 200$									$n = 400$							
	KS $_n$	S $_n^{(1)}$	S $_n^{(2)}$	S $_n^{(3)}$	Z $_n$	T $_n^{(C)}$	T $_n^{(W)}$	T $_n^{(H)}$		KS $_n$	S $_n^{(1)}$	S $_n^{(2)}$	S $_n^{(3)}$	Z $_n$	T $_n^{(C)}$	T $_n^{(W)}$	T $_n^{(H)}$
0.8	53.4	8.4	24.2	41.3	29.5	15.9	25.9	23.8		54.7	6.8	14.1	23.1	17.0	8.8	12.8	12.5
0.5	14.1	6.0	7.4	11.3	8.3	6.5	9.0	9.0		11.1	5.7	6.5	8.1	7.0	4.8	6.4	6.3
0.3	10.6	5.8	5.5	6.3	6.2	5.6	7.7	7.3		8.5	5.2	4.9	4.9	4.8	4.8	6.3	6.2
0	7.4	5.2	3.5	2.5	3.1	4.1	4.7	4.6		5.0	4.2	4.5	4.6	3.8	5.2	4.7	4.2
-0.3	14.6	4.4	2.2	1.5	1.8	5.2	5.9	5.5		10.4	4.9	3.6	2.1	3.1	5.3	5.9	5.8
-0.5	27.6	3.6	1.5	0.6	1.2	5.5	6.1	6.0		19.8	4.7	2.9	1.5	2.3	5.4	6.3	6.4
-0.8	46.9	1.8	0.3	0.0	0.0	8.6	9.0	8.5		41.2	3.7	1.5	0.2	1.0	6.6	7.9	7.3

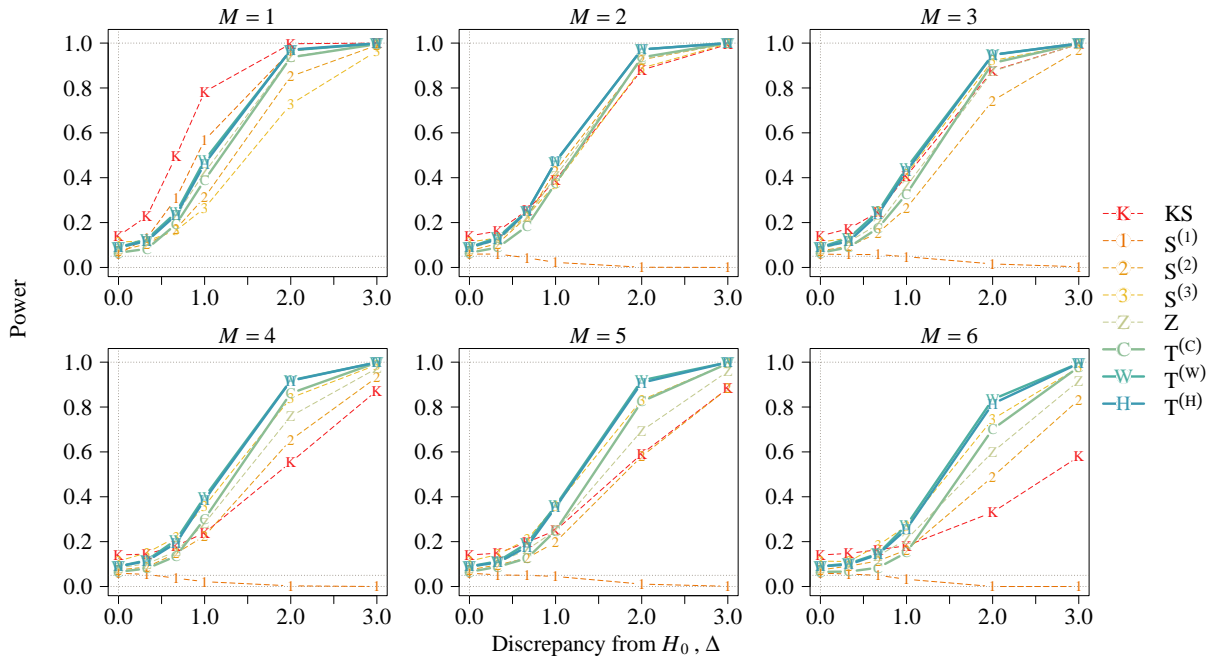


Figure C.28: Power under AR model with $\varpi = 0.5$, mean function (C.1) and innovations following t -distribution.

Table C.6: Null rejection rates (%) at 5% nominal size under BAR model with innovations following t -distribution.

ϑ	ϖ	$n = 200$								$n = 400$							
		KS $_n$	S $_n^{(1)}$	S $_n^{(2)}$	S $_n^{(3)}$	Z $_n$	T $_n^{(C)}$	T $_n^{(W)}$	T $_n^{(H)}$	KS $_n$	S $_n^{(1)}$	S $_n^{(2)}$	S $_n^{(3)}$	Z $_n$	T $_n^{(C)}$	T $_n^{(W)}$	T $_n^{(H)}$
0.8	0.5	15.5	8.1	6.5	3.8	5.7	0.3	4.1	2.2	15.1	7.1	6.3	2.5	4.8	0.8	4.3	3.0
	0.3	17.8	6.7	4.5	2.3	3.4	0.7	3.0	2.7	15.6	7.0	4.2	1.8	3.3	0.9	4.9	4.2
	0	19.7	5.2	2.4	1.1	2.2	0.9	5.7	3.6	16.6	5.9	2.6	0.9	2.0	1.4	6.5	5.1
	-0.3	29.4	5.2	1.9	0.0	1.5	1.0	6.1	4.8	22.6	5.7	1.2	0.4	0.9	0.8	6.9	5.8
	-0.5	31.3	4.7	1.3	0.3	1.0	1.3	7.6	5.0	29.2	6.1	1.6	0.2	0.7	0.8	7.2	5.6
0.5	0.8	27.1	10.3	22.9	20.9	21.3	2.1	10.7	7.5	29.2	8.5	11.6	8.9	11.1	1.0	4.3	4.2
	0.5	14.3	6.0	8.0	6.7	7.2	2.1	4.6	3.8	11.3	5.4	6.8	5.4	6.1	3.0	5.4	4.7
	0.3	12.1	4.8	5.6	3.4	4.6	2.3	4.9	4.1	8.4	5.8	5.6	4.2	5.0	3.9	6.4	6.2
	0	14.6	3.6	3.2	1.7	2.9	2.8	5.4	5.1	10.0	6.6	4.1	2.8	3.7	4.0	6.1	5.7
	-0.3	21.0	3.5	2.1	0.8	1.8	3.3	6.3	5.4	15.7	5.6	2.6	2.1	1.9	4.0	6.2	5.6
-0.5	0.8	28.6	10.4	25.6	22.6	24.4	2.2	10.5	8.3	29.0	9.4	11.2	6.4	10.7	1.3	4.9	3.5
	0.5	13.1	6.9	8.3	6.7	7.5	1.7	4.5	3.7	10.7	6.2	4.2	3.8	3.8	1.8	5.2	4.5
	0.3	11.1	5.4	4.7	2.8	4.6	1.9	4.2	3.7	8.9	5.0	2.9	2.9	2.9	2.2	5.1	4.5
	0	12.5	4.5	2.7	1.7	2.2	2.3	5.4	4.6	9.9	5.4	3.0	1.7	2.0	2.9	5.9	5.2
	-0.3	21.1	4.1	1.8	0.5	1.5	2.3	6.8	6.8	16.1	4.8	2.4	1.2	1.8	3.0	4.9	4.2
-0.8	0.5	18.0	6.9	8.8	3.4	5.9	0.3	4.3	3.1	14.9	5.9	3.6	1.4	3.0	0.2	2.7	1.8
	0.3	17.4	5.6	4.7	1.7	3.7	0.4	4.3	3.2	14.9	6.0	2.7	1.1	2.1	0.7	4.6	3.5
	0	20.4	4.2	2.7	0.9	2.1	0.7	4.9	2.5	16.2	6.1	1.9	0.4	1.5	0.8	4.8	4.1
	-0.3	25.9	5.2	1.3	0.1	1.3	0.7	6.5	5.5	23.7	6.0	2.0	0.7	1.3	0.8	5.5	4.4
	-0.5	34.0	4.8	2.2	0.3	1.7	1.0	7.9	6.0	30.5	5.4	1.7	0.4	0.8	0.7	5.2	4.7

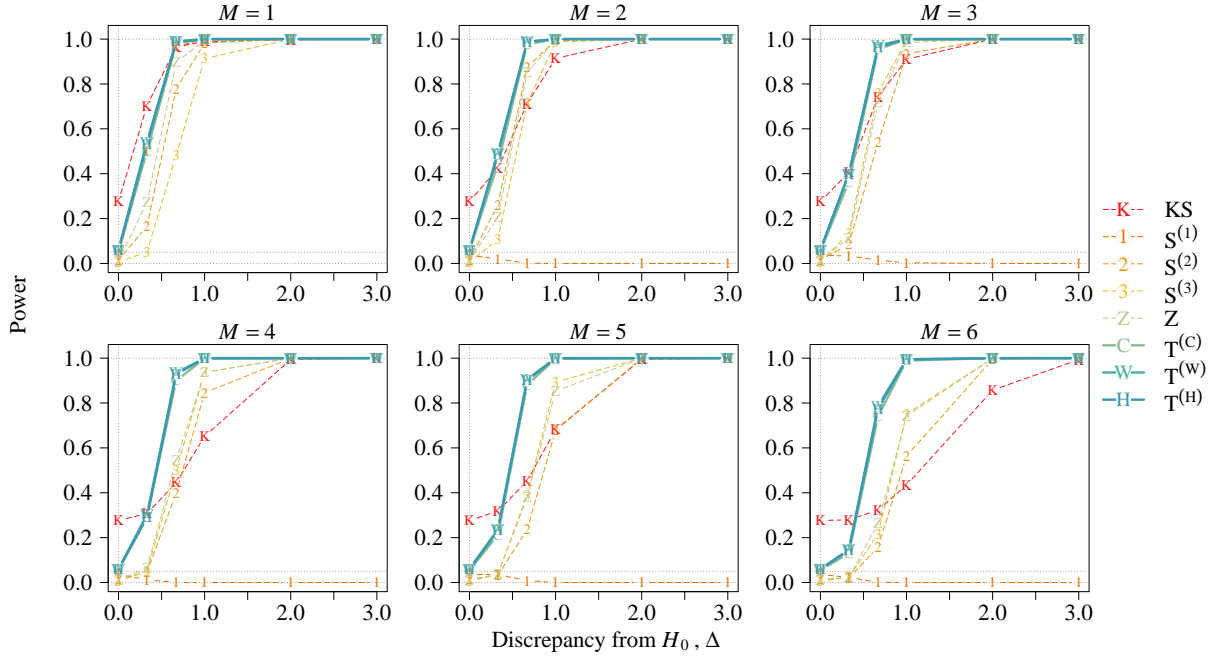


Figure C.29: Power under AR model with $\varpi = -0.5$, mean function (C.1) and innovations following t -distribution.

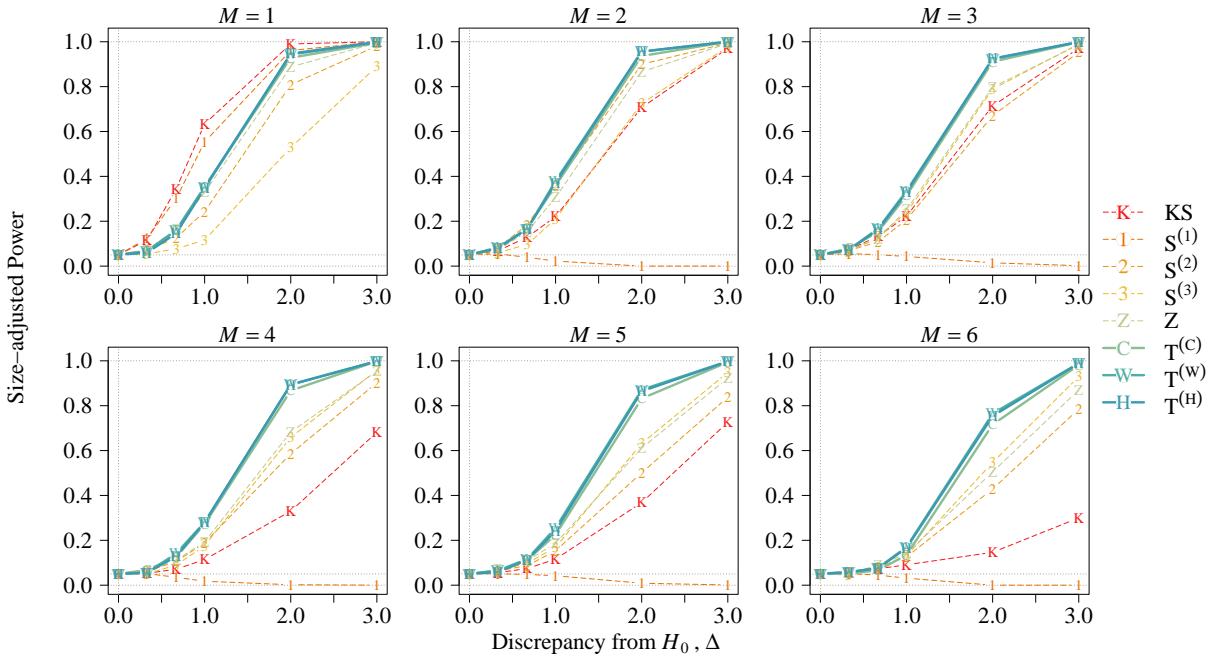


Figure C.30: Size-adjusted power under AR model with $\varpi = 0.5$, mean function (C.1) and innovations following t -distribution.

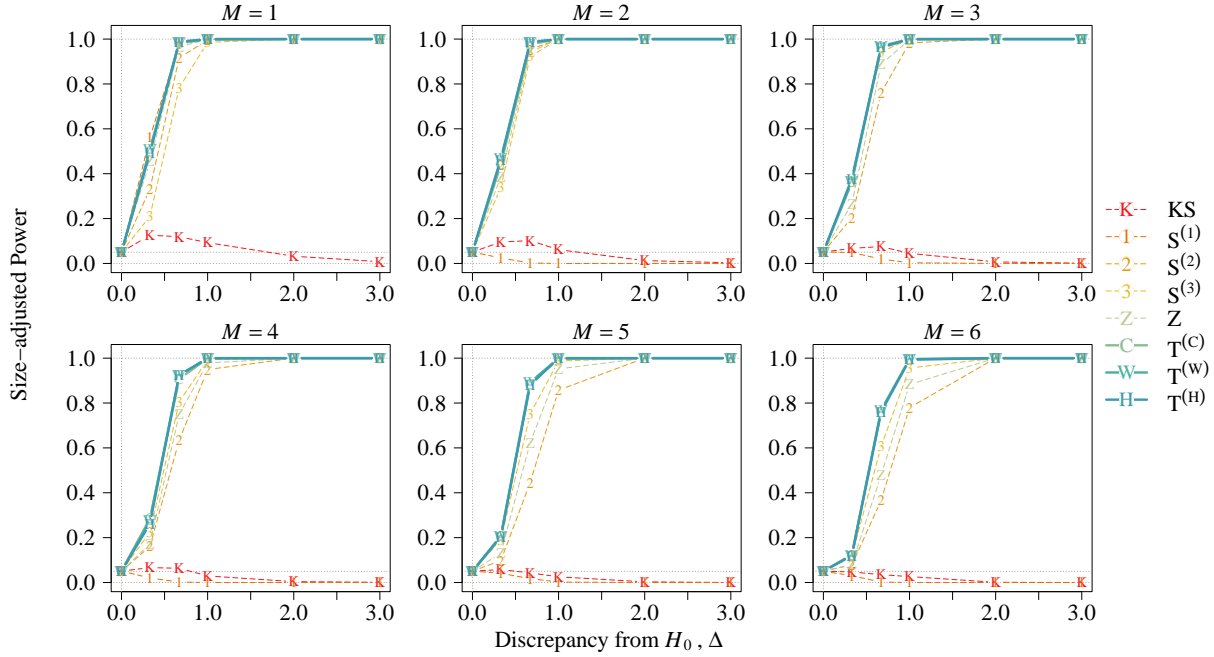


Figure C.31: Size-adjusted power under AR model with $\varpi = -0.5$, mean function (C.1) and innovations following t -distribution.

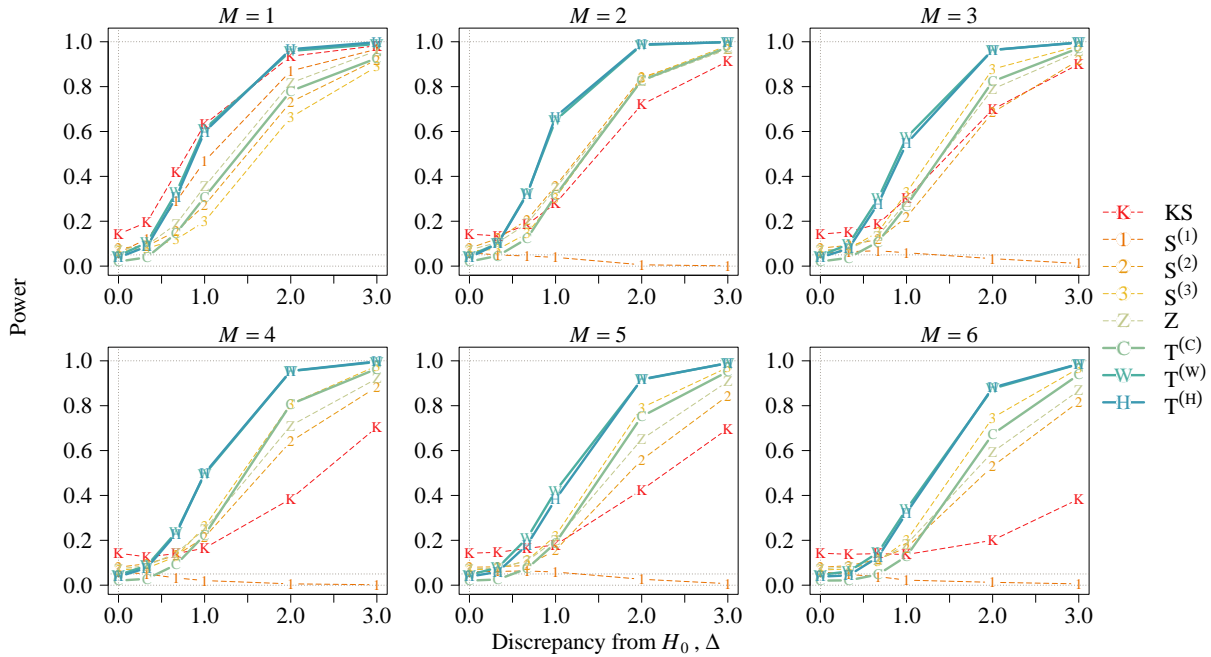


Figure C.32: Power under BAR model with $\varpi = \vartheta = 0.5$, mean function (C.1) and innovations following t -distribution.

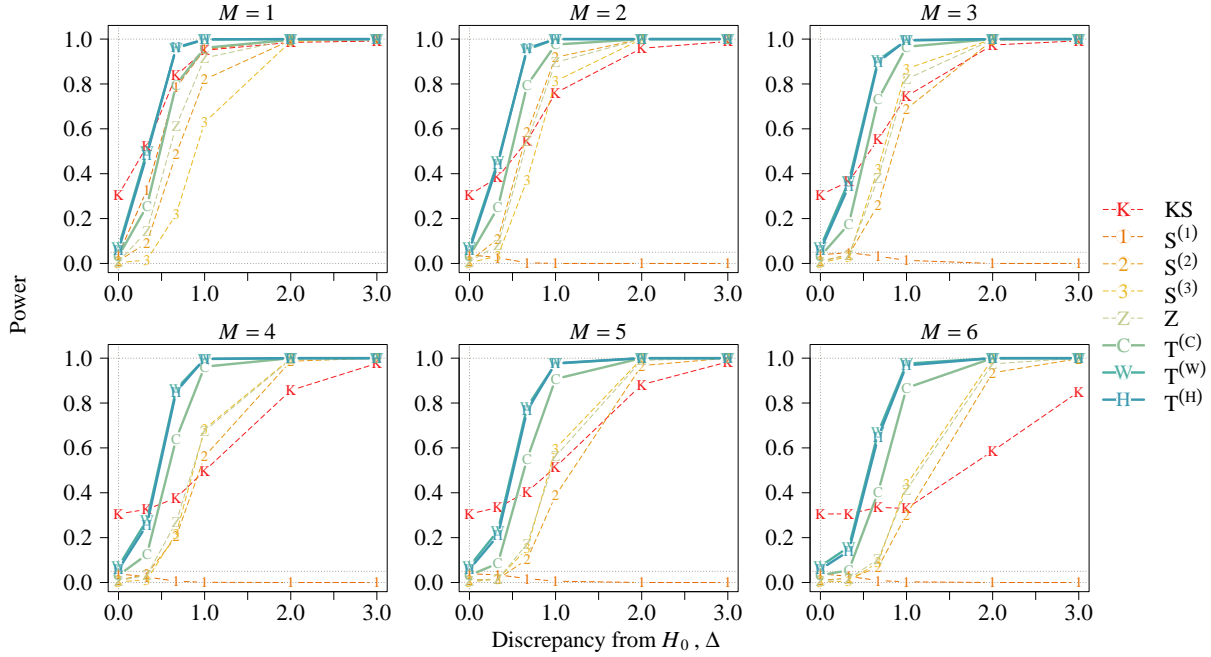


Figure C.33: Power under BAR model with $-\varpi = \vartheta = 0.5$, mean function (C.1) and innovations following t -distribution.

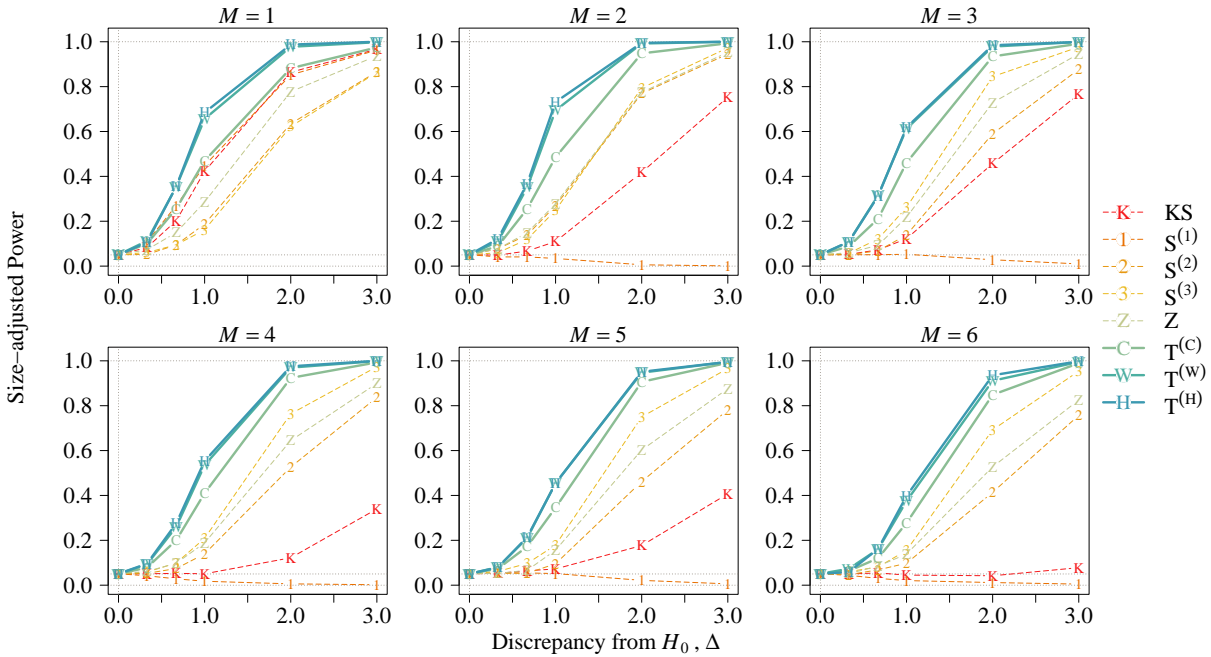


Figure C.34: Size-adjusted power under BAR model with $\varpi = \vartheta = 0.5$, mean function (C.1) and innovations following t -distribution.

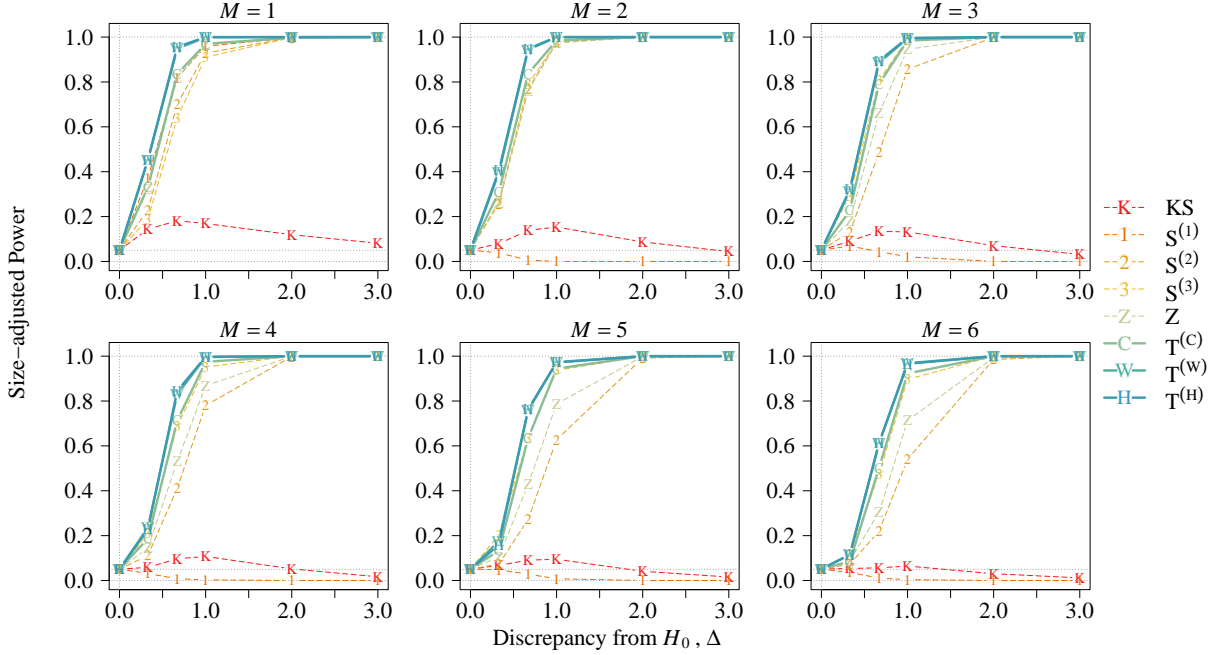


Figure C.35: Size-adjusted power under BAR model with $-\varpi = \vartheta = 0.5$, mean function (C.1) and innovations following t -distribution.

C.8 Unequal change magnitudes

This section extends the simulation results of Section 6.3 in the main text. The CP models, Cases 1 and 2, are defined in Section 6.3 in the main text. Figures C.36–C.37 and C.38–C.40 present the size-adjusted power under the AR and BAR models respectively. The result indicates that Zhang and Lavitas (2018)’s proposed test Z_n suffers larger reduction in power comparing to our proposed tests when the first and the last changes are reduced by half. Therefore, our proposed tests are more general and capable to capture all change structure, while Z_n tends to capture the first and the last CPs.

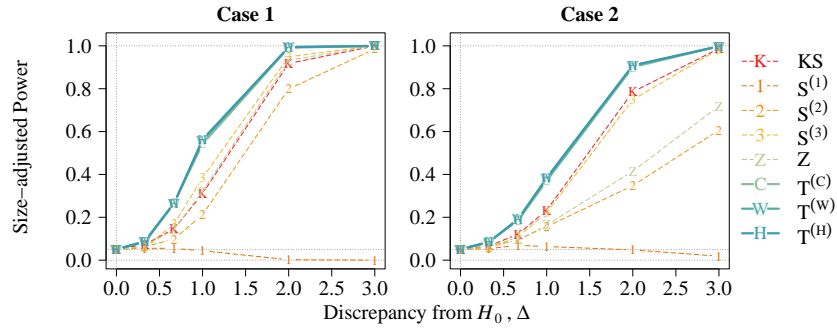


Figure C.36: Size-adjusted power under AR model with $\varpi = 0.5$, $n = 200$ and mean functions in Cases 1 and 2.

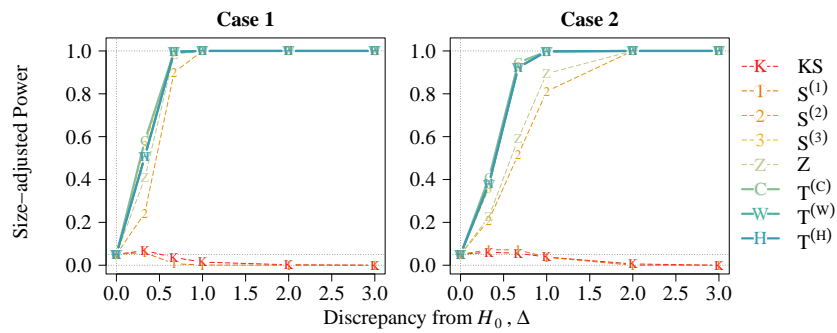


Figure C.37: Size-adjusted power under AR model with $\varpi = -0.5$, $n = 200$ and mean functions in Cases 1 and 2.

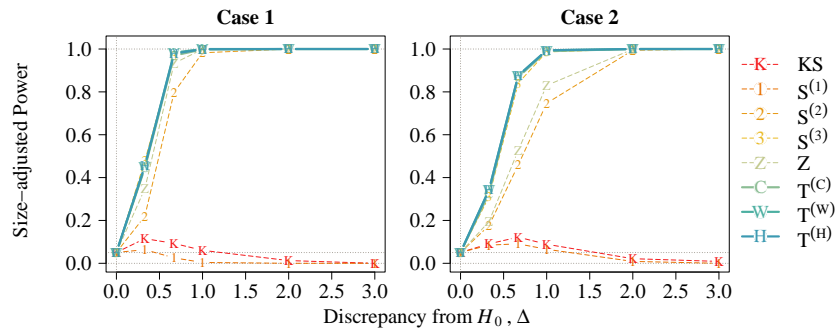


Figure C.38: Size-adjusted power under BAR model with $-\varpi = \vartheta = 0.5$, $n = 200$ and mean functions in Cases 1 and 2.

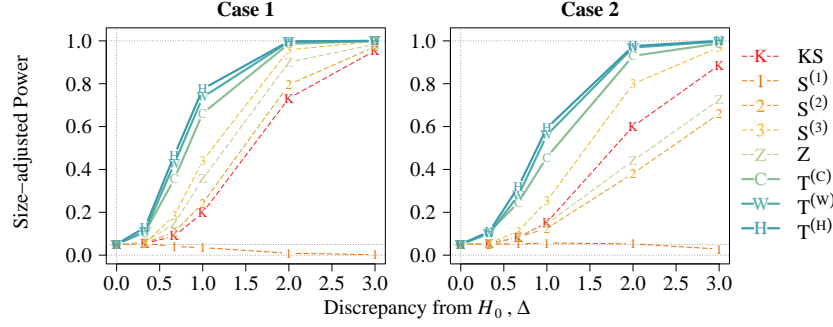


Figure C.39: Size-adjusted power under BAR model with $\varpi = -\vartheta = 0.5$, $n = 200$ and mean functions in Cases 1 and 2.

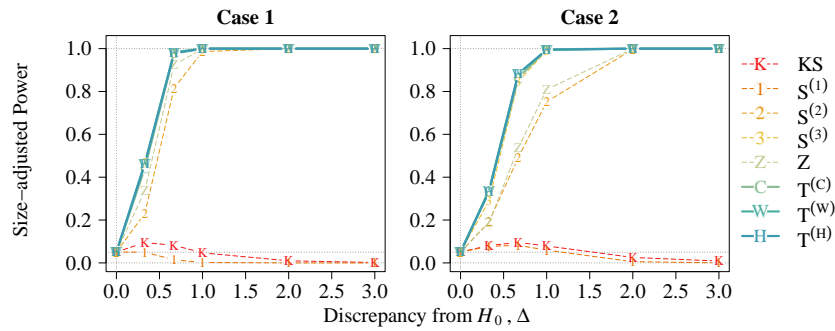


Figure C.40: Size-adjusted power under BAR model with $\varpi = \vartheta = -0.5$, $n = 200$ and mean functions in Cases 1 and 2.

C.9 Nonsymmetric windows

This section presents simulation result supplementing Section 6.4 in the main text. The mean functions, Cases 1 and 3 are defined in Section 6.3 and 6.4 in the main text respectively. The size-adjusted power is presented in Figures C.41–C.42 under the AR model and in Figure C.43 under the BAR model when $-\varpi = \vartheta = 0.5$. From the result, we do not observe significant difference in power after nonsymmetric windows are used. Therefore, using nonsymmetric windows does not give significant improvement in power in general.

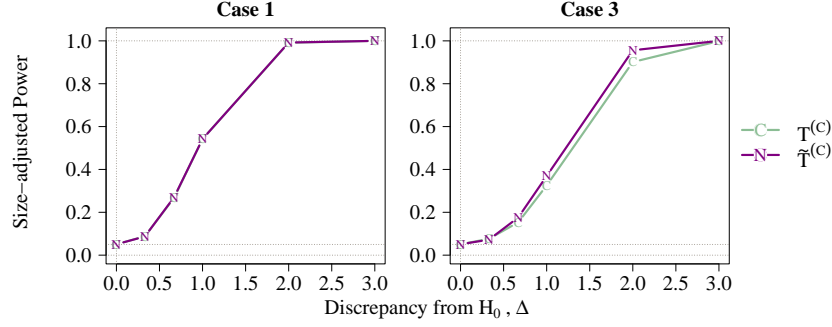


Figure C.41: Size-adjusted power under AR model with $\varpi = 0.5$ and mean functions in Cases 1 and 3.

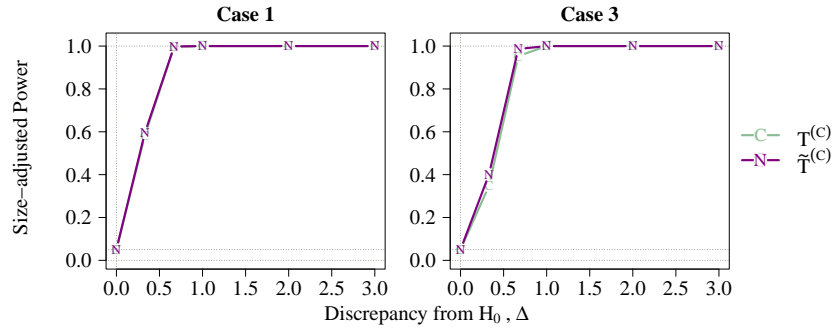


Figure C.42: Size-adjusted power under AR model with $\varpi = -0.5$ and mean functions in Cases 1 and 3.

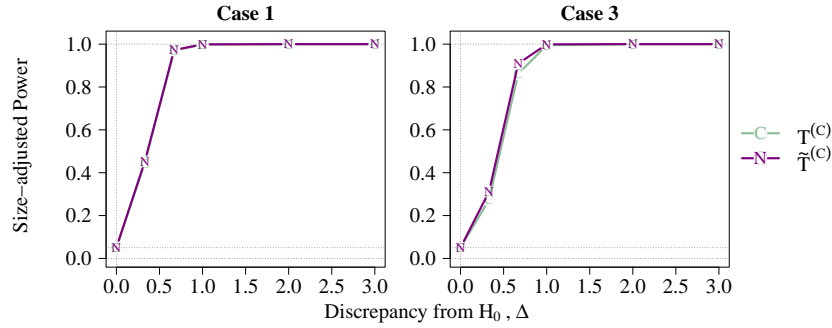


Figure C.43: Size-adjusted power under BAR model with $-\varpi = \vartheta = 0.5$ and mean functions in Cases 1 and 3.

C.10 Conclusion

Our proposed tests in general control the size well. We also observed that non-self-normalized KS test has larger size distortion than self-normalized tests. The results agree to [Kiefer and Vogelsang \(2002\)](#) and [Shao \(2015\)](#). Our proposed tests also have larger power comparing to the state-of-art self-normalized multiple-CP tests, $S_n^{(2)}$, $S_n^{(3)}$ and Z_n . Under

Table D.1: The finite- n adjusted critical values $c_\alpha(n, \rho)$ of $T_n^{(\aleph)}$ under $\alpha = 10\%$ nominal size.

$n \setminus \rho$	-0.9	-0.8	-0.7	-0.6	-0.5	-0.4	-0.3	-0.2	-0.1	0	0.1	0.2	0.3	0.4	0.5	0.6	0.7	0.8	0.9
100	6.8	8.4	9.6	10.7	11.5	12.4	13.1	13.9	14.7	15.5	16.5	17.6	18.9	20.6	22.9	26.2	30.9	38.1	48.0
200	8.5	10.5	11.8	12.8	13.5	14.1	14.7	15.1	15.6	16.1	16.6	17.2	17.9	18.8	20.0	21.7	24.7	30.0	41.2
300	9.8	11.9	13.1	13.9	14.5	15.0	15.4	15.8	16.1	16.4	16.8	17.1	17.6	18.2	18.9	20.1	22.0	25.9	35.6
400	10.7	12.8	13.9	14.6	15.2	15.6	15.9	16.1	16.4	16.6	16.9	17.1	17.4	17.8	18.4	19.2	20.6	23.5	31.6
500	11.4	13.5	14.5	15.1	15.6	15.9	16.1	16.3	16.5	16.7	16.9	17.1	17.3	17.6	18.0	18.7	19.8	22.0	28.8
600	12.0	14.0	14.9	15.5	15.9	16.1	16.4	16.5	16.7	16.8	17.0	17.1	17.3	17.5	17.9	18.4	19.2	21.1	26.8
700	12.5	14.4	15.3	15.8	16.1	16.4	16.5	16.7	16.8	16.9	17.0	17.1	17.3	17.5	17.7	18.1	18.9	20.4	25.3
800	13.0	14.8	15.6	16.0	16.3	16.5	16.6	16.8	16.9	17.0	17.1	17.2	17.3	17.4	17.6	18.0	18.6	19.9	24.2
900	13.3	15.0	15.8	16.2	16.5	16.6	16.8	16.9	17.0	17.0	17.1	17.2	17.3	17.4	17.6	17.9	18.4	19.5	23.3
1000	13.6	15.3	16.0	16.3	16.6	16.7	16.8	16.9	17.0	17.1	17.1	17.2	17.3	17.4	17.6	17.8	18.3	19.3	22.6
2000	16.7	16.9	17.0	17.1	17.2	17.2	17.3	17.2	17.3	17.3	17.3	17.3	17.3	17.3	17.3	17.3	17.4	17.7	18.6
3000	16.9	17.2	17.3	17.3	17.4	17.4	17.4	17.4	17.4	17.4	17.4	17.4	17.4	17.4	17.4	17.4	17.4	17.5	18.0
4000	17.1	17.3	17.4	17.5	17.5	17.5	17.5	17.5	17.5	17.5	17.4	17.4	17.4	17.4	17.4	17.5	17.5	17.5	17.8
5000	17.2	17.4	17.5	17.5	17.6	17.6	17.5	17.5	17.5	17.5	17.5	17.5	17.5	17.5	17.5	17.5	17.4	17.5	17.6
6000	17.3	17.5	17.6	17.6	17.6	17.6	17.6	17.6	17.6	17.5	17.5	17.5	17.5	17.5	17.5	17.5	17.5	17.5	17.6
7000	17.4	17.6	17.6	17.6	17.6	17.6	17.6	17.6	17.6	17.6	17.5	17.5	17.5	17.5	17.5	17.5	17.5	17.5	17.6
8000	17.5	17.6	17.6	17.7	17.6	17.6	17.6	17.6	17.6	17.6	17.6	17.6	17.6	17.5	17.5	17.5	17.5	17.5	17.5
9000	17.5	17.6	17.6	17.7	17.7	17.6	17.6	17.6	17.6	17.6	17.6	17.6	17.6	17.5	17.5	17.5	17.5	17.5	17.5
10000	17.6	17.7	17.7	17.8	17.7	17.7	17.7	17.7	17.6	17.6	17.6	17.6	17.5	17.5	17.5	17.4	17.4	17.4	17.5

the BAR model, our proposed tests even outperform the AMOC tests, $S_n^{(1)}$ and KS_n , in the single CP case. Moreover, the oracle tests $S_n^{(2)}$ and $S_n^{(3)}$ have smaller power comparing to our proposed tests even when the number of CP is correctly specified. It demonstrates that knowing the exact number of CPs does not give a significant advantage in CP detection.

D Finite-sample adjusted critical value

The finite- n adjusted critical values $c_\alpha(n, \rho)$ for $T_n^{(\aleph)}$ at size $\alpha \in \{0.1, 0.05, 0.01\}$ are presented in Tables D.1, D.2 and D.3, respectively, where $n \in \{100, 200, \dots, 1000, 2000, \dots, 10000\}$ and $\rho \in \{0, \pm 0.1, \dots, \pm 0.9\}$. Here the critical values are valid for $\aleph \in \{C, W, H, G\}$. The critical values $c_\alpha(n, \rho)$'s are computed using 200000 replications under autoregressive AR(1) models for each sample sizes $n = 100, \dots, 1000$ and AR parameter $\rho \in \{0, \pm 0.1, \dots, \pm 0.9\}$, with standard normal innovations.

Table D.2: The finite- n adjusted critical values $c_\alpha(n, \rho)$ of $T_n^{(N)}$ under $\alpha = 5\%$ nominal size.

$n \setminus \rho$	-0.9	-0.8	-0.7	-0.6	-0.5	-0.4	-0.3	-0.2	-0.1	0	0.1	0.2	0.3	0.4	0.5	0.6	0.7	0.8	0.9
100	7.6	9.4	10.8	11.9	12.9	13.9	14.7	15.6	16.5	17.5	18.5	19.8	21.3	23.3	25.9	29.5	34.8	42.5	52.9
200	9.5	11.8	13.2	14.2	15.1	15.8	16.3	16.9	17.4	18.0	18.6	19.2	20.0	21.0	22.4	24.4	27.7	33.7	45.7
300	10.9	13.2	14.6	15.5	16.2	16.7	17.2	17.6	18.0	18.3	18.7	19.2	19.7	20.3	21.2	22.5	24.7	29.1	39.8
400	11.9	14.2	15.5	16.3	16.9	17.3	17.7	18.0	18.3	18.5	18.8	19.1	19.5	19.9	20.6	21.5	23.2	26.4	35.5
500	12.7	15.0	16.1	16.8	17.3	17.7	18.0	18.2	18.5	18.7	18.9	19.1	19.4	19.7	20.2	20.9	22.2	24.8	32.4
600	13.4	15.6	16.6	17.3	17.7	18.0	18.2	18.4	18.6	18.8	18.9	19.1	19.3	19.6	20.0	20.6	21.5	23.7	30.1
700	13.9	16.0	17.0	17.5	17.9	18.2	18.4	18.6	18.7	18.9	19.0	19.1	19.3	19.5	19.8	20.3	21.1	22.9	28.5
800	14.4	16.4	17.3	17.8	18.1	18.4	18.5	18.7	18.8	18.9	19.0	19.1	19.3	19.5	19.7	20.1	20.8	22.3	27.2
900	14.8	16.7	17.6	18.0	18.3	18.5	18.7	18.8	18.9	19.0	19.1	19.2	19.3	19.4	19.6	20.0	20.6	21.9	26.2
1000	15.1	17.0	17.7	18.2	18.4	18.6	18.7	18.8	18.9	19.0	19.1	19.1	19.2	19.4	19.6	19.8	20.4	21.5	25.3
2000	18.8	18.8	19.0	19.1	19.1	19.1	19.2	19.2	19.3	19.3	19.3	19.2	19.3	19.3	19.3	19.3	19.4	19.7	20.9
3000	18.9	19.1	19.2	19.3	19.3	19.3	19.4	19.3	19.4	19.4	19.4	19.4	19.3	19.4	19.3	19.4	19.4	19.5	20.1
4000	19.0	19.2	19.3	19.4	19.4	19.5	19.4	19.4	19.5	19.4	19.4	19.4	19.4	19.4	19.4	19.4	19.4	19.5	19.8
5000	19.2	19.3	19.5	19.5	19.5	19.5	19.5	19.5	19.5	19.5	19.5	19.5	19.5	19.5	19.4	19.4	19.5	19.5	19.7
6000	19.3	19.4	19.5	19.5	19.6	19.6	19.5	19.6	19.5	19.5	19.5	19.5	19.5	19.5	19.4	19.4	19.5	19.5	19.6
7000	19.4	19.5	19.5	19.6	19.6	19.6	19.6	19.6	19.6	19.5	19.5	19.5	19.5	19.5	19.5	19.5	19.4	19.5	19.6
8000	19.5	19.6	19.6	19.6	19.6	19.6	19.6	19.6	19.6	19.5	19.5	19.5	19.5	19.5	19.5	19.5	19.5	19.5	19.5
9000	19.5	19.6	19.6	19.6	19.6	19.6	19.6	19.6	19.6	19.5	19.5	19.5	19.5	19.5	19.5	19.5	19.4	19.5	19.5
10000	19.5	19.7	19.7	19.7	19.7	19.6	19.6	19.6	19.6	19.6	19.5	19.5	19.5	19.6	19.4	19.4	19.4	19.4	19.5

Table D.3: The finite- n adjusted critical values $c_\alpha(n, \rho)$ of $T_n^{(N)}$ under $\alpha = 1\%$ nominal size.

$n \setminus \rho$	-0.9	-0.8	-0.7	-0.6	-0.5	-0.4	-0.3	-0.2	-0.1	0	0.1	0.2	0.3	0.4	0.5	0.6	0.7	0.8	0.9
100	9.5	11.6	13.3	14.7	15.9	17.0	18.1	19.2	20.3	21.5	22.9	24.5	26.4	28.8	32.1	36.6	43.0	51.9	63.8
200	11.7	14.4	16.1	17.4	18.4	19.2	20.0	20.7	21.4	22.1	22.8	23.6	24.6	25.9	27.7	30.2	34.3	41.4	55.5
300	13.3	16.1	17.8	18.8	19.7	20.4	20.9	21.4	21.9	22.4	22.9	23.4	24.1	24.9	26.0	27.7	30.5	36.0	49.1
400	14.6	17.4	18.9	19.9	20.6	21.1	21.6	22.0	22.3	22.7	23.0	23.4	23.9	24.4	25.3	26.5	28.5	32.7	43.9
500	15.5	18.3	19.7	20.5	21.2	21.6	22.0	22.3	22.6	22.8	23.1	23.4	23.8	24.3	24.9	25.8	27.4	30.7	40.1
600	16.3	18.9	20.2	21.0	21.5	21.9	22.2	22.4	22.7	22.9	23.1	23.3	23.6	24.0	24.5	25.3	26.5	29.2	37.4
700	16.9	19.4	20.6	21.3	21.7	22.0	22.3	22.5	22.7	22.9	23.1	23.3	23.5	23.8	24.2	24.8	25.9	28.1	35.2
800	17.5	19.9	21.0	21.6	22.0	22.3	22.5	22.7	22.9	23.0	23.2	23.3	23.5	23.7	24.1	24.6	25.5	27.5	33.6
900	18.0	20.2	21.3	21.8	22.2	22.5	22.7	22.8	22.9	23.1	23.2	23.3	23.5	23.7	24.0	24.4	25.3	26.9	32.4
1000	18.4	20.5	21.5	22.0	22.3	22.6	22.7	22.9	23.0	23.1	23.2	23.3	23.5	23.6	23.9	24.3	25.0	26.5	31.4
2000	23.2	22.9	23.0	23.1	23.3	23.3	23.3	23.2	23.4	23.4	23.4	23.4	23.4	23.3	23.4	23.6	23.6	24.1	25.9
3000	23.1	23.1	23.3	23.4	23.4	23.4	23.4	23.4	23.5	23.5	23.5	23.5	23.5	23.5	23.5	23.6	23.6	23.8	24.7
4000	23.2	23.4	23.5	23.6	23.6	23.5	23.6	23.5	23.6	23.6	23.5	23.6	23.7	23.6	23.5	23.6	23.6	23.7	24.3
5000	23.2	23.4	23.5	23.6	23.6	23.7	23.6	23.6	23.6	23.6	23.5	23.6	23.6	23.6	23.5	23.5	23.6	23.7	24.0
6000	23.3	23.5	23.6	23.7	23.7	23.8	23.6	23.6	23.8	23.6	23.6	23.6	23.6	23.7	23.6	23.6	23.6	23.6	23.9
7000	23.5	23.6	23.6	23.8	23.7	23.7	23.7	23.8	23.7	23.6	23.7	23.7	23.7	23.6	23.6	23.6	23.6	23.6	23.8
8000	23.7	23.7	23.7	23.9	23.8	23.7	23.8	23.8	23.8	23.6	23.7	23.8	23.8	23.7	23.6	23.6	23.7	23.7	23.8
9000	23.7	23.8	23.7	23.9	23.8	23.7	23.8	23.8	23.8	23.6	23.7	23.8	23.8	23.7	23.6	23.6	23.6	23.6	23.8
10000	23.7	23.9	23.8	24.0	23.9	23.9	23.8	23.9	23.8	23.7	23.7	23.8	23.7	23.6	23.7	23.6	23.6	23.6	23.8

Algorithm E.1: SaRa for CPs location estimation

- [1] **Input:**
- [2] (i) X_1, \dots, X_n – the data set;
- [3] (ii) $\widehat{T}_n^{(C)}(\cdot)$ – the proposed score function;
- [4] (ii) $\mathcal{C}(\cdot)$ – criterion function to perform CP times selection.
- [5] **begin**
- [6] Compute the initial set of estimated CP locations $\widehat{\Pi} \equiv \{\widehat{k}_1, \dots, \widehat{k}_{\widehat{m}}\}$ by (3.11).
- [7] Rearrange $\widehat{k}_1, \dots, \widehat{k}_{\widehat{m}}$ to $\widehat{k}_{(1)}, \dots, \widehat{k}_{(\widehat{m})}$ such that $T_n^{(C)}(\widehat{k}_{(1)}) \geq \dots \geq T_n^{(C)}(\widehat{k}_{(\widehat{m})})$.
- [8] Select $\widehat{m}' = \arg \min_{1 \leq j \leq \widehat{m}} \mathcal{C}(\widehat{k}_{(1)}, \dots, \widehat{k}_{(j)})$.
- [9] Set $\widehat{\Pi}' = \{\widehat{k}_{(1)}, \dots, \widehat{k}_{(\widehat{m}')}\}$.
- [10] **return** $\widehat{\Pi}'$ – the selected set of estimated CP locations.
-

E Extension to point estimation

Our proposed method can be extended to CP estimation. The first-step estimator for the set of CPs are defined in (3.11). If H_0 is rejected, the proposed score function used in the calculation can be reused and integrated to the screening and ranking algorithm (Niu and Zhang, 2012) to obtain CP estimates; see Algorithm E.1, where $h = \lfloor \epsilon n \rfloor$ and the criterion function \mathcal{C} can be maximum likelihood (Yao, 1987), least-squares estimation (Lavielle and Moulines, 2000), and minimum description length (Davis *et al.*, 2006), etc.

We can also incorporate our CP test and CP location estimator (3.11) into the popular binary segmentation algorithm (Vostrikova, 1981) to produce a potentially better set of CP locations estimator; see Algorithm E.2. The stopping criteria, that is based on the p -values, is also considered by Zhang *et al.* (2022+). They integrated their proposed self-normalized test and the wild binary segmentation proposed by Fryzlewicz (2014).

F Recursively computation

Simplify $V_n^{(Y)}(k | k - d, k + 1 + d) = V_n^{(Y)}(k | d)$. The self-normalizer (SN) using symmetric window, given any input change detecting process $\{Y_n(k)\}_{1 \leq k \leq n}$ are defined as,

$$V_n^{(Y)}(k | d) = \frac{1}{4(d+1)} \left\{ \sum_{j=k-d}^k L_n^{(Y)}(k | k - d, k)^2 + \sum_{j=k+1}^{k+1+d} L_n^{(Y)}(k | k + 1, k + 1 + d)^2 \right\}.$$

Algorithm E.2: Binary segmentation

```

[1] Input:
[2] (i)  $X_1, \dots, X_n$  – the data set;
[3] (ii)  $\widehat{T}_{n'}^{(C)}(\cdot | \mathcal{X})$  – the proposed score function when the a dataset  $\mathcal{X}$  of size  $n'$  is used;
[4] (iv)  $\widehat{p}_{n'}(\mathcal{X})$  – the  $p$ -value function when the a dataset  $\mathcal{X}$  of size  $n'$  is used;
[5] (iii)  $p_0$  – the  $p$ -value threshold to decide whether the CPs exist in the sample;
[6] (iii)  $\lfloor \epsilon n \rfloor$  – minimum window size.
[7] Function getCP(s, e):
[8]   if  $\widehat{p}(X_s, \dots, X_e) < p_0$  and  $e - s + 1 \geq \lfloor \epsilon n \rfloor$  then
[9]     return the set of the most obvious CP location  $\{\arg \max_{s \leq k \leq e} \widehat{T}_{e-s+1}^{(C)}(k | X_{s:e})\}$ .
[10]   else
[11]     return an empty set  $\{\}$ 
[12] begin
[13]   Compute  $\widehat{\Pi}'' = \widetilde{\Pi} = \text{getCP}(1, n)$ .
[14]   while  $\widetilde{\Pi} \neq \emptyset$  do
[15]      $\widetilde{\Pi}_0 = \emptyset$ 
[16]     foreach  $\tilde{k} \in \widetilde{\Pi}$  do
[17]       Set  $\tilde{k}^- = \max\{\widehat{\Pi}'' \cap [1, \tilde{k}]\}$  and  $\tilde{k}^+ = \min\{\widehat{\Pi}'' \cap [\tilde{k} + 1, n]\}$ .
[18]       Update  $\widetilde{\Pi}_0 \leftarrow \widetilde{\Pi}_0 \cup \text{getCP}(\tilde{k}^-, \tilde{k}) \cup \text{getCP}(\tilde{k} + 1, \tilde{k}^+)$ .
[19]     Update  $\widetilde{\Pi} \leftarrow \widetilde{\Pi}_0$  and  $\widehat{\Pi}'' \leftarrow \widehat{\Pi}'' \cup \widetilde{\Pi}_0$ .
[20] return  $\widehat{\Pi}''$  – the selected set of estimated CP locations.

```

For a given k , we want to recursively calculate the SN for $d > 0$. Define $S_{YY}(k) = \sum_{i=1}^k Y_n(i)^2$, $S_Y(k) = \sum_{i=1}^k Y_n(i)$ and $S_{IY}(k) = \sum_{i=1}^k i Y_n(i)$. The SN can be decomposed as

$$\begin{aligned}
V_n^{(Y)}(k | d) &= \frac{n}{4(d+1)^2} \left[(d+1)^2 \left\{ S_{YY}(k+1+d) - S_{YY}(k-d-1) \right\} \right. \\
&\quad + \frac{d(2d+1)}{6} \left\{ Y_n(k-d-1)^2 + Y_n(k)^2 \right\} \\
&\quad + \frac{d(2d+3)}{6} \left\{ Y_n(k)^2 + Y_n(k+1+d)^2 \right\} \\
&\quad + 2 \left\{ S_{IY}(k+1+d) - S_{IY}(k) \right\} \left\{ Y_n(k) - Y_n(k+1+d) \right\} \\
&\quad + 2 \left\{ S_{IY}(k) - S_{IY}(k-d-1) \right\} \left\{ Y_n(k-d-1) - Y_n(k) \right\} \\
&\quad \left. \right]
\end{aligned}$$

$$\begin{aligned}
& + 2 \left\{ S_Y(k+1+d) - S_Y(k) \right\} \left\{ kY_n(k+1+d) - (k+1+d)Y_n(k) \right\} \\
& + 2 \left\{ S_Y(k) - S_Y(k-d-1) \right\} \left\{ (k-d-1)Y_n(k) - kY_n(k-d-1) \right\} \\
& + \frac{d(d+2)}{3} Y_n(k) \left\{ Y_n(k-d-1) + Y_n(k+1+d) \right\} \Big].
\end{aligned}$$

Moreover, simplifying $L_n^{(Y)}(k | k-d, k+1+d) = L_n^{(Y)}(k | d)$, the squared localized process is defined as

$$L_n^{(Y)}(k | d) = \frac{n}{2(d+1)} \left[Y_n(k) - Y_n(k-d-1) - \frac{1}{2} \{Y_n(k+d+1) - Y_n(k-d-1)\} \right]^2.$$

Both $L_n^{(Y)}(k | d)^2$ and $V_n^{(Y)}(k | d)$ requires $O(1)$ time to update as d increases and k being fixed. Therefore, the score at time k , $T_n^{(Y)}(k) = \sup_{[en] \leq d \leq n} L_n^{(Y)}(k | d)^2 / V_n^{(Y)}(k | d)$ can be recursively computed and thus requires $O(n)$ computational complexity. Consequently, the aggregation process takes $O(n^2)$ computational complexity.

References

- Andrews, D. W. (1991) Heteroskedasticity and autocorrelation consistent covariance matrix estimation. *Econometrica*, **59**, 817–858.
- Antoch, J. and Jarušková, D. (2013) Testing for multiple change points. *Comput. Statist.*, **28**, 2161–2183.
- Bai, J. and Perron, P. (1998) Estimating and testing linear models with multiple structural changes. *Econometrica*, **66**, 47–78.
- Bai, Y. and Chow, D. Y. P. (2017) Shanghai-Hong Kong Stock Connect: An analysis of Chinese partial stock market liberalization impact on the local and foreign markets. *J. Int. Financ. Mark. Inst. Money*, **50**, 182–203.
- Bauer, P. and Hackl, P. (1980) An extension of the MOSUM technique for quality control. *Technometrics*, **22**, 1–7.
- Betken, A. (2016) Testing for change-points in long-range dependent time series by means of a self-normalized Wilcoxon test. *J. Time Ser. Anal.*, **37**, 785–809.
- Billingsley, P. (1999) *Convergence of probability measures*. Wiley Ser. Probab. Stat. New York: John Wiley & Sons Inc., second edn.
- Chan, B. S. F., Cheng, A. C. H. and Ma, A. K. C. (2018) Stock market volatility and trading volume: A special case in Hong Kong with Stock Connect turnover. *J. Risk Financ. Manag.*, **11**, 76.

- Chan, K. W. (2022) Mean-structure and autocorrelation consistent covariance matrix estimation. *J. Bus. Econom. Statist.*, **40**, 201–215.
- Chan, K. W. (2022+) Optimal difference-based variance estimators in time series: A general framework. *To appear in Ann. Statist.*
- Chiah, M. and Zhong, A. (2020) Trading from home: The impact of COVID-19 on trading volume around the world. *Finance Res. Lett.*, **37**, 101784.
- Chu, C.-S. J., Hornik, K. and Kaun, C.-M. (1995) MOSUM tests for parameter constancy. *Biometrika*, **82**, 603–617.
- Csörgö, M. and Horváth, L. (1988) 20 nonparametric methods for changepoint problems. *Handbook of Statist.*, **7**, 403–425.
- Csörgö, M. and Horváth, L. (1997) *Limit Theorems in Change-point Analysis*. Wiley Ser. Probab. Stat. New York: John Wiley & Sons Inc.
- Davis, R. A., Lee, T. C. M. and Rodriguez-Yam, G. A. (2006) Structural break estimation for nonstationary time series models. *J. Amer. Statist. Assoc.*, **101**, 223–239.
- Dehling, H., Fried, R., Garcia, I. and Wendler, M. (2015) Change-point detection under dependence based on two-sample U -statistics. In *Asymptotic Laws and Methods in Stochastics* (eds. D. Dawson, R. Kulik, M. Ould Haye, B. Szyszkowicz and Y. Zhao), 195–220. New York: Springer.
- Dehling, H., Fried, R. and Wendler, M. (2020) A robust method for shift detection in time series. *Biometrika*, **107**, 647–660.
- Dehling, H., Rooch, A. and Taqqu, M. S. (2013) Non-parametric change-point tests for long-range dependent data. *Scand. J. Statist.*, **40**, 153–173.
- Eichinger, B. and Kirch, C. (2018) A MOSUM procedure for the estimation of multiple random change points. *Bernoulli*, **24**, 526–564.
- Fryzlewicz, P. (2014) Wild binary segmentation for multiple change-point detection. *Ann. Statist.*, **42**, 2243–2281.
- Ge, L., Lin, T.-C. and Pearson, N. D. (2016) Why does the option to stock volume ratio predict stock returns? *J. Financ. Econ.*, **120**, 601–622.
- Gormsen, N. J. and Koijen, R. S. (2020) Coronavirus: Impact on stock prices and growth expectations. *Rev. Asset Pricing Stud.*, **10**, 574–597.
- Herrndorf, N. (1984) A functional central limit theorem for weakly dependent sequences of random variables. *Ann. Probab.*, **12**, 141–153.
- Huang, Y., Volgushev, S. and Shao, X. (2015) On self-normalization for censored dependent data. *J. Time Ser. Anal.*, **36**, 109–124.
- Huo, R. and Ahmed, A. D. (2017) Return and volatility spillovers effects: Evaluating the impact of Shanghai-Hong Kong Stock Connect. *Economic Modelling*, **61**, 260–272.

- Jiang, F., Zhao, Z. and Shao, X. (2022+) Modelling the COVID-19 infection trajectory: A piecewise linear quantile trend model. *To appear in J. R. Stat. Soc. Ser. B Stat. Methodol.*
- Johnson, T. L. and So, E. C. (2012) The option to stock volume ratio and future returns. *J. Financ. Econ.*, **106**, 262–286.
- Kiefer, N. M. and Vogelsang, T. J. (2002) Heteroskedasticity-autocorrelation robust standard errors using the Bartlett kernel without truncation. *Econometrica*, **70**, 2093–2095.
- Kiefer, N. M. and Vogelsang, T. J. (2005) A new asymptotic theory for heteroskedasticity-autocorrelation robust tests. *Econometric Theory*, **21**, 1130–1164.
- Koenker, R. W. and d’Orey, V. (1987) Algorithm as 229: Computing regression quantiles. *J. R. Stat. Soc., C: Appl. Stat.*, **36**, 383–393.
- Künsch, H. (1987) Statistical aspects of self-similar processes. *Proceedings of the First World Congress of the Bernoulli Society (Yu. Prohorov and V. V. Sazanov, eds.)*, **1**, 67–74.
- Lavielle, M. and Moulines, E. (2000) Least-squares estimation of an unknown number of shifts in a time series. *J. Time Ser. Anal.*, **21**, 33–59.
- Lee, C.-B. (1995) Estimating the number of change points in a sequence of independent normal random variables. *Statist. Probab. Lett.*, **25**, 241–248.
- Lobato, I. N. (2001) Testing that a dependent process is uncorrelated. *J. Amer. Statist. Assoc.*, **96**, 1066–1076.
- Niu, Y. S. and Zhang, H. (2012) The screening and ranking algorithm to detect DNA copy number variations. *Ann. Appl. Stat.*, **6**, 1306–1326.
- Ortmann, R., Pelster, M. and Wengerek, S. T. (2020) COVID-19 and investor behavior. *Finance Res. Lett.*, **37**, 101717.
- Palma, W. (2007) *Long-Memory Time Series: Theory and Methods*, vol. 662. John Wiley & Sons.
- Pan, J. and Poteshman, A. M. (2006) The information in option volume for future stock prices. *Rev. Financ. Stud.*, **19**, 871–908.
- Pipiras, V. and Taqqu, M. S. (2017) *Long-Range Dependence and Self-Similarity*, vol. 45 of *Camb. Ser. Stat. Probab. Math.* Cambridge University Press.
- Rao, T. S. and Gabr, M. M. (1984) *An Introduction to Bispectral Analysis and Bilinear Time Series Models*, vol. 24. Springer-Verlag, New York, 1 edn.
- Ruan, Q., Zhang, S., Lv, D. and Lu, X. (2018) Financial liberalization and stock market cross-correlation: MF-DCCA analysis based on Shanghai-Hong Kong Stock Connect. *Phys. A: Stat. Mech. Appl.*, **491**, 779–791.
- Shao, X. (2010) A self-normalized approach to confidence interval construction in time series. *J. R. Stat. Soc. Ser. B Stat. Methodol.*, **72**, 343–366.

- Shao, X. (2011) A simple test of changes in mean in the possible presence of long-range dependence. *J. Time Ser. Anal.*, **32**, 598–606.
- Shao, X. (2015) Self-normalization for time series: a review of recent developments. *J. Amer. Statist. Assoc.*, **110**, 1797–1817.
- Shao, X. and Wu, W. B. (2007) Local Whittle estimation of fractional integration for nonlinear processes. *Econometric Theory*, **23**, 899–929.
- Shao, X. and Zhang, X. (2010) Testing for change points in time series. *J. Amer. Statist. Assoc.*, **105**, 1228–1240.
- Taqqu, M. S. (1975) Weak convergence to fractional Brownian motion and to the Rosenblatt process. *Zeitschrift für Wahrscheinlichkeitstheorie und verwandte Gebiete*, **31**, 287–302.
- Vogelsang, T. J. (1999) Sources of nonmonotonic power when testing for a shift in mean of a dynamic time series. *J. Econometrics*, **88**, 283–299.
- Vostrikova, L. Y. (1981) Detection disorder in multidimensional random processes. *Soviet Math. Dokl.*, **259**, 55–59.
- Wang, R., Zhu, C., Volgushev, S. and Shao, X. (2022) Inference for change points in high-dimensional data via self-normalization. *Ann. Statist.*, **50**, 781–806.
- Wasserman, L. (2006) *All of Nonparametric Statistics*. Springer-Verlag, New York, 1 edn.
- Wu, W. B. (2007) Strong invariance principles for dependent random variables. *Ann. Probab.*, **35**, 2294–2320.
- Wu, W. B. (2011) Asymptotic theory for stationary processes. *Statistics and its Interface*, **4**, 207–226.
- Xu, K., Zheng, X., Pan, D., Xing, L. and Zhang, X. (2020) Stock market openness and market quality: evidence from the Shanghai-Hong Kong Stock Connect program. *Journal of Financial Research*, **43**, 373–406.
- Yao, Y.-C. (1987) Approximating the distribution of the maximum likelihood estimate of the change-point in a sequence of independent random variables. *Ann. Statist.*, 1321–1328.
- Yao, Y.-C. (1988) Estimating the number of change-points via Schwarz’ criterion. *Statist. Probab. Lett.*, **6**, 181–189.
- Yau, C. Y. and Zhao, Z. (2016) Inference for multiple change points in time series via likelihood ratio scan statistics. *J. R. Stat. Soc. Ser. B Stat. Methodol.*, 895–916.
- Zhang, T. and Lavitas, L. (2018) Unsupervised self-normalized change-point testing for time series. *J. Amer. Statist. Assoc.*, **113**, 637–648.
- Zhang, Y., Wang, R. and Shao, X. (2022+) Adaptive inference for change points in high-dimensional data. *J. Amer. Statist. Assoc.*